

**IMPACTS OF ZOOPLANKTON ABUNDANCE AND COMMUNITY
COMPOSITION ON LARVAL FISH HABITAT QUALITY AND LARVAL
COREGONID DIETS**

by

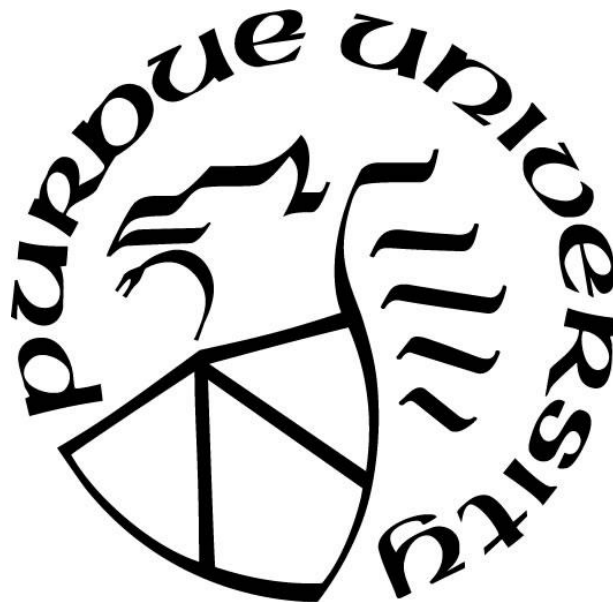
Marissa Cubbage

A Thesis

Submitted to the Faculty of Purdue University

In Partial Fulfillment of the Requirements for the degree of

Master of Science



Department of Forestry and Natural Resources

West Lafayette, Indiana

December 2021

THE PURDUE UNIVERSITY GRADUATE SCHOOL
STATEMENT OF COMMITTEE APPROVAL

Dr. Paris Collingsworth, Chair

Department of Forestry and Natural Resources

Dr. Tomas Höök

Department of Forestry and Natural Resources

Dr. David Bo Bunnell

USGS Great Lakes Science Center

Approved by:

Dr. Robert Wagner

Dedicated to Kim, the inspiration to always push myself to be a better scientist

ACKNOWLEDGMENTS

I would like to thank my advisors Paris Collingsworth and Tomas Höök for their support of my research, especially during the height of the Covid-19 pandemic. I would also like to thank my additional committee member Bo Bunnell for project advice and thesis revisions. I thank past and present members of the Höök lab, including Suse LaGory, Patricia Nease, Scott Koenigbauer, Annie Scofield, Josh Tellier, Jay Beugly, and Matt Hamilton supporting me with my research and my mental health through my master's studies. I would also like to thank the Little Traverse Bay Bands of Odawa Indians for assistance in sample collection. I would especially like to thank Patty Dieter and technicians at USGS Great Lakes Science Center for zooplankton training and processing.

TABLE OF CONTENTS

LIST OF TABLES	7
LIST OF FIGURES	8
ABSTRACT.....	11
CHAPTER 1. INTRODUCTION	13
1.1 Introduction.....	13
1.2 References.....	16
CHAPTER 2. LARVAL COREGONID DENSITY AND DIET COMPOSITION IN NEARSHORE AREAS OF NORTHERN LAKE MICHIGAN	19
2.1 Introduction.....	19
2.2 Methods.....	21
2.2.1 Field Collections.....	21
2.2.2 Selection of zooplankton and larval fish samples for analysis	22
2.2.3 Zooplankton Sample Processing.....	22
2.2.4 Larval Fish Processing.....	22
2.2.5 Statistical Analysis.....	23
2.3 Results.....	26
2.3.1 Zooplankton Abundance and Community Composition	26
2.3.2 Coregonid Abundance	27
2.3.3 Coregonid Size Structure.....	27
2.3.4 Coregonid Diet.....	28
2.3.5 Diet Selectivity	28
2.4 Discussion	28
2.5 Tables and Figures	32
2.6 References	41
CHAPTER 3. LARVAL FISH HABITAT QUALITY OBTAINED USING HIGH- FREQUENCY SENSOR DATA AND GROWTH RATE POTENTIAL MODELLING.....	45
3.1 Introduction.....	45
3.2 Methods.....	48
3.2.1 Data collection and preparation	48
3.2.2 Model environment setup	49
3.2.3 Model Overview	51

3.2.4	Foraging model	52
3.2.5	Summarizing outputs across a transect group	55
3.3	Results	56
3.3.1	Larvae size throughout the summer.....	56
	May 6 mm larvae	56
	June 11 mm larvae	57
	July 11 and 14 mm larvae.....	57
3.4	Discussion	58
3.5	Tables and Figures	62
3.6	References	75

LIST OF TABLES

Table 2. 1 Number of sampling events used in four major sections of results (larval abundance, zooplankton abundance, diet composition, and diet selectivity) for each year 2015-2019.	32
Table 3. 1 Nearshore-offshore TUV transects location, length, depth station range, month(s) sampled, TUV used in data collection, and transect group used for figures and summary analysis. Transect lengths are listed in chronological order for Lake Huron (May, June July) and Lake Michigan (May, July).....	62
Table 3. 2 Description of zooplankton groups used as prey types in the foraging model. The median length of the size bin is used in the model for all particles of that size bin. All particles in the LOPC size bin are assumed to have similar energy densities, according to reported energy densities of the taxonomic group designated. Energy densities sourced from Cummings and Wuycheck (1971), as grouped by Fernandez et al (2009).	63
Table 3. 3 Yellow perch and European Smelt bioenergetic parameters. Yellow perch equations and parameters sourced from post 1990 and Worishka and Mehner (1998). European smelt paramters sourced from Karjalainen et al (1997a).	64

LIST OF FIGURES

Figure 2. 1. Map of Lake Michigan with locations of four study sites: Petoskey State Park, Big Stone Bay, Bliss Beach, and Elk Rapids..... 32

Figure 2. 2 Scatterplot of Zooplankton density (total zooplankton count m^{-3}) based on collection date. Collection year is represented by point color and collection site is represented by point shape. Samples that were included in zooplankton community description and analysis, but did not have viable larvae from a corresponding neuston net tow, are designated with a plus sign over the point. Collection dates ranged from the last week of March to the first week of June. While most zooplankton collections occurred throughout the month of May, peak zooplankton abundances were measure the last two weeks of April through the first two weeks of May. 33

Figure 2. 3 Scatterplot of mean percent abundance of each major zooplankton group (small cladocerans, adult calanoid copepods, calanoid copepodites, adult cyclopoid copepods, cyclopoid copepodites, daphnia species, dreissenid veligers, harpacticoids, and copepod nauplii) each sampling year (A) and collection site (B) in zooplankton samples collected in northern Lake Michigan. Standard deviation of each mean is represented by dotted lines. Nauplii and calanoid copepods had high percent zooplankton community composition, whether samples were grouped by year (top) or year (bottom). In some samples from Petoskey State Park and the 2017 collection year had relatively high cyclopoid percent zooplankton community composition. 34

Figure 2. 4 Scatterplot of density (number of zooplankton per cubic meter) of nine major zooplankton groups (small cladocerans, adult calanoid copepods, calanoid copepodites, adult cyclopoid copepods, cyclopoid copepodites, daphnia species, dreissenid veligers, harpacticoids, and copepod nauplii) each sampling year (A) and collection site (B). Standard deviation of each mean is represented by dotted lines. Nauplii and calanoid copepods were the most abundant prey types, whether samples were grouped by year (top) or site (bottom). 35

Figure 2. 5 Scatterplots of coregonid larvae density of each neuston net tow in northern lake Michigan 2015-2019 (number of larvae m^{-3}) in reference to water temperature at time of collection (A), and collection date (B). Water temperature was unavailable for 26 of the 115 neuston net tows collected 2015-2019 due to uncalibrated sampling instruments. Collection dates ranged from the last week of March to the last week of June. Larvae density ranged from 0 to 91.8 larvae m^{-3} , with highest coregonid larvae density during May and when water temperatures were between 7-11°C. 36

Figure 2. 6 Histogram of coregonid larvae length from all neuston sample 2015-2019 with and without a yolk-sac (A). Scatterplot of number of diet items vs. larvae length with associated linear regressions for yolk-sac larvae ($y = 0.28x - 1.12$, $R^2 = < 0.001$, $p = 0.31$), non yolk sac larvae ($y = 2.93x - 31.04$, $R^2 = 0.21$, $p = < 0.001$), and all larvae ($y = 3.07x - 34.17$, $R^2 = 0.24$, $p = < 0.001$) (B). Scatterplot of gut empty status (0=empty gut, 1=gut with at least 1 diet item) vs. larvae length with predicted logistic regression (C). Scatterplot of biomass of items in gut (mg) vs. larvae length (mm) and associated linear regressions for yolk-sac larvae ($y = 0.01x - 0.05$, $R^2 = 0.03$, $p = 0.06$), non yolk sac larvae ($y = 0.02x - 0.18$, $R^2 = 0.19$, $p = < 0.001$), and all larvae ($y = 0.02x - 0.19$, $R^2 = 0.21$, $p = < 0.001$) (D). Yolk-sac larvae regressions are indicated in red, larvae without a yolk

sac regression are indicated by gray, and all larvae regressions are indicated by black throughout the plot panels. 37

Figure 2. 7 Barplot of coregonid diet composition (% biomass) for all larvae collected 2015-2019 in northern Lake Michigan by larvae length (grouped by mm, 8-23 mm). Diet item groups include calanoid copepods, cyclopoid copepods, unknown copepods (could not be identified as calanoid or cyclopoid), chironomids, harpacticoids, small cladocerans, large cladocerans, and other prey items. Common diet items by number and biomass include, calanoid copepods, cyclopoid copepods, and chironomids, while cladocerans were rarely found in diets and no copepod nauplii were found in diets. Numbers placed above each bar denote the number of larvae in the size bin. 38

Figure 2. 8 Barplot of coregonid diet composition (%) in biomass for small (8-15 mm) and large (15-24) larvae each sampling year (A) and collection site (B). Diet item groups include calanoid copepods, cyclopoid copepods, unknown copepods (could not be identified as calanoid or cyclopoid), chironomids, harpacticoids, small cladocerans, large cladocerans, and other prey items. Common diet items by number and biomass include, calanoid copepods, cyclopoid copepods, and chironomids, while cladocerans were rarely found in diets and no copepod nauplii were found in diets. 39

Figure 2. 9 Mean Chesson's index of larvae for five prey types within each sampling year (A) and site (B). 95% confidence interval for each mean is represented by solid black lines. The five prey groups used in calculating Chesson's index include calanoid copepods (adult and copepodid), cyclopoid adult copepods, cyclopoid copepodites, cladocerans, and copepod nauplii. The horizontal line represents 1 divided by the number of prey types in zooplankton samples. Chesson's index values above the horizontal line are prey groups that larvae positively select for, values near the line are prey groups that larvae neutrally select for, and values below the line are prey groups that larvae negatively select for. Each year, larvae positively selected for calanoid copepods and adult cyclopoid copepods, but negatively selected for cyclopoid copepodites, cladocerans, and copepod nauplii. 40

Figure 3. 1. Locations of nearshore-offshore TUV transects in Lake Michigan (2015) and Lake Huron (2017). 65

Figure 3. 2 Boxplots of lengths of a subset of larvae collected in oblique larval fish tows at bathymetric depths of 18, 46, and an additional offshore site (68-110 m depth contour) in Lake Huron in 2017 and Lake Michigan in 2015. For rainbow smelt, larvae were only collected at 18 m bathymetric depth in May (A), but in all depth stations in June (B) and July (C) in southern Lake Huron transects. Larval yellow perch were only collected at 18 and 46 m bathymetric depths in June and July (combined data of these 2 months, D). Larval yellow perch from central and southern lake Michigan transects were only collected in July (E). Numbers placed above each boxplot represent sample size. 66

Figure 3. 3 Relationship between larvae reactive distance and zooplankton length (top), and the relationship between larvae reactive distance and light availability ($\mu\text{E m}^{-2} \text{sec}^{-1}$) (bottom) for 6 mm, 11 mm, and 14 mm larvae. 67

Figure 3. 4 Mean percent positive GRP in 16 sections of the water column among southern Lake Huron transects for 6 mm yellow perch in May (A), 11 mm yellow perch in June (B), and 11 mm and 14 mm yellow perch in July (C,D). Labels are the percent positive GRP value for each transect in the following order: Maitland, Harbor Beach, Saugeen River.	68
Figure 3. 5 Mean percent positive GRP in 16 sections of the water column among southern Lake Huron transects for 6 mm smelt in May (A), 11 mm smelt in June (B), and 11 mm and 14 mm smelt in July (C,D). Labels are the percent positive GRP value for each transect in the following order: Maitland, Harbor Beach, Saugeen River.	69
Figure 3. 6 Mean percent positive GRP in 16 sections of the water column among southern Lake Michigan transects for 11 mm and 14 mm yellow perch (A,B) and smelt (C,D). Labels are the percent positive GRP value for each transect in the following order: : Frankfort, Sturgeon Bay, Manitowoc, Ludington.	70
Figure 3. 7 Southern Lake Huron means of mean individual transect averages of GRP in cells within the 95 th percentile for 16 designated areas of the water column in May for 6 mm yellow perch (A), June for 11 mm yellow perch (B), and July for 11 mm and 14 mm yellow perch (C,D).	71
Figure 3. 8 Southern Lake Huron means of mean individual transect averages of GRP in cells within the 95 th percentile for 16 designated areas of the water column in May for 6 mm smelt (A), June for 11 mm smelt (B), July for 11 mm and 14 mm smelt (C,D).	72
Figure 3. 9 Central Lake Michigan means of mean individual transect averages of GRP in cells within the 95 th percentile for 16 designated areas of the water column by month and species in May for 6 mm yellow perch (A) and July for 11 mm and 14 mm yellow perch (B,C).	73
Figure 3. 10 Central Lake Michigan means of mean individual transect averages of GRP in cells within the 95 th percentile for 16 designated areas of the water column by month and species in May for 6 mm smelt (A) and July for 11 mm and 14 mm smelt (B,C).	74

ABSTRACT

Offshore spring zooplankton biomass in northern Lake Michigan is currently dominated by calanoid copepods and lacking in cyclopoid copepod biomass, which is a preferred prey type for larval coregonids in the Great Lakes. As such, we survey nearshore beach zooplankton to determine if nearshore environments are following offshore trends and describe larval coregonid diets and prey selectivity during spring 2015-2019. Copepod nauplii and calanoid copepods were the most abundant prey types in the nearshore beach environments, and although larvae did not consume copepod nauplii, larvae did incorporate substantial later life stages of calanoid copepods into their diet. Additionally, larvae exhibited positive selectivity for both calanoid and cyclopoid copepods. High consumption of and selectivity for calanoid copepods in small larval coregonids is not a common observation in the Great Lakes, as previous diets of small larvae have been comprised of mainly cyclopoid copepods and cladocerans. Future research into the foraging costs and nutritional benefits of larval diets with differing ratios of cyclopoid to calanoid biomass should be investigated to understand the potential impacts of differing diets on larval growth and survival.

Many species of larval fish in Lakes Michigan and Huron experience a prolonged offshore pelagic stage as during early life, but environmental conditions in offshore environments have changed in the past quarter century. Under current conditions, offshore habitats may be unsuitable for larval fish, given recent increases in offshore water clarity and decreases in offshore primary production and zooplankton biomass in both lakes. To evaluate habitat suitability for larval fish, we characterized ambient environmental conditions using data streams from multiple high frequency sensors to develop growth rate potential models as an index of habitat quality of nearshore-offshore transects in central Lake Michigan and southern Lake Huron. Since temperature regimes differ throughout the summer, we compare habitat quality throughout the summer for larval yellow perch and smelt, two species that have demonstrated offshore pelagic stages as larvae. Early in the summer, high habitat quality was concentrated nearshore, while later in the summer high habitat quality was concentrated near the thermocline, at depths where larvae are unlikely to inhabit due to limited swimming ability. The offshore (15-60 m depth contour) surface waters of both lakes provide poor habitat quality in May and July, although the surface waters of transects collected during June in southern Lake Huron provided high quality habitat at all distances from shore. These results suggest that offshore advection and prolonged offshore

pelagic stage duration during early life of fish could contribute to decreased growth and survival of larval fish in lakes Michigan and Huron.

CHAPTER 1. INTRODUCTION

1.1 Introduction

The Laurentian Great Lakes of North America provide recreational, commercial, and subsistence fishing to surrounding communities (Ebener et al 2008, Chiarappa et al 2005, Melstrom and Lupi 2013), but many fish populations in these lakes are in decline (Gorman 2019). In Lake Huron, pelagic and demersal fish abundance and biomass decreased in the early 2000s (Riley et al 2008, Warner et al 2009), and Lake Michigan prey fish abundances also exhibited declines beginning at the turn of the 20th century (Gorman 2019). Declining fish biomass in lakes Michigan and Huron have occurred alongside several other ecosystem level changes, including exotic species invasions, oligotrophication of offshore waters, increased water clarity, and shifting zooplankton community composition (Barbiero et al 2019, Evans et al 2011, Hutton-Stadig 2020). Considering the multiple changes lakes Michigan and Huron have undergone over the last century, it is difficult to concretely identify the mechanisms behind declining fish population in these lakes. However, one possible contribution to reduced fish abundances is declining zooplankton abundances contributing to reduced growth and survival of larval fish (Bunnell et al 2018).

Survival rates at the larval fish stage can greatly impact subsequent adult abundances. As organisms that exhibit type three survivorship curves, early life stages of fish have relatively high mortality rates in comparison to adult life stages (Houde and Zastrow 1993, Pauly 1980). As such, slight increases in survival rates during early life stages could dramatically increase subsequent adult abundances. In freshwater systems, the juvenile stage has been identified as the most critical stage because 1) freshwater juveniles experience higher over-winter mortality and competition for resources, and 2) freshwater larvae hatch at larger sizes and have a reduced pelagic stage in comparison to marine larvae, reducing mortality at the larval stage (Houde 1994). However, due to the large size and currents of the Great Lakes, many freshwater species in this system experience a substantial offshore pelagic stage as larvae (Dettmers 2005, Janssen et al 2014, Nash and Geffen 1991). The offshore pelagic stage for larvae has been identified as a stage with higher mortality than the subsequent nearshore benthic larval and juvenile stages of yellow perch in Lake Michigan (Weber et al 2011). Exacerbated baseline mortality rates of larvae in the Great Lakes through increased predation, starvation, or reduced growth, could reduce year class strength.

Prey availability is important for the survival of fish larvae. If appropriate prey are not available after larvae have absorbed their yolk sac and must begin exogenous feeding, large die-off events can occur (Hjort 1914). Instances of low prey availability during the larval stage could occur when timing of peak prey abundances and larval transition to exogenous feeding do not match. A mismatch in peak prey abundance and peak larval emergence can cause larvae to die from starvation (Cushing 1990). Even for species resistant to starvation, reduced prey availability can slow larval growth rates, increasing the length of the pelagic larval stage and exposing larvae to high predation risk.

Most fish species in the Great Lakes utilize zooplankton as prey during the larval stage, and the importance of zooplankton for fish larvae in these systems is well documented. Larval lake whitefish growth during the spring is correlated with zooplankton density in Lake Ontario (Hoyle 2011) and catch per unit effort (CPUE) of age -0 yellow perch has been related to early summer zooplankton densities in Lake Michigan (Hoyle 2011, Dettmers et al 2003). High zooplankton abundance, in addition to alewife abundance and water temperature, was associated with strong year class strength of yellow perch over two decades in Lake Michigan (Redman et al 2011). Overall, 46% of studies on fish recruitment in the Great Lakes found that lower trophic levels influenced recruitment of fish populations (Pritt et al 2014).

Changes in the lower trophic levels of offshore environments in lakes Michigan and Huron include decreased spring zooplankton abundances, which could exacerbate larval fish mortality through increased starvation and reduced growth. The late winter phytoplankton bloom in these lakes has over time been characterized by reduced chlorophyll-a, increased water clarity, and increased soluble silica (increased free silica indicates less silica being used by diatoms) (Mida et al 2010, Fahnenstiel et al 2010, Kerfoot et al 2010, Barbiero et al 2012). As the late winter phytoplankton bloom is reduced, less primary production is available to support the early spring zooplankton community. Over the past quarter century, the spring zooplankton community in Lake Michigan has been increasingly dominated by calanoid copepods, which have largely replaced cyclopoid copepods (Kerfoot et al 2010, Barbiero et al 2019). In addition to reduced cyclopoid biomass in spring zooplankton communities, Lake Huron has exhibited decreased overall biomass of spring zooplankton over time (Barbiero et al 2019).

Coregonids, specifically lake whitefish (*Coregonus clupeaformis*) and cisco (*Coregonus artedii*), are an important group of fish that rely on spring zooplankton as larvae in the Great Lakes.

To understand foraging of coregonid larvae under an altered zooplankton regime, we quantified the spring beach zooplankton community and described coregonid larvae early life feeding in northern lake Michigan from 2015-2019. The zooplankton community in the nearshore beach environment consisted of mainly copepod nauplii and adult calanoid copepods; cyclopoid copepods and cladocerans consistently made up less than 10% of total zooplankton abundance. However, relative abundances of nauplii and calanoid copepods varied widely among sample collections. Coregonid larvae mainly consumed adult calanoid and cyclopoid copepods. While cyclopoid copepods occurred in lower abundances than calanoid copepods, larvae positively selected for both prey types. These diet observations are in contrast with previous studies that have documented low consumption of calanoid copepods by small coregonid larvae in the Great Lakes (Hoyle et al 2011, Lucke et al 2020, Pothoven et al 2020). As Lakes Michigan and Huron continue to support oligotrophic species of calanoid copepods, there may be energetic and foraging consequences of a larval coregonid diet consistent of more calanoid copepods.

Ecosystem changes in lakes Michigan and Huron could also impact fish larvae that hatch in late spring and summer, such as yellow perch (*Perca Flavescens*) and rainbow smelt (*Osmerus mordax*). The offshore environment of these lakes have experienced substantial oligotrophication that seem to be related to decreased nutrient loading and filtering by invasive dreissenid mussels (Evans et al 2011). In addition to intense oligotrophication, biomass of offshore summer zooplankton has decreased in both lake Michigan and Lake Huron (Barbiero et al 2019). Late-spring/summer hatching larvae, such as yellow perch and rainbow smelt, have documented offshore pelagic stages where they will experience the oligotrophic, decreased prey environment.

Despite overall oligotrophication and declines in zooplankton abundance, advection and natural ‘patchiness’ of zooplankton ensures larvae experience varied habitat throughout the offshore pelagic stage. Thus, we describe variation in habitat quality for larval fish within nearshore to offshore transects of lakes Michigan and Huron. In the southern basin of Lake Huron, our analysis suggests that the location of high quality habitat for larval fish shifts from shallow nearshore areas in the late spring to the thermocline offshore as thermal stratification sets in. In contrast, the best quality habitat remained in surface waters nearshore throughout the entire summer in central Lake Michigan. In transects across the lakes, warm offshore surface waters in late summer provided poor habitat quality for larval fish due to low prey densities.

1.2 References

- Barbiero, R.P., Lesht, B.M. and Warren, G.J., 2012. Convergence of trophic state and the lower food web in Lakes Huron, Michigan and Superior. *Journal of Great Lakes Research*, 38(2), pp.368-380.
- Barbiero, R.P., Rudstam, L.G., Watkins, J.M. and Lesht, B.M., 2019. A cross-lake comparison of crustacean zooplankton communities in the Laurentian Great Lakes, 1997–2016. *Journal of Great Lakes Research*, 45(3), pp.672-690.
- Bunnell, D.B., Carrick, H.J., Madenjian, C.P., Rutherford, E.S., Vanderploeg, H.A., Barbiero, R.P., Hinchey-Malloy, E., Pothoven, S.A., Riseng, C.M., Claramunt, R.M. and Bootsma, H.A., 2018. *Are changes in lower trophic levels limiting prey-fish biomass and production in Lake Michigan?* (No. 2018-01). Great Lakes Fishery Commission.
- Chiarappa, M.J., 2005. Overseeing the family of whitefishes: The priorities and debates of coregonid management on America's Great Lakes, 1870-2000. *Environment and History*, pp.163-194.
- Cushing, D.H., 1990. Plankton production and year-class strength in fish populations: an update of the match/mismatch hypothesis. In *Advances in marine biology* (Vol. 26, pp. 249-293). Academic Press.
- Dettmers, J.M., Raffenberg, M.J. and Weis, A.K., 2003. Exploring zooplankton changes in southern Lake Michigan: implications for yellow perch recruitment. *Journal of Great Lakes Research*, 29(2), pp.355-364.
- Dettmers, J.M., Janssen, J., Pientka, B., Fulford, R.S. and Jude, D.J., 2005. Evidence across multiple scales for offshore transport of yellow perch (*Perca flavescens*) larvae in Lake Michigan. *Canadian Journal of Fisheries and Aquatic Sciences*, 62(12), pp.2683-2693.
- Ebener, M.P., Kinnunen, R.E., Schneeberger, P.J., Mohr, L.C., Hoyle, J.A. and Peeters, P., 2008. Management of commercial fisheries for lake whitefish in the Laurentian Great Lakes of North America. *International governance of fisheries ecosystems: learning from the past, finding solutions for the future*. American Fisheries Society, Bethesda, Maryland, pp.99-143.
- Evans, M.A., Fahnenstiel, G. and Scavia, D., 2011. Incidental oligotrophication of North American great lakes. *Environmental science & technology*, 45(8), pp.3297-3303.
- Fahnenstiel, G., Pothoven, S., Vanderploeg, H., Klarer, D., Nalepa, T. and Scavia, D., 2010. Recent changes in primary production and phytoplankton in the offshore region of southeastern Lake Michigan. *Journal of Great Lakes Research*, 36, pp.20-29.
- Gorman, O.T., 2019. Prey fish communities of the Laurentian Great Lakes: A cross-basin overview of status and trends based on bottom trawl surveys, 1978-2016. *Aquatic Ecosystem Health & Management*, 22(3), pp.263-279.

- Hjort, J., 1914. Fluctuations in the great fisheries of northern Europe viewed in the light of biological research. ICES.
- Houde, E.D., 1994. Differences between marine and freshwater fish larvae: implications for recruitment. *ICES Journal of Marine Science*, 51(1), pp.91-97.
- Houde, E.D. and Zastrow, C.E., 1993. Ecosystem-and taxon-specific dynamic and energetics properties of larval fish assemblages. *Bulletin of marine science*, 53(2), pp.290-335.
- Hoyle, J.A., Johannsson, O.E. and Bowen, K.L., 2011. Larval lake whitefish abundance, diet and growth and their zooplankton prey abundance during a period of ecosystem change on the Bay of Quinte, Lake Ontario. *Aquatic Ecosystem Health & Management*, 14(1), pp.66-74.
- Janssen, J., Marsden, J.E., Hrabik, T.R. and Stockwell, J.D., 2014. Are the Laurentian Great Lakes great enough for Hjort?. *ICES Journal of Marine Science*, 71(8), pp.2242-2251.
- Kerfoot, W.C., Yousef, F., Green, S.A., Budd, J.W., Schwab, D.J. and Vanderploeg, H.A., 2010. Approaching storm: disappearing winter bloom in Lake Michigan. *Journal of Great Lakes Research*, 36, pp.30-41.
- Melstrom, R.T. and Lupi, F., 2013. Valuing recreational fishing in the Great Lakes. *North American Journal of Fisheries Management*, 33(6), pp.1184-1193.
- Mida, J.L., Scavia, D., Fahnenstiel, G.L., Pothoven, S.A., Vanderploeg, H.A. and Dolan, D.M., 2010. Long-term and recent changes in southern Lake Michigan water quality with implications for present trophic status. *Journal of Great Lakes Research*, 36, pp.42-49.
- Nash, R.D. and Geffen, A.J., 1991. Spatial and temporal changes in the offshore larval fish assemblage in southeastern Lake Michigan. *Journal of Great Lakes Research*, 17(1), pp.25-32.
- Lucke, V.S., Stewart, T.R., Vinson, M.R., Glase, J.D. and Stockwell, J.D., 2020. Larval Coregonus spp. diets and zooplankton community patterns in the Apostle Islands, Lake Superior. *Journal of Great Lakes Research*, 46(5), pp.1391-1401.
- Pauly, D., 1980. On the interrelationships between natural mortality, growth parameters, and mean environmental temperature in 175 fish stocks. *ICES journal of Marine Science*, 39(2), pp.175-192.
- Pothoven, S.A., 2020. The influence of ontogeny and prey abundance on feeding ecology of age-0 Lake Whitefish (*Coregonus clupeaformis*) in southeastern Lake Michigan. *Ecology of Freshwater Fish*, 29(1), pp.103-111.
- Pritt, J.J., Roseman, E.F. and O'Brien, T.P., 2014. Mechanisms driving recruitment variability in fish: comparisons between the Laurentian Great Lakes and marine systems. *ICES Journal of Marine Science*, 71(8), pp.2252-2267.

- Redman, R.A., Czesny, S.J., Dettmers, J.M., Weber, M.J. and Makauskas, D., 2011. Old tales in recent context: current perspective on yellow perch recruitment in Lake Michigan. *Transactions of the American Fisheries Society*, 140(5), pp.1277-1289.
- Riley, S.C., Roseman, E.F., Nichols, S.J., O'Brien, T.P., Kiley, C.S. and Schaeffer, J.S., 2008. Deepwater demersal fish community collapse in Lake Huron. *Transactions of the American Fisheries Society*, 137(6), pp.1879-1890.
- Stadig, M.H., Collingsworth, P.D., Lesht, B.M. and Höök, T.O., 2020. Spatially heterogeneous trends in nearshore and offshore chlorophyll a concentrations in lakes Michigan and Huron (1998–2013). *Freshwater Biology*, 65(3), pp.366-378.
- Warner, D.M., Schaeffer, J.S. and O'Brien, T.P., 2009. The Lake Huron pelagic fish community: persistent spatial pattern along biomass and species composition gradients. *Canadian Journal of Fisheries and Aquatic Sciences*, 66(8), pp.1199-1215.
- Weber, M.J., Dettmers, J.M. and Wahl, D.H., 2011. Growth and survival of age-0 yellow perch across habitats in southwestern Lake Michigan: early life history in a large freshwater environment. *Transactions of the American Fisheries Society*, 140(5), pp.1172-1185.

CHAPTER 2. LARVAL COREGONID DENSITY AND DIET COMPOSITION IN NEARSHORE AREAS OF NORTHERN LAKE MICHIGAN

2.1 Introduction

Lake Michigan has undergone multiple ecosystem changes over the past quarter century. Zebra mussels *Dreissena polymorpha* were first observed in the late 1980s in the lake, and by 1997 the more prolific quagga mussels *Dreissena rostriformis bugensis* were found in northern Lake Michigan (Nalepa et al. 2001, NY Sea Grant 2002). The subsequent rapid spread of quagga mussels coincided with declines in primary production and increased water clarity (Fahnenstiel et al. 2010, Mida et al. 2010). In particular, Lake Michigan experienced reductions in the spring phytoplankton bloom, which is the foundation for the early spring zooplankton bloom (Kerfoot et al. 2010). From 2000 to 2015, total biomass of offshore zooplankton in Lake Michigan during the spring declined and in particular, the biomass of cyclopoid copepods declined. As such, as of 2005, calanoid copepods were the dominant taxonomic group in the offshore spring zooplankton bloom (Barbiero et al. 2019). Changes in the density and community structure of zooplankton could impact higher trophic levels, especially during the spring when cold temperatures limit overall productivity and availability of prey types. This could particularly affect the growth of first feeding larval fish that utilize zooplankton as their primary food source. Reduced growth of larvae postpones diet shifts and the ability to escape gape limited predators, increasing the baseline high mortality rate of the larval stage. One potential explanation for recent low recruitment of some Great Lakes fish populations is that suboptimal zooplankton availability during the larval stage reduces larval growth, thereby increasing larval predation and starvation risk and ultimately contributing to reduced overall recruitment.

Altered spring zooplankton regimes in Lake Michigan could affect the growth and mortality of native species that hatch in early spring, such as some Coregonine species including lake whitefish and cisco. Since historic lows in the mid 1900's, lake whitefish recruitment in the eastern portion of the northern basin of Lake Michigan remains very low, even in comparison to other areas of the lake (Caroffino and Seider 2020). Coregonids are culturally and economically important to Indigenous tribes of Michigan and Wisconsin, and lake whitefish *Coregonus clupeaformis* support the largest commercial fishery in Lake Michigan (Chiarappa et al. 2005,

Ebener et al. 2008). One possible explanation for persistent low recruitment of coregonids in this area is a lack of sufficient zooplankton. Diet studies of small larval coregonids in the Great Lakes show high consumption of (Claramunt et al. 2010, Hoyle et al. 2011) and selection for (Pothoven et al. 2014, Pothoven 2020) cyclopoid copepods. Cyclopoid copepods on average are smaller and have more complex swimming patterns than calanoid copepods, which can increase capture success and visual detection by larval coregonids (Anneville et al. 2011, Jonsson and Tiselius 1990, Strickler et al. 1975). The recent lack of cyclopoid copepods in the spring zooplankton community could affect larval fish diet and growth.

Reductions in offshore zooplankton during the spring in Lake Michigan over the last two decades has been documented, but zooplankton biomass and community composition in more nearshore areas such as shallow beach environments have yet to be described in any amount of detail, especially in the northern basin. Studies on larval fish diet and prey availability in Lake Michigan have previously focused on species whose larvae emerge in late spring or summer, such as alewife *Alosa pseudoharengus* or yellow perch *Perca flavescens* (Bremigan et al. 2003, Eppenhimer et al. 2019, Withers et al. 2015). The few recent studies that have focused on early spring-hatching larval fish in Lake Michigan compared diets to zooplankton sampled in areas deeper than ten meters (Claramunt et al. 2010), except for one recent study in southern Lake Michigan that assessed zooplankton in the beach environment (Pothoven 2020). However, findings reported by Pothoven (2020) may not represent zooplankton availability of the northeastern beach environment in Lake Michigan, given the spatial variation in zooplankton composition that is inherent in this system (Barbiero et al. 2019, Bunnell et al. 2018).

While little is known about the nearshore zooplankton community in Lake Michigan, this understudied environment is likely critical for coregonine recruitment because larvae emerge and begin feeding in this environment, and because larval densities are particularly high in nearshore beach environments (Lahnsteiner and Wanzenböck 2004, Mckenna and Johnson 2009). In this study, we aim to describe the nearshore (≤ 1 m depth, beach environment) zooplankton community in northeastern Lake Michigan during early spring 2015-2019. Additionally, we describe the diet of larval coregonids preying upon this particular zooplankton community. We hypothesize that larval coregonids will consume and positively select for cyclopoid copepods due to previously documented positive selection of this zooplankton prey (Pothoven et al 2014, Pothoven 2020). However, given declines in offshore cyclopoid abundance during spring in

northern Lake Michigan, we also expect that calanoid copepods will be consumed at high levels as an alternate prey.

2.2 Methods

2.2.1 Field Collections

During 2015-2019, zooplankton and larval fish were sampled by fisheries biologists from the Little Traverse Bay Band of Odawa Indians at four beaches in northeastern Lake Michigan: Big Stone Bay, Elk Rapids, Petoskey State Park, and Bliss Beach, Michigan (Figure 2.1). During March-June of each year, each sampling location was sampled up to five times for water temperature, zooplankton, and larval fish. One exception to this routine was in 2019 when Elk Rapids was not sampled. As such, a total of 86 sampling events were conducted from 2015-2019 (Table 2.1). Surface water temperature was measured using a YSI Professional Plus multiparameter probe. Larval fish were sampled using a 1 x 2 m, 1000 μm mesh neuston net that was pulled by hand parallel to shore in depths ranging from 0.4 -1.0 m. During the sampling years 2015-2018, a single 20 m neuston net tow was conducted during each sampling event. In 2019, sampling protocol changed with the intention of conducting three 20 m neuston net tows during each sampling event. However, if the initial 20 m tow resulted in larval catch preliminarily judged to be low, which occurred at 2 of the sampling events, the subsequent additional 1-2 tows were increased to up to 80 m or 100 m. Additionally, due to varying field conditions during collection, only one neuston tow measuring 30 m or 100 m was conducted at 5 sampling events. In total, 115 neuston net tows were conducted from 2015-2019. Zooplankton were sampled using a 0.3 m diameter, 1.5 m long, 63 μm mesh zooplankton net towed horizontally in the water column along a single 30 m transect during each sampling event. In 2015, 2016, and 2017, horizontal zooplankton tows were conducted with the net located towards the middle of the water column. In contrast, paired surface and bottom zooplankton tows were conducted in 2018 and a sinusoidal zooplankton path through the water column was conducted in 2019. Despite differences in sampling protocol for zooplankton among years, zooplankton distribution is likely uniform within the water column at depths sampled in this study (≤ 1 m). Larval fish and zooplankton were stored in 95% ethanol prior to processing.

2.2.2 Selection of zooplankton and larval fish samples for analysis

Of the 86 sampling events, samples from 43 sampling events were selected for further processing and analysis. Included in these 43 sampling events were at least 1 pair of zooplankton and larval fish samples from each sampling location per year and any additional paired zooplankton and larval fish samples where more than 5 larvae were caught during the sampling event.

2.2.3 Zooplankton Sample Processing

Zooplankton samples from the 43 selected sampling events were processed at the USGS Great Lake Science Center in Ann Arbor, MI using methods similar to Eppeheimer et al (2019). To initiate processing, all zooplankton from a sample were transferred to at least 40 ml of water treated with reverse osmosis. The resulting samples were then transferred to a counting wheel in 1 ml increments and all organisms were enumerated. This procedure was repeated with subsequent 1 ml subsamples until 200 individuals (not including copepod nauplii and dreissenid veligers) were counted. All zooplankton were identified to the genus level, and when possible, some zooplankton were identified to species. The whole sample was processed to count predatory cladocerans and aquatic insects. Some of the samples contained a large amount of debris and less than 10 individuals per 1 mL aliquot. Owing to the excessive amount of time it would have taken to process the samples at that rate (e.g., >16 hours) and uncertainty about the quality of the sample, nine of the 43 zooplankton samples were not processed (Table 2.1). Many of the aborted zooplankton samples were collected from the bottom in 2018; thus we only used surface zooplankton samples in our analysis for that year.

2.2.4 Larval Fish Processing

Immediately after neuston tows, larval samples were picked visually by washing the sample into a white plastic container and preserved in 95% ethanol. For neuston tows that resulted in large catches, a sub sample of 30-100 larvae were picked and preserved, while the remainder of the larvae were enumerated by slowly pouring out the remaining contents of the container and counting larvae as they exited the container. However, most samples were enumerated in a lab after leaving the study site.

Larval fish samples from six of the original selected 43 sampling events were in poor condition (Table 2.1), and thus a total of 753 of the collected coregonid larvae from 37 separate sampling events were processed for lengths, diet, and DNA analysis. When samples contained fewer than 30 larvae, all larvae in the sample were processed, while samples that contained over 30 larvae were subsampled by spreading the sample onto a gridded tray of 16 numbered squares and picking 30 larvae from squares that were selected by a random number generator. Each individual larvae was photographed using a Micrometrics LE camera mounted to a dissecting microscope and the presence or absence of a yolk sac was recorded. After extracting the digestive tract from esophagus to anus, diet items were enumerated, identified, and imaged using a dissecting or compound microscope at 4.5x-10x magnification. Diet items were identified to major taxonomic groups, including cyclopoid and calanoid copepods, harpacticoida, *Daphnia* spp., Chydoridae, Bosminidae, Chironomidae, and other. Cyclopoid copepodite stages were easily separated from cyclopoid adults by the length of the last urosomal segment, the fifth legs of calanoid copepods (which are used to delineate adults from copepodite life stages) were often distorted or missing. Thus, at 4.5x magnification, we identified cyclopoid adults from cyclopoid copepodite life stages, but we did not discriminate between adult and copepodite calanoid copepods. To avoid double counting of partial copepods, we counted heads (cephalosome) and headless items (items with complete metasome and urosome but missing cephalosome), and only included the larger enumerated group (heads or headless items) in total item count. Biomass for each imaged diet item was calculated by measuring each item in ImageJ and applying established length- dry weight regressions for major groups of taxa (Benke et al. 1999, Bottrell 1976, Rosen 1981). For partial copepods in a larval diet, each partial individual was assigned a length equal to the average length of whole copepods in the same larvae's gut. Fifteen larvae contained partial copepods but no whole copepods, and thus these diet items were assigned a length equal to the average length of whole copepods in larvae diets within the same sampling event.

2.2.5 Statistical Analysis

To estimate zooplankton density in the environment, the estimated number of zooplankton in each of the 86 samples were divided by the estimated total volume of water sampled and for each zooplankton sample density was expressed as individuals m^{-3} . Flowmeters were not used

during field collections, and as such total volume of water sampled was estimated using equation 1.

$$\text{Water volume sampled} = \text{net tow length} * \pi * \text{net diameter}^2 \quad \text{Equation 1}$$

Zooplankton density and community composition estimates are comparable among years, despite differing sampling methods, due to the likelihood that zooplankton communities are likely uniform at the depth strata of collection (<1 m). We tested for differences in the zooplankton community composition among sites and among years using ANOSIM. As a non-parametric test that uses a rank dissimilarity matrix to compare dissimilarity within groups to dissimilarity among groups, ANOSIM has been used to assess differences among groups of many taxa, including zooplankton assemblages (Marchant et al. 2000, Duggan et al. 2020, Pothoven and Fahnenstiel 2015). Pairwise R-values from ANOSIM are a measure of separation between groups. R-values range from -1 to +1, where 0 represents indistinguishable similarities within and among groups and +1 indicates that similarities within groups are all less than any similarity between groups. Thus, in this study, ANOSIM was used to compare differences in zooplankton community composition among years or sites to differences in zooplankton community composition within year or site.

To estimate larval coregonid density in the environment, the number of larvae in each sample was divided by the estimated total volume of water sampled. The neuston net used for collection measured 2 m wide and 1 m tall, but sampling occurred in 0.4 – 1 m depths, and as such we estimated total volume of water sampled using equation 2.

$$\text{Water volume sampled} = \text{net tow length} * \text{net width} * \text{water depth} \quad \text{Equation 2}$$

In equation 2, we assume that the bottom of the neuston net was positioned on the lakebed for the entirety of the tow length and that depth. In addition, we assume that depth sampled was consistent for the entirety of the neuston tow. Considering the presence of lakebed gradients and waves in beach nearshore environments, the estimates of larval coregonid density reported in this study are likely underestimates of true densities.

The relationship between the number or biomass of diet items in larval guts and larvae length was assessed using linear regressions after ensuring that this data followed assumptions of homoscedasticity and normality. Previous observations of a positive linear relationship between

fish larvae length and diet biomass have been observed in multiple fish species (Young et al. 1990, Roswell et al. 2014, Roseman et al. 2014). To determine whether the likelihood of an individual larvae having an empty digestive tract was related to larvae length, logistic regression was used due to the binomial status of presence or lack of presence of diet items in larval guts. Since diet composition can vary with larvae length (Claramunt et al. 2010), we calculated the percent biomass of major prey groups (cyclopoid and calanoid copepods, harpacticoida, *Daphnia* spp., Chydoridae, Bosminidae, Chironomidae, and other) in guts of small larvae (8-15 mm) and large larvae (15-24 mm) collected each year and at each sampling location. Additionally, we calculated the percent biomass of major prey groups among all larvae collected throughout the study period 2015-2019 in each mm size class (8-23 mm).

For each larval fish in a subset of samples, individual diet selectivity was calculated for five major prey groups: copepod nauplii, cyclopoid copepod adults, cyclopoid copepodites, calanoid copepods (included copepedite and adult stages), and cladocerans. Using sampling events with concurrent zooplankton and neuston tows, selectivity of each prey type for each individual larvae was calculated using Chesson's index, also known as Manly's alpha, as described by equation 3,

$$\alpha_i = \frac{r_i}{n_i} * \frac{1}{\sum_{i=1}^m \frac{r_i}{n_i}} \quad \text{Equation 3}$$

where r_i is the proportion of prey type i in the larvae gut, n_i is the proportion of prey type i in the environment, and m is the total number of prey types. Manly's alpha ranges 0-1, where $\alpha = 0$ if larvae completely avoids the prey type, and $\alpha = 1$ if larvae has complete preference for one prey type and avoids others. Using the null hypothesis that larvae show no preference to any available prey type, $\alpha = 1/5$ for all prey types, considering five prey types were included in the analysis and the sum of alpha values equals 1. To summarize individual larvae selectivity, we averaged alpha values for each prey type among larvae collected at the same site (all years) and larvae collected within the same year (all sites) and calculated the 95% confidence interval of these means using equation 4.

$$95 \% \text{ C.I.} = 1.96 * \sqrt{\frac{\sum(x-\bar{x})^2}{n-1}} / \sqrt{n} \quad \text{Equation 4}$$

In equation 4, \bar{x} is average alpha value for a prey type, x is the alpha value for each larva used in calculation of the mean, and n is the number of larvae used in the calculation of the mean. If 95% confidence intervals of averaged alpha values from larvae of each site or year for a prey type did not overlap with 0.2, we rejected the null hypothesis, meaning that larvae exhibited preference for or avoidance of that particular prey type. Zooplankton samples without a corresponding neuston tow sample, or vice versa, were not included in diet selectivity analysis, but were included in larvae diet analysis, zooplankton community composition, and zooplankton density. Additionally, 10 of the remaining 31 concurrent zooplankton collections lacked detection of cladocerans. However, cladocerans were detected in low densities in some samples each year and at each study site, and thus we assume that the cladocerans were present at all zooplankton collections, but sampling protocol used was not sufficient to detect cladocerans in 10 of the samples due to rarity of cladocerans in this environment. In order to calculate larvae selectivity for cladocerans at sampling events where cladoceran density was not estimated by the zooplankton net tow, we added the lowest non-zero estimate of cladoceran density recorded during sample collection (0.465 ind/m³) to density estimates of all taxa, using similar methods as Bunnell et al (2012).

2.3 Results

2.3.1 Zooplankton Abundance and Community Composition

Zooplankton density ranged from 17 to 5942 individuals m⁻³ among 34 samples collected between March 29 and June 6 (Figure 2.2). While most sample collections occurred throughout May, peak zooplankton abundance may have occurred prior to the period of most frequent sampling, as indicated by a few collections with relatively higher zooplankton densities April 15 - May 15. Copepod nauplii and adult calanoid copepods were the most abundant zooplankton categories among samples (Figures 2.3 and 2.4). However, even these dominant zooplankton groups varied widely among samples, with nauplii contributing 0 to 99% and calanoid copepods contributing 0 to 67% of the total zooplankton density within a given sample (Figures 2.3 and 2.4). ANOSIM analysis revealed no significant difference in the zooplankton community composition

among years ($R=-0.03084$, $p=0.6409$, but there was a significant difference in the zooplankton community among sites ($R=0.1459$, $p = 0.0164$). In particular, some Petoskey State Park samples had relatively high densities of cyclopoid copepods, while one Petoskey State Park sample in 2018 had relatively high proportion of dreissenid veligers (Figure 2.3).

2.3.2 Coregonid Abundance

Coregonid density ranged from 0 to 91.88 individuals per cubic meter among the 115 neuston net tows collected from 86 sampling events 2015-2019 throughout the collection season (March 29 – June 27, Figure 2.5A). In general, coregonid larval densities were lowest during April and June, and variable throughout May. 20% of larval coregonid density estimates were greater than 1 individual m^{-3} , and 77% of density estimates were greater than 0 individuals m^{-3} . Peak larval density occurred in May during 2015, 2016, 2017 and 2019, and in early June in 2018. Sites with the highest larval density varied 2015-2017, but Bliss Beach and Big Stone Bay exhibited the highest larval densities in 2018 and 2019 (Figure 2.5A). Water temperature during larval fish collections ranged from 3.0 to 17.2 °C (Figure 2.5B). Overall, larval density increased with increasing water temperature, peaking at 8 or 9°C, and then declined with increasing water temperatures higher than 11°C. Peak larval density occurred between 8 and 11°C during 2015, 2017, 2018, and 2019. In 2016, peak larval density occurred at approximately 7.6 °C, the highest temperature recorded during collections that year. The lower temperature at peak larval fish abundance in 2016 most likely occurred due to earlier larval collections that were conducted from the last week of March to the first week of May (Figure 2.5B).

2.3.3 Coregonid Size Structure

Larval lengths ranged from 8.9 to 23.4 mm, with 90% of larvae measuring between 11.8 and 18.8 mm (Figure 2.6A). Yolk sac larvae, which represented 16% of total catch, ranged from 10.7 to 18.4 mm in total length, averaging 13.8 mm. The lengths of larvae that had totally absorbed the yolk sac ranged from 8.9 to 23.4 mm, averaging 15.2 mm (Figure 2.6A). 32% of yolk sac larvae had empty stomachs, while only 9% of non-yolk sac larvae had empty stomachs.

2.3.4 Coregonid Diet

The number and biomass of diet items in larval stomachs increased with larval length ($p < 0.001$, $R^2 = 0.237$, $df = 751$, $y = 3.07x - 34.17$, Figure 2.6B, 2.6D). Common diet items included calanoid copepods, cyclopoid copepods, and chironomids (Figure 2.7). Small and large cladocerans, respectively, represented less than 1.5 % of diet biomass in either size class (8-15 mm or 15-24 mm) when grouped by year or site. The percent biomass of chironomids was higher in diets of large larvae than small larvae, increasing by 2.5%-40% in the larger size class, depending on the collection site (Figure 2.8B). Calanoid copepods consistently contributed to diets of small and large larvae within each year and site, typically comprising >30% of diet biomass, except for large larvae groups in Big Stone Bay and 2016, when larvae consumption was dominated by chironomid biomass. Large larvae consumed relatively more calanoid copepod biomass 2017-2019 than small larvae, but the opposite was seen in 2015 and 2016 (Figure 2.8A). Percent biomass of cyclopoid copepods in larval stomachs was similar for small and large larvae, differing by less than 5% between size groups each year. However, the proportion of cyclopoids in larval coregonid diets varied among years and sites, ranging from approximately 4% to 37% of diet biomass among years and 8% to 45% of diet biomass among sites (Figure 2.8). Larval fish collected at Petoskey State Park consumed the most cyclopoid diet biomass, especially in 2017 (Figure 2.8B).

2.3.5 Diet Selectivity

Larval coregonids consistently selected for calanoid copepods and adult cyclopoid copepods. In 2015, calanoid copepods had the highest mean diet selectivity, while larvae collected the remaining four years had highest mean selectivity for adult cyclopoid copepods (Figure 2.9). Larvae exhibited negative selectivity for the three remaining prey types (copepod nauplii, cladocerans, and cyclopoid copepodites, Figure 2.9).

2.4 Discussion

In the present study, larval coregonid densities ranged from 0 – 91.8 larvae m^{-3} , with estimated densities often exceeding 1 larvae m^{-3} during May. Larval abundance varied during the present study period, but 20% of neuston tows estimated abundances higher than previously reported densities in the Great Lakes, which typically value <1 larvae/ m^3 (Hoyle et al. 2011, Lucke

et al. 2021, Pothoven et al. 2020). Peak larvae abundances consistently occurred as water temperatures reached between 8-11 °C each year 2015-2019. Water temperature during peak larval densities of this study are similar to other studies conducted in the Great Lakes. For example, in an eight year study in the Bay of Quinte, Lake Ontario, peak larval abundance occurred between 7 and 11 °C, and during 2018 in the Apostle Islands, peak larval density occurred around 9 °C (Hoyle et al. 2011, Lucke et al. 2020).

Throughout the sample period, zooplankton abundance in the nearshore beach environment varied widely. Despite large variations in abundance, copepod nauplii and calanoid copepods consistently contributed the most to zooplankton community composition, while cyclopoid copepods did not occur in large abundances in zooplankton samples. The contributions of cladocerans to the zooplankton community were minimal in comparison to copepods. As such, the community composition of the nearshore beach environment in this study area likely reflects recent spring offshore community composition in the northern basin of Lake Michigan (Barbiero et al. 2019).

While the zooplankton community of beach environments sampled in northern Lake Michigan reflect offshore trends, these patterns may not be consistent throughout the lake. For example, a four year study (2014-2017) of beach zooplankton samples in the southern basin of Lake Michigan showed that the zooplankton community in this portion of the lake was mainly composed of cyclopoid copepods, small cladocerans, and copepod nauplii (Pothoven 2020), whereas the offshore spring zooplankton in the southern basin is primarily dominated by calanoid copepods (Barbiero et al. 2019, Pothoven and Fahnenstiel 2014). Thus, the contrast between shallow beach zooplankton and offshore zooplankton communities in the southern basin of Lake Michigan may not be present in the northern basin. Considering the potential for beach environment zooplankton to vary throughout Lake Michigan as showcased by this study and Pothoven (2020), more beach environments throughout the lake should be surveyed for spring zooplankton community composition in order to determine how zooplankton prey availability for larval coregonids varies throughout Lake Michigan.

Although prey availability, measured as zooplankton density, was variable among sampling events, few small coregonid larvae (< 24 mm) had an empty gut tract. Larval coregonids 8-23 mm mainly consumed calanoid copepods, cyclopoid copepods, and chironomids. We hypothesized that larvae would mainly consume cyclopoid copepods due to previous studies of

coregonid larvae diets, but larvae often consumed more calanoid copepod biomass than cyclopoid copepod biomass. Nonetheless, coregonid larvae still positively selected for cyclopoid copepods despite low abundances of this prey type in the environment. Larval coregonids may have higher capture success rates when targeting cyclopoids than calanoids, probably due to different swimming behaviors of the two taxa (Anneville et al. 2011). As such, there could be foraging and energetic consequences to increased calanoid consumption over cyclopoid consumption. On the other hand, incorporation of calanoid copepods into diets, even in small larvae, may not affect condition or survival since coregonids evolved in oligotrophic systems. In oligotrophic systems, calanoid copepods normally dominate, and thus a coregonid larvae may be more adapted to a diet similar to one before anthropogenic alterations to the Great Lakes. Future research into the energetic demand of capture, energetic assimilation, and nutritional benefits of different types of copepods could inform potential effects of differing diet compositions.

While several observed diet patterns were consistent with past studies, there were notable differences between the diets of small coregonid larvae in this study and diets of coregonids located in other areas of the Great Lakes. Low frequency of larvae with empty stomachs is a common observation in larval coregonid diet studies, especially for larvae longer than 11 mm (present study, Lucke et al. 2020, Pothoven 2020). This study, and previous diet studies in Bay of Quinte, Lake Ontario, Saginaw Bay, Lake Huron, and southern Lake Michigan observe a lack of copepod nauplii in diets despite high availability in the environment (Hoyle et al. 2011, Pothoven et al. 2014, Pothoven 2020). However, larval coregonids measuring less than < 24 mm in the Apostle Islands, Lake Superior, readily consumed nauplii (Lucke et al. 2020). Calanoid copepods, previously observed in low abundances in larvae (< 25 mm) diets (Hoyle et al. 2011, Pothoven et al. 2014, Pothoven 2020), were a major component of larval diet biomass in this study. The incorporation of calanoid copepods to the diets of larvae examined in this study could be due to limited availability of other prey types, such as cyclopoid copepods and cladocerans, in the nearshore environment. For example, consumption of cyclopoid copepod biomass was highest at Petoskey State Park collection site, which coincidentally was the site with highest mean cyclopoid abundance in the environment. From this study and others, it appears young coregonid larvae in the Great Lakes primarily consume calanoid and cyclopoid copepods, generally consuming more of the copepod type that is readily available in the environment.

Climate change, especially changes in spring warming rates, could impact the egg stage duration and foraging efficiency of larval coregonids in Lake Michigan. Incidences of empty stomachs in coregonids are often reported at a lower rate than in other species of larval fish in the Great Lakes (Withers et al 2015). High feeding efficiency of coregonid larvae relative to other species is partially due to an extended egg stage duration that contributes to larvae with increased gape size, swimming ability, and visual acuity. However, the relatively long egg stage duration of coregonids could be shortened with climate change. The effect of spring warming on hatch timing may be more important than the effect of spawn timing on hatch timing for coregonids considering their egg stage duration lasts multiple months. Additionally, temperature can signal spawning of adult coregonids (Wahl and Loffler 2009, Hartmann 1984), such that warmer temperatures farther into the fall season could delay spawning. As such, the combination of delayed cooling in the fall signaling delayed spawning in coregonids and rapid warming rates in the spring signaling earlier hatch could shorten egg incubation, shorten larvae size at hatch, and ultimately, limit feeding efficiency of larvae (Colby and Brooke 1970).

This study documented consistent consumption and positive selectivity for both calanoid and cyclopoid copepods in coregonid larvae less than 24 mm. The dominant zooplankton available for consumption in the nearshore beach environment of the study area seem to be copepod nauplii and calanoid copepods. When considering this study in the context of other studies focused on coregonids, it appears that nearshore spring zooplankton and small larval coregonid diets vary in different areas of Lake Michigan. Despite low instances of empty stomachs documented in this study and others, this differing diet composition of larvae could alter foraging behavior, growth, and even potentially recruitment of coregonids.

2.5 Tables and Figures

Table 2. 1 Number of sampling events used in four major sections of results (larval abundance, zooplankton abundance, diet composition, and diet selectivity) for each year 2015-2019.

	Larval Abundance	Zooplankton Abundance and Community Composition	Diet Composition	Diet Selectivity
Total 2015-2019	86	34	37	31
2015	19	6	6	3
2016	17	6	6	3
2017	11	5	5	4
2018	18	11	10	6
2019	21	6	10	5

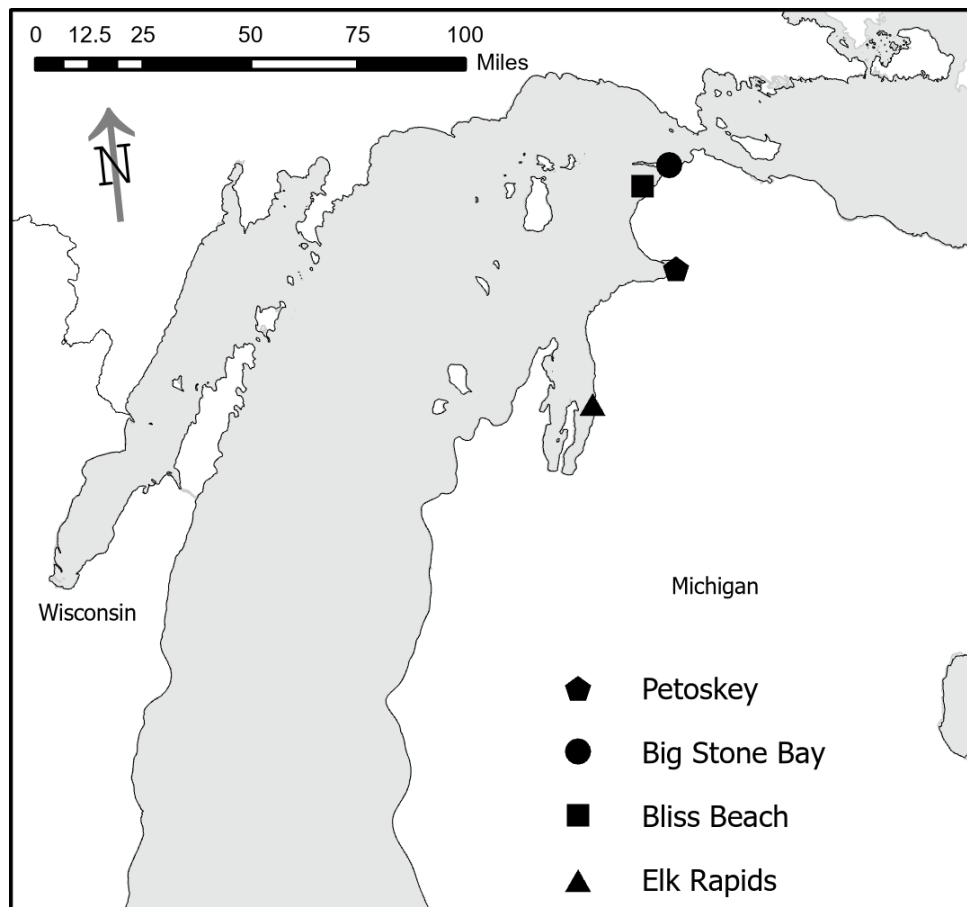


Figure 2. 1. Map of Lake Michigan with locations of four study sites: Petoskey State Park, Big Stone Bay, Bliss Beach, and Elk Rapids.

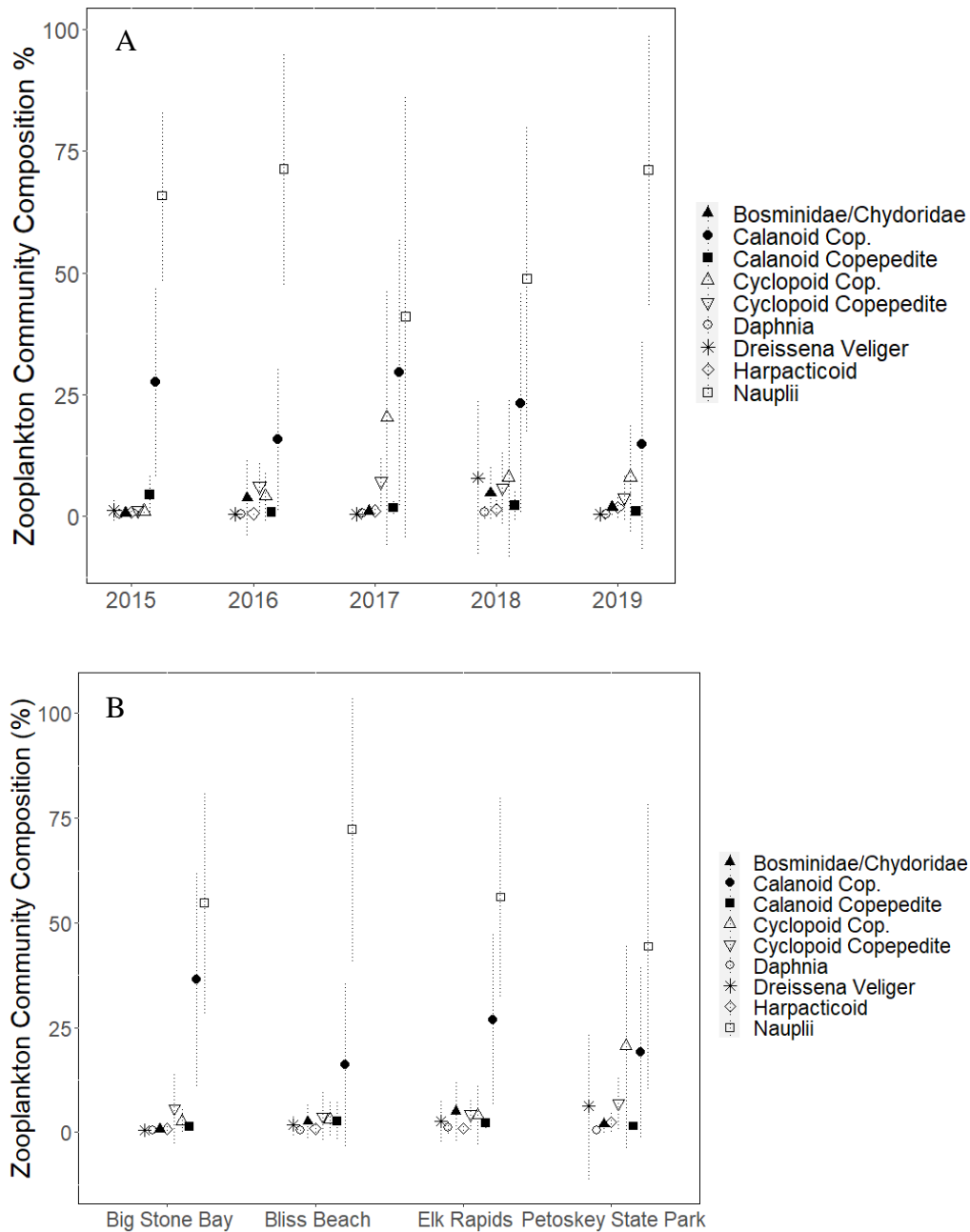


Figure 2. 3 Scatterplot of mean percent abundance of each major zooplankton group (small cladocerans, adult calanoid copepods, calanoid copepodites, adult cyclopoid copepods, cyclopoid copepodites, daphnia species, dreissenid veligers, harpacticoids, and copepod nauplii) each sampling year (A) and collection site (B) in zooplankton samples collected in northern Lake Michigan. Standard deviation of each mean is represented by dotted lines. Nauplii and calanoid copepods had high percent zooplankton community composition, whether samples were grouped by year (top) or year (bottom). In some samples from Petoskey State Park and the 2017 collection year had relatively high cyclopoid percent zooplankton community composition.

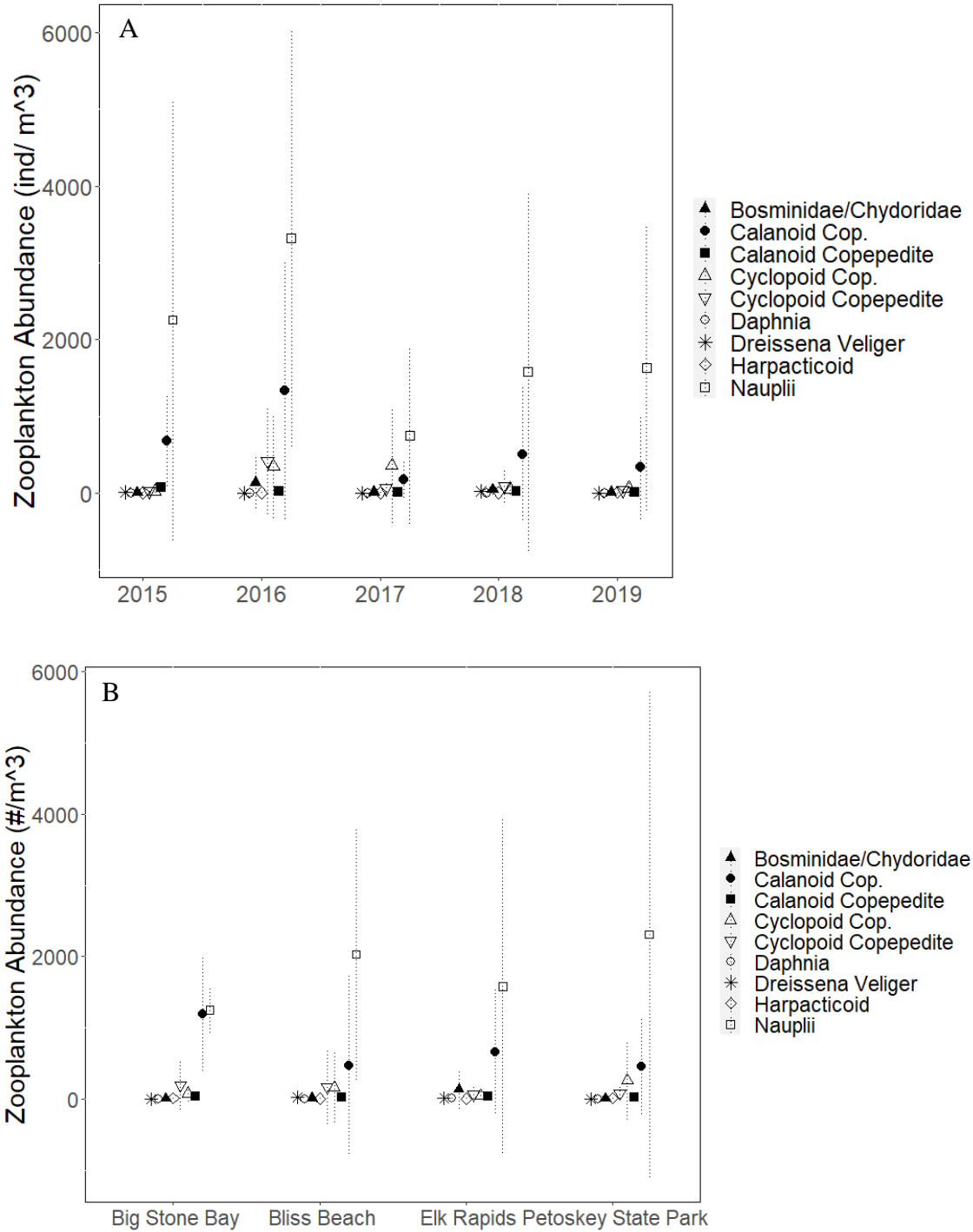


Figure 2. 4 Scatterplot of density (number of zooplankton per cubic meter) of nine major zooplankton groups (small cladocerans, adult calanoid copepods, calanoid copepodites, adult cyclopoid copepods, cyclopoid copepodites, daphnia species, dreissenid veligers, harpacticoids, and copepod nauplii) each sampling year (A) and collection site (B). Standard deviation of each mean is represented by dotted lines. Nauplii and calanoid copepods were the most abundant prey types, whether samples were grouped by year (top) or site (bottom).

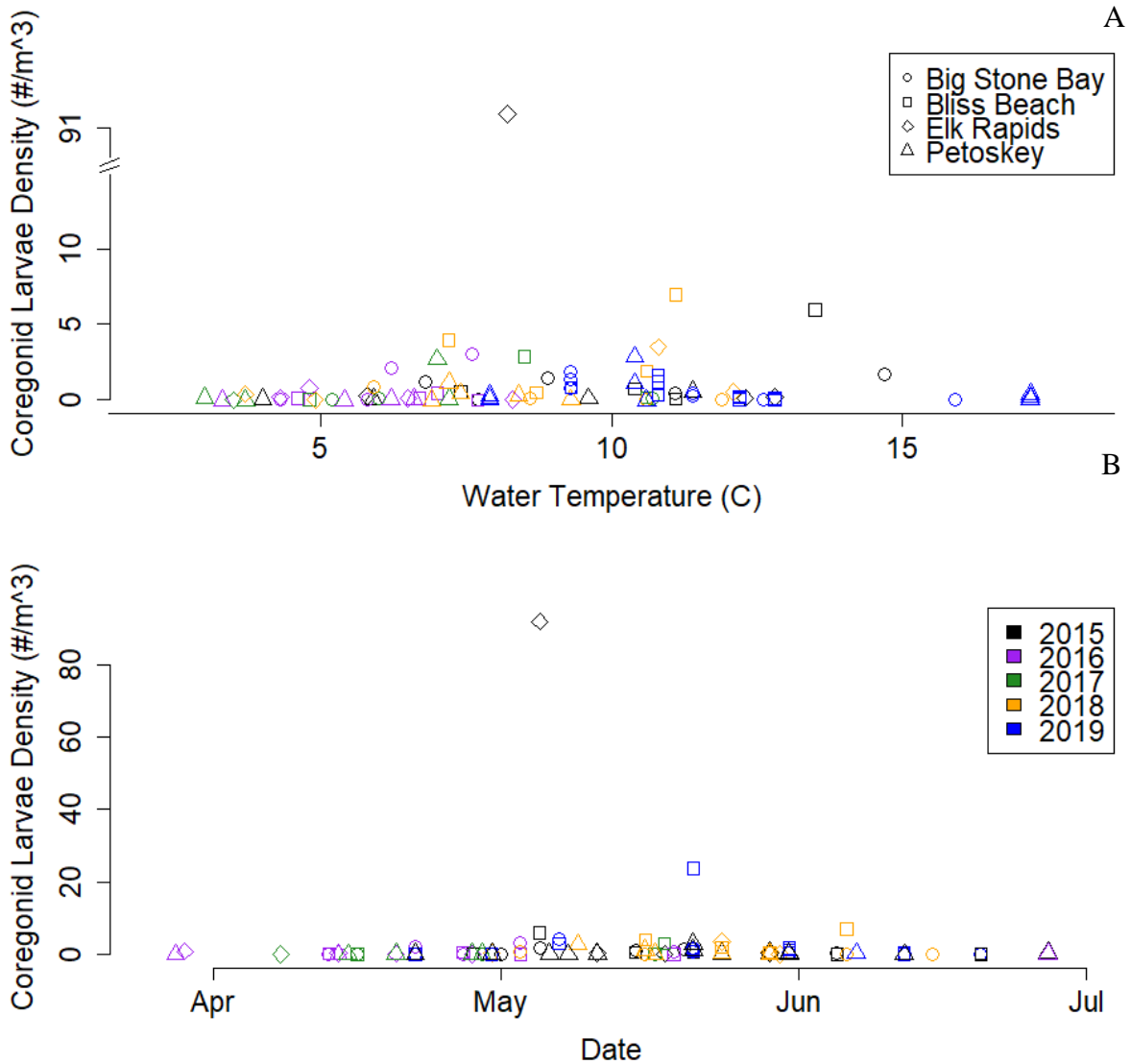


Figure 2. 5 Scatterplots of coregonid larvae density of each neuston net tow in northern lake Michigan 2015-2019 (number of larvae m^{-3}) in reference to water temperature at time of collection (A), and collection date (B). Water temperature was unavailable for 26 of the 115 neuston net tows collected 2015-2019 due to uncalibrated sampling instruments. Collection dates ranged from the last week of March to the last week of June. Larvae density ranged from 0 to 91.8 larvae m^{-3} , with highest coregonid larvae density during May and when water temperatures were between 7-11°C.

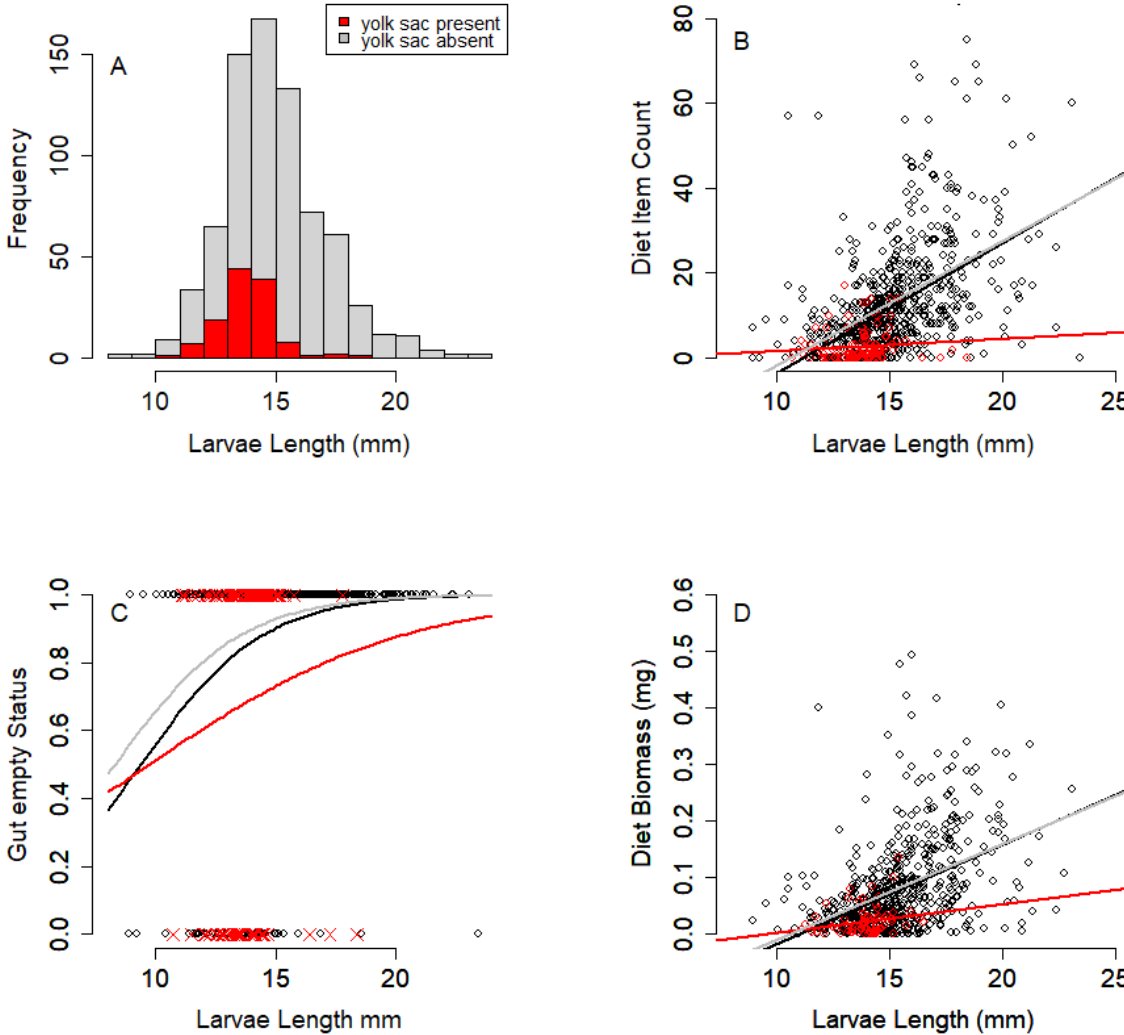


Figure 2. 6 Histogram of coregonid larva length from all neuston sample 2015-2019 with and without a yolk-sac (A). Scatterplot of number of diet items vs. larva length with associated linear regressions for yolk-sac larvae ($y = 0.28x - 1.12$, $R^2 = < 0.001$, $p = 0.31$), non yolk sac larvae ($y = 2.93x - 31.04$, $R^2 = 0.21$, $p = < 0.001$), and all larvae ($y = 3.07x - 34.17$, $R^2 = 0.24$, $p = < 0.001$) (B). Scatterplot of gut empty status (0=empty gut, 1=gut with at least 1 diet item) vs. larva length with predicted logistic regression (C). Scatterplot of biomass of items in gut (mg) vs. larva length (mm) and associated linear regressions for yolk-sac larvae ($y = 0.01x - 0.05$, $R^2 = 0.03$, $p = 0.06$), non yolk sac larvae ($y = 0.02x - 0.18$, $R^2 = 0.19$, $p = < 0.001$), and all larvae ($y = 0.02x - 0.19$, $R^2 = 0.21$, $p = < 0.001$) (D). Yolk-sac larvae regressions are indicated in red, larvae without a yolk sac regression are indicated by gray, and all larvae regressions are indicated by black throughout the plot panels.

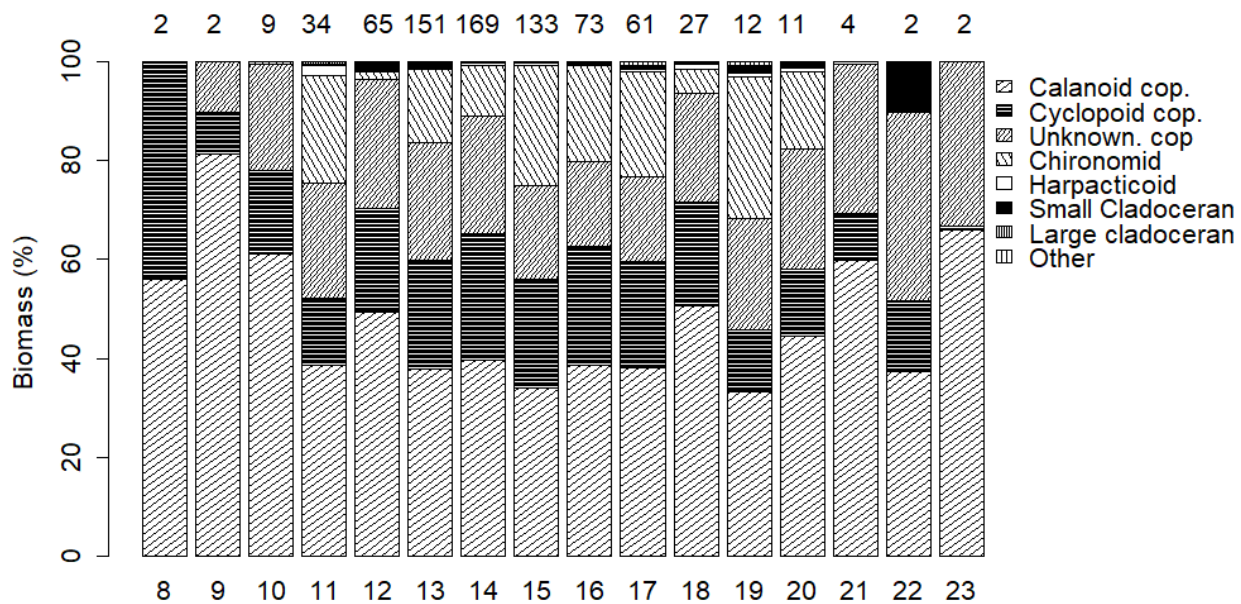


Figure 2. 7 Barplot of coregonid diet composition (% biomass) for all larvae collected 2015-2019 in northern Lake Michigan by larvae length (grouped by mm, 8-23 mm). Diet item groups include calanoid copepods, cyclopoid copepods, unknown copepods (could not be identified as calanoid or cyclopoid), chironomids, harpacticoids, small cladocerans, large cladocerans, and other prey items. Common diet items by number and biomass include, calanoid copepods, cyclopoid copepods, and chironomids, while cladocerans were rarely found in diets and no copepod nauplii were found in diets. Numbers placed above each bar denote the number of larvae in the size bin.

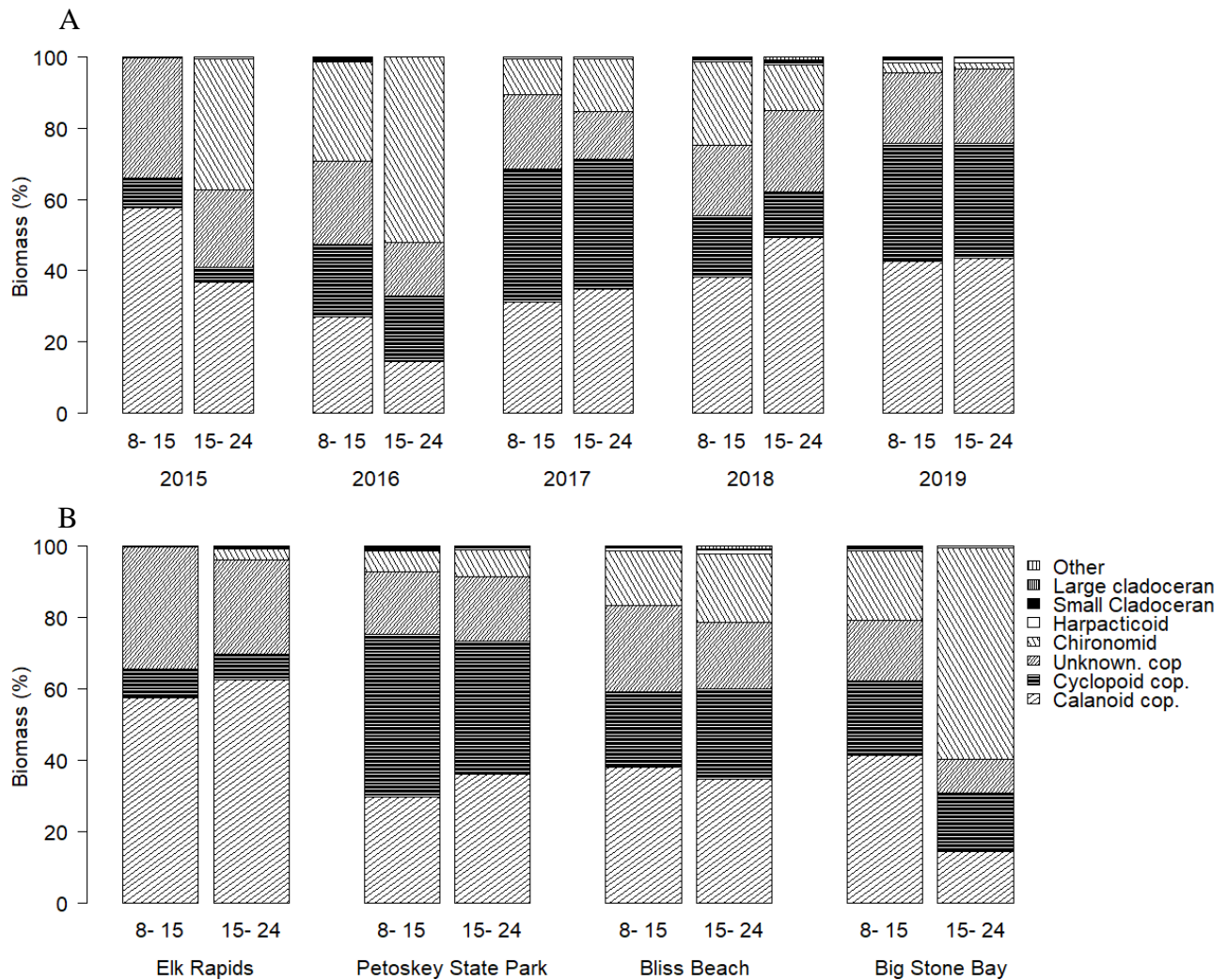


Figure 2. 8 Barplot of coregonid diet composition (%) in biomass for small (8-15 mm) and large (15-24) larvae each sampling year (A) and collection site (B). Diet item groups include calanoid copepods, cyclopoid copepods, unknown copepods (could not be identified as calanoid or cyclopoid), chironomids, harpacticoids, small cladocerans, large cladocerans, and other prey items. Common diet items by number and biomass include, calanoid copepods, cyclopoid copepods, and chironomids, while cladocerans were rarely found in diets and no copepod nauplii were found in diets.

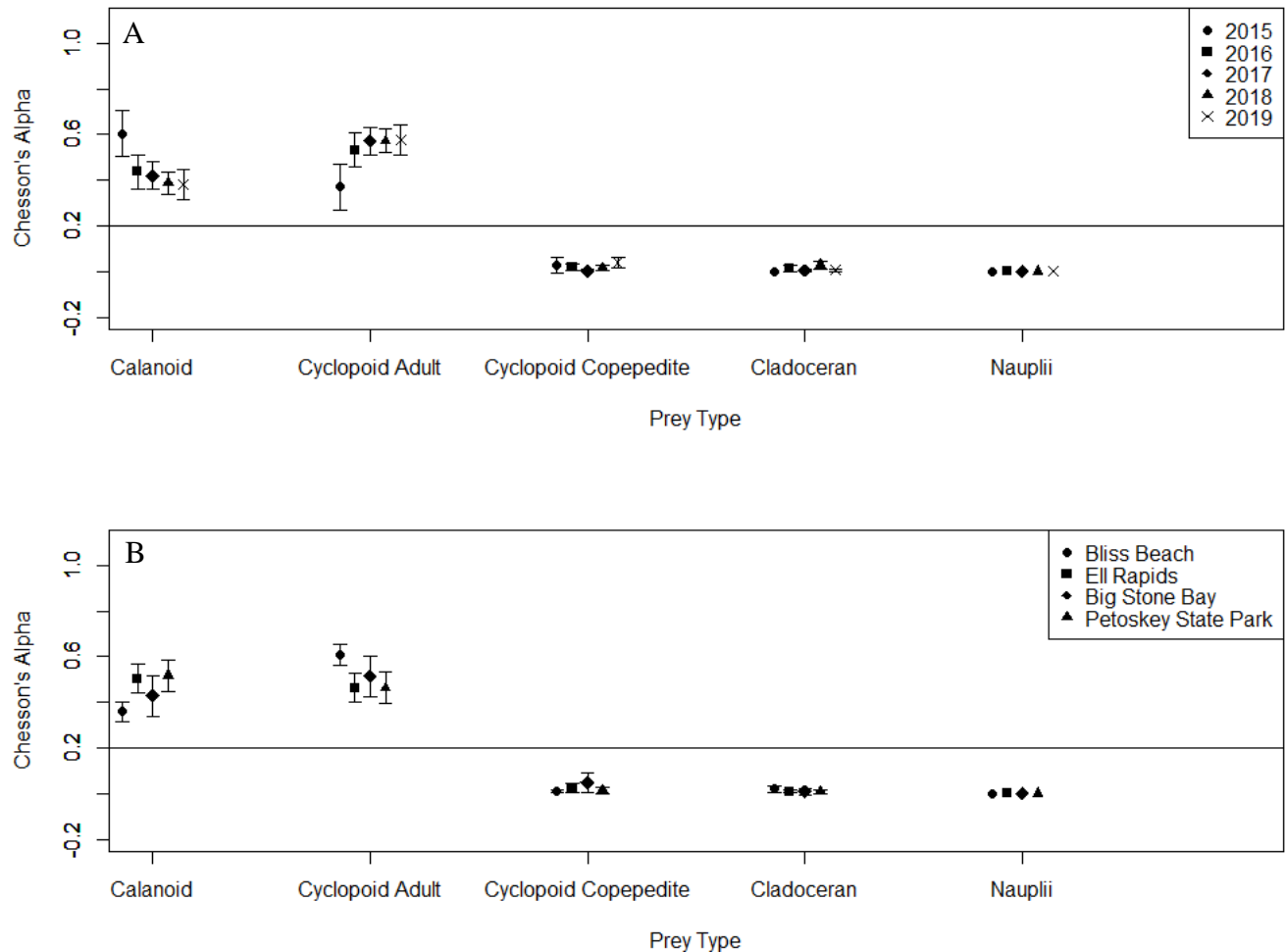


Figure 2. 9 Mean Chesson's index of larvae for five prey types within each sampling year (A) and site (B). 95% confidence interval for each mean is represented by solid black lines. The five prey groups used in calculating Chesson's index include calanoid copepods (adult and copepodid), cyclopoid adult copepods, cyclopoid copepodites, cladocerans, and copepod nauplii. The horizontal line represents 1 divided by the number of prey types in zooplankton samples. Chesson's index values above the horizontal line are prey groups that larvae positively select for, values near the line are prey groups that larvae neutrally select for, and values below the line are prey groups that larvae negatively select for. Each year, larvae positively selected for calanoid copepods and adult cyclopoid copepods, but negatively selected for cyclopoid copepodites, cladocerans, and copepod nauplii.

2.6 References

- Anneville, O., Berthon, V., Glippa, O., Mahjoub, M.S., Molinero, J.C. and Souissi, S., 2011. Ontogenetic dietary changes of whitefish larvae: insights from field and experimental observations. *Environmental biology of fishes*, 91(1), pp.27-38.
- Barbiero, R.P., Rudstam, L.G., Watkins, J.M. and Lesht, B.M., 2019. A cross-lake comparison of crustacean zooplankton communities in the Laurentian Great Lakes, 1997–2016. *Journal of Great Lakes Research*, 45(3), pp.672-690.
- Benke, A.C., Huryn, A.D., Smock, L.A. and Wallace, J.B., 1999. Length-mass relationships for freshwater macroinvertebrates in North America with particular reference to the southeastern United States. *Journal of the North American Benthological Society*, 18(3), pp.308-343.
- Bootsma, M.L., Gruenthal, K.M., McKinney, G.J., Simmons, L., Miller, L., Sass, G.G. and Larson, W.A., 2020. A GT-seq panel for walleye (*Sander vitreus*) provides important insights for efficient development and implementation of amplicon panels in non-model organisms. *Molecular Ecology Resources*, 20(6), pp.1706-1722.
- Bottrell, H.C. and HH, B., 1976. A review of some problems in zooplankton production studies.
- Bremigan, M.T., Dettmers, J.M. and Mahan, A.L., 2003. Zooplankton selectivity by larval yellow perch in Green Bay, Lake Michigan. *Journal of Great Lakes Research*, 29(3), pp.501-510.
- Bunnell, D.B., Eshenroder, R.L., Krause, A.E. and Adams, J.V., 2012. Depth segregation of deepwater ciscoes (*Coregonus* spp.) in Lake Michigan during 1930–1932 and range expansion of *Coregonus hoyi* into deeper waters after the 1990s. *Advances in Limnology*, 63, pp.3-24.
- Bunnell, D.B., Carrick, H.J., Madenjian, C.P., Rutherford, E.S., Vanderploeg, H.A., Barbiero, R.P., Hinchey-Malloy, E., Pothoven, S.A., Riseng, C.M., Claramunt, R.M. and Bootsma, H.A., 2018. *Are changes in lower trophic levels limiting prey-fish biomass and production in Lake Michigan?* (No. 2018-01). Great Lakes Fishery Commission.
- Caroffino, D.C. and Seider, M.J. 2020. Status of Lake Whitefish populations in Caroffino, D.C. and Seider, M.J., eds. Technical Fisheries Committee Administrative Report 2020: Status of Lake Trout and Lake Whitefish Populations in the 1836 Treaty-Ceded Waters of Lakes Superior, Huron and Michigan, with Recommended Yield and Effort Levels for 2020. <https://www.michigan.gov/greatlakesconsentdecree>
- Campbell, N.R., Harmon, S.A. and Narum, S.R., 2015. Genotyping-in-Thousands by sequencing (GT-seq): A cost effective SNP genotyping method based on custom amplicon sequencing. *Molecular ecology resources*, 15(4), pp.855-867.

- Chiarappa, M.J., 2005. Overseeing the family of whitefishes: The priorities and debates of coregonid management on America's Great Lakes, 1870-2000. *Environment and History*, pp.163-194.
- Claramunt, R.M., Muir, A.M., Johnson, J. and Sutton, T.M., 2010. Spatio-temporal trends in the food habits of age-0 lake whitefish. *Journal of Great Lakes Research*, 36, pp.66-72.
- Duggan, I.C., Pearson, A.A. and Kusabs, I.A., 2020. Effects of a native New Zealand freshwater mussel on zooplankton assemblages, including non-native *Daphnia*: a mesocosm experiment. *Marine and Freshwater Research*, 72(5), pp.709-717.
- Ebener, M.P., Kinnunen, R.E., Schneeberger, P.J., Mohr, L.C., Hoyle, J.A. and Peeters, P., 2008. Management of commercial fisheries for lake whitefish in the Laurentian Great Lakes of North America. *International governance of fisheries ecosystems: learning from the past, finding solutions for the future*. American Fisheries Society, Bethesda, Maryland, pp.99-143.
- Eppehimer, D.E., Bunnell, D.B., Armenio, P.M., Warner, D.M., Eaton, L.A., Wells, D.J. and Rutherford, E.S., 2019. Densities, diets, and growth rates of larval alewife and bloater in a changing Lake Michigan ecosystem. *Transactions of the American Fisheries Society*, 148(4), pp.755-770.
- Eshenroder, R.L., Vecsei, P., Gorman, O.T., Yule, D., Pratt, T.C., Mandrak, N.E., Bunnell, D.B. and Muir, A.M., 2016. *Ciscoes (Coregonus, subgenus Leucichthys) of the Laurentian Great Lakes and Lake Nipigon*. Great Lakes Fishery Commission.
- Fahnenstiel, G., Pothoven, S., Vanderploeg, H., Klarer, D., Nalepa, T. and Scavia, D., 2010. Recent changes in primary production and phytoplankton in the offshore region of southeastern Lake Michigan. *Journal of Great Lakes Research*, 36, pp.20-29.
- Hartmann, J., 1984. 11-year cycle of spawning time and growth of the whitefish (*Coregonus lavaretus*) of Lake Constance. *Schweizerische Zeitschrift für Hydrologie*, 46(1), pp.163-170.
- Hoyle, J.A., Johannsson, O.E. and Bowen, K.L., 2011. Larval lake whitefish abundance, diet and growth and their zooplankton prey abundance during a period of ecosystem change on the Bay of Quinte, Lake Ontario. *Aquatic Ecosystem Health & Management*, 14(1), pp.66-74.
- Kerfoot, W.C., Yousef, F., Green, S.A., Budd, J.W., Schwab, D.J. and Vanderploeg, H.A., 2010. Approaching storm: disappearing winter bloom in Lake Michigan. *Journal of Great Lakes Research*, 36, pp.30-41.
- Kristineberg Marine Biological Station, S. and Sweden, F., 1990. Foraging behaviour of six calanoid copepods: observations and hydrodynamic analysis. *Marine ecology progress series*, 66, pp.23-33.

- Lahnsteiner, B. and Wanzenböck, J., 2004, January. Variability in the spatio-temporal distribution of larval European whitefish (*Coregonus lavaretus* (L.)) in two Austrian lakes. In *Annales Zoologici Fennici* (pp. 75-83). Finnish Zoological and Botanical Publishing Board.
- Lucke, V.S., Stewart, T.R., Vinson, M.R., Glase, J.D. and Stockwell, J.D., 2020. Larval *Coregonus* spp. diets and zooplankton community patterns in the Apostle Islands, Lake Superior. *Journal of Great Lakes Research*, 46(5), pp.1391-1401.
- McKenna Jr, J.E. and Johnson, J.H., 2009. Spatial and temporal variation in distribution of larval lake whitefish in eastern Lake Ontario: signs of recovery?. *Journal of Great Lakes Research*, 35(1), pp.94-100.
- Marchant, R., Wells, F. and Newall, P., 2000. Assessment of an ecoregion approach for classifying macroinvertebrate assemblages from streams in Victoria, Australia. *Journal of the North American Benthological Society*, 19(3), pp.497-500.
- Mida, J.L., Scavia, D., Fahnenstiel, G.L., Pothoven, S.A., Vanderploeg, H.A. and Dolan, D.M., 2010. Long-term and recent changes in southern Lake Michigan water quality with implications for present trophic status. *Journal of Great Lakes Research*, 36, pp.42-49.
- Pothoven, S.A. and Fahnenstiel, G.L., 2015. Spatial and temporal trends in zooplankton assemblages along a nearshore to offshore transect in southeastern Lake Michigan from 2007 to 2012. *Journal of Great Lakes Research*, 41, pp.95-103.
- Pothoven, S.A., 2020. The influence of ontogeny and prey abundance on feeding ecology of age-0 Lake Whitefish (*Coregonus clupeaformis*) in southeastern Lake Michigan. *Ecology of Freshwater Fish*, 29(1), pp.103-111.
- Pothoven, S.A., Höök, T.O. and Roswell, C.R., 2014. Feeding ecology of age-0 lake whitefish in Saginaw Bay, Lake Huron. *Journal of Great Lakes Research*, 40, pp.148-155.
- Roseman, E.F., 2014. Diet and habitat use by age-0 deepwater sculpins in northern Lake Huron, Michigan and the Detroit River. *Journal of Great Lakes Research*, 40, pp.110-117.
- Rosen, R.A., 1981. Length-dry weight relationships of some freshwater zooplanktona. *Journal of Freshwater Ecology*, 1(2), pp.225-229.
- Strickler, J.R., 1975. Swimming of planktonic Cyclops species (Copepoda, Crustacea): pattern, movements and their control. In *Swimming and flying in nature* (pp. 599-613). Springer, Boston, MA.
- Jonsson, P.R. and Tiselius, P., 1990. Feeding behaviour, prey detection and capture efficiency of the copepod *Acartia tonsa* feeding on planktonic ciliates. *Marine Ecology Progress Series*, pp.35-44.
- Wahl, B. and Löffler, H., 2009. Influences on the natural reproduction of whitefish (*Coregonus lavaretus*) in Lake Constance. *Canadian Journal of Fisheries and Aquatic Sciences*, 66(4), pp.547-556.

- Withers, J.L., Sesterhenn, T.M., Foley, C.J., Troy, C.D. and Höök, T.O., 2015. Diets and growth potential of early stage larval yellow perch and alewife in a nearshore region of southeastern Lake Michigan. *Journal of Great Lakes Research*, 41, pp.197-209.
- Young, J.W. and Davis, T.L., 1990. Feeding ecology of larvae of southern bluefin, albacore and skipjack tunas (Pisces: Scombridae) in the eastern Indian Ocean. *Marine Ecology Progress Series*, pp.17-29.

CHAPTER 3. LARVAL FISH HABITAT QUALITY OBTAINED USING HIGH-FREQUENCY SENSOR DATA AND GROWTH RATE POTENTIAL MODELLING

3.1 Introduction

Oligotrophication in the Laurentian Great Lakes of North America has dramatically altered food web processes in recent decades. In lakes Michigan and Huron, the introduction of invasive *Dreissena* mussel species and their subsequent spread has resulted in a host of rapid changes, including reduced spring phytoplankton biomass, surface chlorophyll-a, and diatom biomass (Evans et al., 2011, Fahnenstiel et al., 2010, Stadig et al., 2020). These symptoms of oligotrophication have corresponded with changes in zooplankton biomass and community composition. For example, offshore zooplankton biomass during the period of 2004-2016 declined 66 and 29% from levels measured in 1997- 2003 in the northern and southern basins of Lake Huron, respectively, while in Lake Michigan offshore zooplankton biomass between these two time periods declined 37 and 35% in the northern and southern basins (Barbiero et al., 2019). In addition, the community composition of zooplankton has shifted, with higher relative abundance of calanoid copepods and decreasing proportions of cyclopoid copepods and cladocerans since the late 1990's in both of these lakes (Barbiero et al., 2019). Reduced zooplankton availability can influence organisms farther up the food web. For example, insufficient zooplankton prey can negatively affect the performance of larval fish by limiting foraging success, growth, survival, and ultimately affect fish population sizes. Fish larvae are likely to experience altered offshore habitats when prevailing wind patterns produce lake currents that advect larvae offshore or along the coastline (Beletsky et al., 2007). Incidentally, prey fish biomass has decreased in Lakes Michigan and Huron (GLFC USGS report, Gorman 2019), which may be related to reduced prey fish population abundances and/or growth. Assessing habitat quality during the larval stage in these lakes can help determine if insufficient offshore habitat quality could be a contributing factor to declines in fish populations in the Great Lakes.

Spatial variation in ambient environmental conditions in Lakes Michigan and Huron will ultimately influence the spatial distribution of habitat quality for larval fish. Increased water clarity caused by dreissenid mussel water filtration could impact larval fish foraging efficiency and predator avoidance (Bunnell et al., 2021). Recent declines in zooplankton, which are especially

pronounced in offshore habitats, could increase larvae mortality rates either directly through starvation, or indirectly through increased likelihood of experiencing size-selective predation due to slow growth (Miller et al 1988). These aforementioned environmental factors interact with lake thermal regimes such spring warming rates and the seasonal progression of thermal stratification to influence larval growth through the effect of temperature on metabolic rate, consumption, and activity rate of individual larvae. Considering the various habitats larvae are expected to encounter and the multiple environmental factors interacting to influence their growth and survival, using just one environmental factor (i.e. zooplankton density or temperature or light availability) as an index of larval fish habitat may be insufficient. Growth rate potential (GRP) models that are based on foraging and bioenergetic models have been used as an index of habitat quality in many systems and for many species due to their incorporation of various environmental factors into a single index (Brandt et al., 2011, Höök et al., 2004, Nislow et al., 2000).

Recent ecosystem change in lakes Michigan and Huron necessitate a re-evaluation of the spatial distribution of habitat quality for larval fish habitat in these lakes that incorporates multiple environmental variables. The use of high frequency sensors can provide information at a much finer spatial grain within the water column than typical sampling methods. For example, typical sampling of physiochemical characteristics with a water quality meter (such as a YSI) would be extremely time consuming if used to obtain fine scale measurements across of broad vertical or horizontal plane of the water column. Additionally, traditional whole water column zooplankton net tows cannot detect changes in zooplankton abundance within the depth strata of a single tow, but laser optical plankton counters (LOPC) can estimate finely spatially resolved zooplankton abundance by counting particles along a towed path (Watkins et al., 2017, Yurista et al., 2009). While offshore zooplankton biomass has declined lakewide, zooplankton availability within the water column has been observed to vary with depth, temperature, and distance from shore (Bordeau et al., 2015, Nowicki et al., 2017, Pothoven and Fahnenstiel 2015, Scofield et al., 2020, Watkins et al., 2017), and thus fine scale measurements from an LOPC are useful to quantify spatial patterns in zooplankton abundance. In recent years, multiple sensors have been attached to towed undulating vehicles (TUV) to collect simultaneous measurements of water quality (Watkins et al., 2017, Xu et al., 2017, Yurista et al., 2009) while towed in a sinusoidal motion through the water column. Using fine scale TUV measurements of ambient environmental conditions as inputs to growth rate potential models, it is possible incorporate multiple environmental factors into an

assessment of habitat quality for larval fish across broad spatial areas and throughout the water column.

Fish species with prolonged pelagic larval stages may experience offshore habitat conditions that have changed over the past quarter century. Rainbow smelt are invasive in the Great Lakes, yet they are an important prey fish for larger sport fish and are caught ubiquitously during the larval stage throughout the summer in pelagic waters (Roseman et al., 2013, 2017 CSMI ichthyoplankton surveys, Figure 3.2). As larvae that are present throughout the summer, rainbow smelt are an appropriate species to examine changes in habitat quality as thermal regimes and zooplankton availability vary throughout the season. An additional species with a strong propensity for prolonged offshore advection during the larval stage is yellow perch (Beletsky et al., 2007), that have historically supported large commercial and recreational fisheries in the Great Lakes. Studies conducted prior to thorough establishment of dreissenid mussels in Lake Michigan show that offshore habitats may be more conducive to larval yellow perch growth and survival than nearshore habitats (Dettmers et al., 2005, Weber et al., 2011). However, current conditions such as offshore reductions in zooplankton biomass may mitigate the benefits of the offshore environment observed before mussel establishment and subsequent oligotrophication of offshore environments.

The purpose of this study is to assess current spatial and seasonal distribution in habitat quality within nearshore-offshore transects during the period of peak larval abundance (May-July) in Lakes Michigan and Huron. We calculate relative growth rate potential as a proxy for habitat quality within transects using towed undulating vehicle (TUV) data streams as inputs to a bioenergetics model with a foraging submodel. We conduct this analysis for larval rainbow smelt and yellow perch due to their observed substantial offshore pelagic larval stages. In general, we predict poor habitat quality earlier in the summer in comparison to later in the summer due to observed reductions in spring phytoplankton and zooplankton blooms. Additionally, we hypothesize that locations of high habitat quality will shift with changes in the thermal habitat and spatial distribution of prey items throughout the spring and summer. In early summer, we predict that offshore regions of the water column will provide poor habitat for larval fish due to concentrated warm temperatures and zooplankton nearshore (thermal bar). Later in the summer as waters become thermally stratified, we predict high habitat quality to be located near the thermocline where zooplankton are often concentrated, and expect poor habitat quality in the

surface waters, where warm temperatures increase metabolic rate but scarce zooplankton limit consumption.

3.2 Methods

3.2.1 Data collection and preparation

As part of the Cooperative Science and Monitoring Initiative (CSMI) field efforts in 2015 and 2017, several US federal agencies completed daytime nearshore to offshore surveys of Lake Michigan (2015) and Lake Huron (2017) utilizing traditional sampling techniques as well as high frequency sensors and towed undulating vehicles (TUV). Equipped with multiple data loggers and sensors, the TUVs surveyed temperature, zooplankton density and size, dissolved oxygen, and light availability at approximately nine second intervals while towed vertically and horizontally through the water column in a sinusoidal motion. The common sensors mounted on each TUV included a laser optical plankton counter (LOPC), CTD (conductivity, temperature, depth), and a fluourometer. The EPA Great Lakes National Program Office R/V Lake Guardian vessel completed daytime transect tows for Lake Huron in 2017 with the TRIAXUS towed undulating vehicle, equipped with a Seabird CTD, BBE Moeldaecke Fluoroprobe fluorometer, WETlab C-Star transmissometer (660 nm wavelength, 25 cm path-length), and a Rolls Royce laser optical plankton counter (LOPC) (Figure 3.1). Along the transects in Lake Huron, oblique larval fish tows were completed at bathymetric depths of 18 m, 46 m, and an additional bathymetric depth between 68 and 82 m using a 1 m diameter circular net with a mesh size of 500 μm . At the same bathymetric depth stations, vertical zooplankton tows were completed using a 0.5 m diameter circular net with a 63 μm mesh. At the 18 m depth contour zooplankton net tows sampled depths 0-10 m, while at the 46 m depth contour net tows sampled depths 0-35 m, and at the most offshore depth contour (68-82 m) net tows sampled depths 0-40 m. The EPA Mid-Continent Ecology Division R/V Lake Explorer II completed daytime TUV transects for central Lake Michigan in 2015 with the Vfin TUV, equipped with a SeaBird SBE19plus CTD, SeaBird C-Star with a 10 cm path-length, and a Rolls Royce laser optical plankton counter (Figure 3.1). Along the transects in Lake Michigan, vertical zooplankton net tows were completed at 18 m, 46 m, and 110 m depth contours using a 0.5 m circular net with 153 μm mesh. At the 18 m depth contour zooplankton net tows sampled depths 0-18 m, while at the 46 m depth contour net tows sampled depths 0-46 m, and at the 110 m

depth contour net tows sampled depths 0-100 m. Nighttime larval fish tows in Lake Michigan were conducted by the USGS at 18 m, 46 m, and 91-110 m depth stations using a 1 m diameter circular net with a 500 μ m mesh size within 14 days of the TUV transect tows.

The resulting dataset was comprised of water quality data collected by two separate towed undulating vehicles and two different lakes, and therefore we define two major groups of transects for summarizing results: southern Lake Huron and central Lake Michigan. Transect group designation, year, location, length, and TUV type for each transect are described in Table 3.1 and Figure 3.1.

3.2.2 Model environment setup

To estimate environmental parameters throughout the water column, the nearshore-offshore water column transect was split into equally sized cells, and values of environmental variables were assigned to each cell by interpolating the TUV data streams. Xu et al (2017) developed an automated algorithm that uses kriging interpolation to synch and interpolate data streams from multiple sensors across the sinusoidal path of the TUV along transects. The spatial extent of interpolation, including grain size, can influence outputs of growth rate potential (Mason and Brandt 1996). Therefore, a grain size that mimics temperature gradients within the water column along the vertical and horizontal axes were used because temperature is the primary variable influencing metabolic rate and maximum consumption in the calculation of growth rate potential. A smaller grain size of 0.2 m along the vertical axis accounts for fine scale changes in environmental conditions with depth, especially during months of strong thermal stratification. In contrast, changes in conditions from nearshore to offshore are more gradual, and thus a larger grain size of 0.2 km was used along the horizontal axis that still captures the patchiness of zooplankton biomass within the water column. Temperature measured along the sinusoidal path of the TUV was directly interpolated to each 0.2 km by 0.2 m cell, while zooplankton density and beam attenuation were adjusted before or after interpolation for optimal usage in subsequent foraging and bioenergetic models.

Although we assumed all particles counted by the LOPC were zooplankton, this may not be the case. Previous applications of LOPC use zooplankton net tows to calibrate LOPC estimates, although these efforts tend to focus on biomass instead of density (Watkins et al., 2017 and Yurista et al., 2009). To calibrate LOPC data, we calculated a calibration number for each major transect

group by dividing the average of all LOPC measurements within the transect group by the average of all net tow zooplankton density measurements within the transect group, excluding organisms outside of the size range measured by the LOPC (0.2 - 4.0 mm) from net tow density estimates. We divided total LOPC particle counts by the calibration number before interpolation (Table 3.1). In addition to enumeration, the LOPC measured each particle that passed through a laser beam in the unit of equivalent spherical diameter (ESD), which we then converted to length in millimeters using methods described in Watkins et al (2017). As such, we grouped the calibrated LOPC particle counts into seven defined size bins that represent typical zooplankton taxa sizes in the Great Lakes (Table 3.2, Scofield et al., 2020). After calibrating particle abundance and grouping particles into the seven size bins, we interpolated particle abundance of each of the seven size bins for each 0.2 km by 0.25 m cell. After interpolation, each cell in the water column contained a particle density measurement for each of the seven size bins that we used as estimates of zooplankton density in subsequent foraging and bioenergetic models. We assumed the two smallest size bins were composed of copepod nauplii, while we assumed the remaining five size bins were composed of 75% copepods and 25% cladocerans (Table 3.2). We skewed the composition of the five largest bins towards copepods due to recent declines in cladocerans in offshore environments of Lake Michigan and Lake Huron (Barbiero et al 2019). Additionally, after excluding copepod nauplii, copepods on average represented 92.4 % +/- 12.9 % (mean +/- standard deviation) of Lake Michigan zooplankton net tows and 92.9 % +/- 17.0 % of Lake Huron zooplankton net tows.

The TUV measured beam attenuation in units of m^{-1} , but larval foraging models are based on estimated of light availability. Consequently, a value for beam attenuation was assigned to each grid cell using kriging interpolation, and then downwelling irradiance in each grid cell was calculated from interpolated beam attenuation coefficients. First, beam attenuation coefficients were converted into diffuse attenuation coefficients (K_d) using equations 1 and 2 from Arst et al (2002).

$$b(580 \text{ nm}) = 0.3c(580 \text{ nm}) \quad \text{Equation 1}$$

$$K_d = \frac{1}{\cos\theta} * ((c - b)^2 + (0.425 \cos\theta - 0.190) * (c - b)b)^{0.5} \quad \text{Equation 2}$$

Pheta (Θ) in the equation is the angle in degrees of photon in the solar beam compared to the vertical right below the surface of the water, which was set to 0. A conversions rate of 0.3 was used to convert c into the scattering coefficient (b) in equation 1 because of the relatively low beam attenuation values in the dataset (Arst et al 2002). The diffuse coefficient (K_d) of a certain depth is affected by the light above it, and thus the final K_d value for a grid cell of a certain depth was the average of the K_d values of the grid cells above it in the water column. K_d was then converted to downwelling irradiance using the beer-lambert law.

$$I(z) = I(0)e^{(-k_f*z)} \quad \text{Equation 3}$$

In this equation, I is the downwelling irradiance in $\mu\text{E}/\text{m}^2/\text{sec}$, $I(0)$ is the downwelling irradiance just beneath the surface of the water, K_f is the final diffuse attenuation coefficient value for the grid cell, and z is depth in meters. Typical measurements of photosynthetically active radiation (PAR) just beneath the surface were used as values for $I(0)$ because PAR measures light in the wavelength range of 400-700 nm, which is appropriate for the visual range of larval fish and PAR has the same units as downwelling irradiance. The plankton survey system (PSS), operated by NOAA, provided typical surface PAR measurements for the Great Lakes during this time of year at <https://www.glerl.noaa.gov/res/PSS/>. Surface PAR values used in the model are 500 $\mu\text{E}/\text{m}^2/\text{sec}$ for May transects, 750 $\mu\text{E}/\text{m}^2/\text{sec}$ for June transects, and 1000 $\mu\text{E}/\text{m}^2/\text{sec}$ for July transects.

3.2.3 Model Overview

Measurements of temperature, light availability, and size-based zooplankton density are used in subsequent foraging and bioenergetic models to estimate larval fish growth rate potential (GRP) in each 0.2 km by 0.25 m cell of individual transects. In the GRP model output, cells with higher GRP values represent locations with relatively better habitat quality for larval fish growth based on prevailing environmental conditions. In this study, foraging and bioenergetic models were used to estimate habitat quality for yellow perch and rainbow smelt due to the substantial offshore pelagic stages of these two species in the Great Lakes, but larval rainbow smelt bioenergetic parameters are not available, and thus we use larval European smelt *Osmerus eperlanus* parameters as a proxy (heretofore referred to as smelt). We used lengths of a subset of

larval fish collected in ichthyoplankton tows along TUV transects (Figure 3.2) and previous length measurements of larval yellow perch in Lake Michigan (Dettmers et al., 2005) to determine larval lengths used in the current model. Larval fish size increases throughout the summer for yellow perch (Dettmers et al., 2005) and rainbow smelt (Figure 3.2), and thus we model habitat for 6 mm larvae in May, 11 mm larvae in June, and 11 and 14 mm larvae in July.

We calculated growth rate potential of fish larvae using the following model

$$GRP = C - (R * A) - (C - (FA * C) * SDA) - (FA * C) - (UA * (C - FA * C))$$

GRP is growth rate potential and C is consumption, which is calculated by the foraging submodel described below. Other physiological processes in this model were derived from literature and include metabolism (R), specific dynamic action (SDA), and wastes (egestion FA and excretion UA) (Hewett and Johnson 1992). Table 3.3 lists bioenergetics calculations and parameters for smelt and yellow perch.

3.2.4 Foraging model

In the foraging submodel, larvae consume zooplankton. In our foraging model, we assume that larvae can only consume zooplankton within their gape height, as modelled by Schael et al (1991) for yellow perch and Hrabik et al (2001) for smelt.

$$Gape\ Height\ (mm) = 0.159 * L(mm) - 0.597 \text{ (yellow perch)} \quad \text{Equation 4}$$

$$Gape\ Height\ (mm) = L(mm) * 0.042 \text{ (smelt)} \quad \text{Equation 5}$$

In addition to gape height, we used optimal foraging theory to determine which of the seven prey types to include in larval diet. First, we ranked prey types (i) based on equation 6.

$$Profitability_i = \frac{ZPW_i * ZPE_i * P_i}{HT_i} \quad \text{Equation 6}$$

After ranking prey type profitability, prey types are added to larval diet in order of most to least profitable until the value of accumulated profitability started to decrease

$$accumulated\ profitability = \frac{\sum_i(ZPW_i * ZPE_i * P_i)}{1 + \sum_i(HT_i * ER_i)} \quad \text{Equation 7}$$

In equations 6 and 7, ZPW is zooplankton prey type weight and ZPE is zooplankton prey type energy density. Handling time (HT) and capture success (P) of each prey type i depend on larvae length and zooplankton prey length. We used a handling time model described by Walton et al (1992) for larvae equal to or less than 19 mm

$$HT = e^{0.26410^{7.0151}(\frac{ZPL}{L})} \quad \text{Equation 8}$$

where HT is handling time in seconds, ZPL is zooplankton length (mm), and L is fish length (mm). Table 3.2 lists zooplankton lengths assigned to each size bin. We defined capture success for each prey type using a model proposed by Letcher et al (1996).

$$P = \frac{CSNum * L^2}{CSDen + L^2} \quad \text{Equation 9}$$

L is larvae length(mm), and CSNum and CSDen are parameters configured for each zooplankton group based on larvae size used in the model and capture success rates measured in previous published studies on larval fish (Anneville et al., 2007, Hoagman 1974, Mahjoub et al., 2008). Larvae typically have higher capture success for copepods than cladocerans, and thus we first defined CSNum and CSDen parameters for copepods (CSNum=0.8, CSDen=150) and cladocerans (CSNum=0.7, CSDen=50) separately. Then, we calculated a weighted average of cladoceran and copepod parameters based on the assumption that 75% of zooplankton in each bin were copepods, which resulted in a CSNum of 0.775 and CSDen of 125.

For prey types (i) within larvae gape that were added to larval fish diets based on optimal foraging theory, we calculated encounter rates (ER) as a function of zooplankton density and search volume.

$$ER_i = ZD_i * SV_i \quad \text{Equation 10}$$

In this equation, ER is the encounter rate (items/sec), ZD is the zooplankton density ($1/m^3$) of the grid cell, and SV is the search volume (m^3/s). Larval fish foraged for 15 hours per day, which represents an approximation of daylight hours in mid-summer at the latitudes of the transect sites. Search volume for each prey type (i) depends on larvae swimming speed and reactive distance according to the following equation derived by Varpe and Fiksen (2010):

$$SV_i = \frac{1}{2} * \pi * RD_i^2 * SS \quad \text{Equation 11}$$

We set larval swimming speed (SS) to one body length per second. Reactive distance (RD) for each prey type (i) depends on fish length, light availability, and prey size. Aknes and Utne (1997) defined reactive distance as shown in equation 12, following the assumption that maximum reactive distance is less than 0.5 meters (Aknes and Utne 1997).

$$RD_i = \sqrt{C * A_i * E' * \frac{I}{I+K_e}} \quad \text{Equation 12}$$

RD is reactive distance (m), C is the contrast between the prey and its environment, A is the area of the prey in m^2 , and I is downwelling irradiance in $\mu E/m^2/sec$. Downwelling irradiance is calculated from beam attenuation reported by the TUV. We set visual contrast of the prey to 0.3 (Utne-Palm 1999) and used a value of $10 \mu E/m^2/sec$ for K_e , considering below $10 \mu E/m^2/sec$ larval foraging is substantially reduced (Fiksen et al., 1998, Richmond et al., 2004). E' is a unitless parameter representing eye acuity and development which increases with fish length. We calculated a separate E' for each larvae size used in the model using equation 13 modelled by Fiksen et al (1998) for larval herring. Figure 3.3 depicts how reactive distance changes with light availability and prey size.

$$\log_{10}(E') = \frac{4.88}{1 + e^{-(L - (\frac{10.98}{1.34}))}} \quad \text{Equation 13}$$

Zooplankton prey area is calculated using methods described in Watkins et al (2017).

$$Prey Area_i = ZPL_i * \frac{ZPL_i}{b} \quad \text{Equation 14}$$

In equation 14, Watkins et al (2017) set b to 1.6 for prey types representing cladocerans and set b to 3 for prey types representing copepods (Table 3.2). Considering the composition of zooplankton in model inputs were 75% copepods 25% cladocerans, we calculated a weighted average of 1.6 and 3.0, resulting in a b value of 2.65.

We capped encounter rates at maximum consumption, which was determined by temperature and species-specific maximum consumption models for larval yellow perch (Post 1990), and larval smelt (Karjalainen et al., 1997a). The parameters used to calculate maximum consumption are provided in Table 3.3. After calculating encounter rate for each prey type, we estimated consumption of each prey types using a multi-prey Hollings Type 2 foraging model. Type 2 foraging models assume that handling time limits consumption at high prey densities, which is appropriate for larval fish because they do not filter feed, but are ‘sprint pursuit’ predators that actively ingest larvae within close proximity (Fuiman et al., 2009, Holling 1965).

$$Cons_i = P_i * \left(\frac{ER_i}{1 + \sum_i (HT_i * ER_i)} \right) \quad \text{Equation 15}$$

3.2.5 Summarizing outputs across a transect group

To compare habitat quality throughout the water column, we divided each output transect of GRP values into 16 sections, henceforth referred to as ‘water column sections’, to conduct further analysis. We defined the 16 sections by sub-dividing the transects based on bathymetric depth on the horizontal axis and water column depth on the vertical axis. From this point, the four horizontal boundaries based on bathymetric depth will be referred to as nearshore (15-30 m), mid-nearshore (30-45 m), mid-offshore (45-60 m), and offshore (60 m – end of transect), while the vertical boundaries based on water column depth will be referred to as surface (0-10 m), sub-surface (10-20 m), mid-depth (20-30 m), and deep (30-60 m maximum in southern Lake Huron transects, 30-70 m maximum in central lake Michigan transects). For each transect, the 5 % of

cells with the highest GRP values in each of the 16 water column sections were identified and averaged. In addition, we calculated the percent of cells within each water column section with positive GRP values in each transect. Individual transect GRP values of mean top 5% cells and percent positive GRP are then averaged across transects of the same transect group and sampling month for each of the 16 sections to evaluate trends in location of high quality habitat for larval fish.

3.3 Results

3.3.1 Larvae size throughout the summer

In Lake Huron, smelt larvae were caught in all 3 months, and mean larvae length increased from 6 mm in May to 9 mm in June to 21 mm in July. In May, smelt larvae were only caught at the 18 m depth contour, while larvae were caught at 18 m, 46 m, and most offshore (68-82m) depth contours in June and July (Figure 3.2 A-C). Yellow perch larvae were not caught in Lake Huron in May, and 1 and 6 yellow perch larvae were caught in June and July, respectively. The few yellow perch larvae caught in Lake Huron were caught at the 18 and 46 m depth contours (Figure 3.2D). No larval smelt were caught in Lake Michigan, and yellow perch larvae were only caught in July at 18, 46, and 110 m depth contours. Only one yellow perch larval fish was caught in the central lake Michigan transects at the Ludington transect, while the remaining yellow perch larvae were caught in southern Lake Michigan transects located at Saugatuck, St. Joes, and Waukegan (Figure 3.2E). The southern lake Michigan transects are not assessed for habitat quality in the present study, but the lengths of larval fish collected in these transects help inform selection of larval sizes used in the GRP model.

May 6 mm larvae

Habitat quality for small larvae was poor in May and varied little among water column sections due low zooplankton densities and narrow temperature gradients. In both Lake Michigan and Lake Huron, no water column sections supported positive GRP for either species (Figures 3.4, 3.5, 3.6). Low zooplankton densities throughout the water column limited consumption, while temperature decreased with distance from shore (Appendix A: Figures 3,4,5,6), leading to slightly increasing GRP values of averaged top 5 % cells with increased distance from shore due to lower

metabolic rates at lower temperatures (Figures 3.7A, 3.8A, 3.9A, 3.10A). The GRP values of averaged top 5 % cells in Lake Huron ranged from -0.024 to -0.022 g g⁻¹ day⁻¹ among the 16 designated water column sections for yellow perch, and -0.029 to -0.025 g g⁻¹ day⁻¹ for smelt (Fig. 3.7A, 3.8A). The GRP values of averaged top 5 % cells in Lake Michigan ranged from -0.026 to -0.022 g g⁻¹ day⁻¹ among the 16 designated water column sections for yellow perch, and -0.030 to -0.026 g g⁻¹ day⁻¹ for smelt (Figure 3.9A, 3.10A).

June 11 mm larvae

Weak thermal stratification and pockets of concentrated zooplankton in surface waters during June across southern Lake Huron transects (Appendix A: Figures 1,2) led to vertical variation in GRP, with higher GRP values closer to the warm surface waters that contained pockets of high zooplankton availability (Figures 3.7B, 3.8B). For 11 mm yellow perch, over 70% of cells in surface waters at all bathymetric depths supported positive GRP in southern Lake Huron transects (Figure 3.4B). For 11 mm smelt, percent positive GRP was highest in surface waters nearshore, but pockets of zooplankton offshore in some transects provided positive GRP offshore as well (Figure 3.5B). 11 mm yellow perch have a larger gape than 11 mm European smelt, and as such, yellow perch were able to consume more in areas with densities of larger zooplankton offshore, whereas smelt could not. The GRP values of averaged top 5 % cells in June ranged from -0.015 to 0.050 g g⁻¹ day⁻¹ among the 16 water column sections for yellow perch, and -0.019 to 0.004 g g⁻¹ day⁻¹ for smelt (Figure 3.5B, 3.6B), with highest GRP values of averaged top 5% cells occurring in surface and subsurface waters across the transect for both species.

July 11 and 14 mm larvae

Habitat quality for 11 and 14 mm larvae in July was driven by strong thermal stratification and zooplankton availability. Zooplankton were concentrated primarily at the thermocline in southern Lake Huron transects, while zooplankton were concentrated in surface waters nearshore in central Lake Michigan transects (Figure 3.10, Appendix A: Figures 7,8,9), leading to differing patterns in the spatial distribution of habitat quality between lakes. In Lake Huron, scarce zooplankton availability in surface water offshore led to few cells that could support positive GRP for 11 mm yellow perch and rainbow smelt in these areas (Figures 3.4C, 3.5D). However, increased

foraging ability of 14 mm rainbow smelt and yellow perch led to positive GRP throughout the water column (3.4D, 3.5D). GRP of averaged top 5% of cells in surface waters decreased with distance from shore for 11 mm larvae, and the highest GRP values of averaged top 5% of cells occurred along the thermocline (Figures 3.7C, 3.8C). GRP values of averaged top 5% cells in July ranged from -0.028 to 0.155 g g⁻¹ day⁻¹ among the 16 water column sections for yellow perch, and -0.049 to 0.092 g g⁻¹ day⁻¹ for smelt. For 14 mm larvae, GRP of averaged top 5% of cells were highest in surface waters, with little variation in habitat quality nearshore-offshore (Figures 3.7D, 3.8D). GRP values of averaged top 5% cells in July ranged from 0.253 to 0.806 g g⁻¹ day⁻¹ among the 16 water column sections for yellow perch, and 0.202 to 0.316 g g⁻¹ day⁻¹ for smelt.

In central Lake Michigan, zooplankton was concentrated nearshore during July, (Appendix A: Figures 3,4,5,6), and as such, nearshore water column sections contained the highest percentage of cells with positive GRP for both species. For 11 mm larvae, cells that supported positive GRP only occurred in surface waters nearshore of Frankfort and Ludington transects for yellow perch, and only Ludington transect for smelt (Figure 3.6A,3.6C). Although additional water column sections contained cells that supported GRP for 14 mm larvae, highest percent positive GRP occurred in surface waters nearshore (Figure 3.6B,3.6D). Additionally, the highest GRP values of averaged top 5% of cells occurred in surface waters nearshore for both 11 mm and 14 mm larvae. For 11 mm larvae, GRP values of averaged top 5% cells in July ranged from -0.023 to -0.001 g g⁻¹ day⁻¹ among the 16 water column sections for yellow perch, and -0.033 to -0.011 g g⁻¹ day⁻¹ for smelt (Figure 3.9B, 3.10B). For 14 mm larvae, GRP values of averaged top 5% cells in July ranged from -0.014 to 0.340 g g⁻¹ day⁻¹ among the 16 water column sections for yellow perch, and -0.021 to 0.224 g g⁻¹ day⁻¹ for smelt (Figure 3.10C, 3.10C).

3.4 Discussion

The location of best habitat quality shifted throughout the summer in Lakes Michigan and Huron, but not always in congruence with our hypotheses. In May, we expected high quality habitat to occur in surface waters closer to shore due to a horizontal thermal bar nearshore to offshore along transects. This hypothesis was not supported in Lake Huron or Lake Michigan, considering habitat quality in surface water slightly increased with distance from shore due to low zooplankton densities throughout the transects. In July, we expected high habitat quality to occur along the thermocline. This hypothesis was supported in the southern Lake Huron transect group

for 11 mm larvae, but high quality habitat occurred throughout the top 20 m of the water column for larger larvae with increased foraging abilities. In the southern Lake Michigan transect group, high habitat quality was still located nearshore during July where zooplankton densities were the highest for most transects.

Growth rate potential ideally increases with increased temperature until critical temperatures, as at higher temperatures maximum consumption increases at a greater rate than the increased energetic demand for respiration (Hewett and Johnson 1992). However, some warmer areas of transects in this study displayed relatively lower GRP than cooler areas, a result of limited foraging ability of larval fish and low zooplankton densities. Larval fish, unlike adult life stages, do not have efficient control of where they forage due to limited visual and swimming ability (Fuiman et al., 2009). As such, larvae experience increased energetic demand for respiration in environments with high temperatures and low zooplankton densities but do not have a sufficiently high encounter rate to take advantage of increased maximum consumption rate. While densities were relatively highest nearshore during May in many transects, these zooplankton densities were not sufficient to overcome increased metabolic demand of warmer nearshore areas, and thus nearshore surface waters provided slightly lower habitat quality than offshore environments. Surface waters had the highest temperatures in July due to thermal stratification, yet surface waters offshore provided poor habitat quality for 11 mm larvae in Lake Huron and 11 and 14 mm larvae in Lake Michigan due to low zooplankton densities. However, pockets of concentrated zooplankton in nearshore warm surface waters of July central Lake Michigan transects resulted in positive growth and highest GRP values for those transects. A lack of overlap of areas with high temperatures and high food availability could limit larval fish habitat quality in offshore waters of these lakes.

During the larval stage, yellow perch and rainbow smelt likely undergo an offshore pelagic stage in the Great Lakes, as larvae with poor swimming ability are advected offshore by lake currents (Dettmers et al., 2005). This study emphasizes the range of habitat quality larvae could experience before transitioning to nearshore habitats as juveniles. In May, advection offshore may only slightly benefit larvae, as habitat quality is poor throughout the water column. During June in southern Lake Huron, advection offshore may not be detrimental, but also does not provide increased habitat quality in comparison to nearshore habitats. However, this varied between the two species modelled, where smaller-gaped smelt experienced decreasing habitat quality farther

offshore than larger gaped yellow perch in June. While pockets of high zooplankton densities occurred at all bathymetric depths in June, the offshore zooplankton community was generally larger, which limited consumption for smelt. In July, offshore habitats seem to provide worse habitat conditions than nearshore areas for larvae in central Lake Michigan and for smaller larvae in southern Lake Huron. However, Lake Huron transects provided high quality habitat quality in surface waters across the transect for larger larvae with increased foraging abilities. Previous work measuring habitat quality with distance from shore has shown increased zooplankton densities and growth rates of yellow perch larvae offshore in Lake Michigan (Dettmers et al., 2005, Weber et al., 2011). However, these habitat evaluations were conducted prior to major oligotrophication and decrease in small zooplankton biomass in the offshore waters of lakes Michigan and Huron. In the present study, we conclude that the habitat quality of offshore surface waters of Lakes Michigan and Huron is similar to nearshore habitat quality in May, and generally worse than nearshore habitat quality in July.

Considering shifts in the location of best habitat quality throughout the summer were driven by thermal regime for many transects, future spring and summer warming rates may affect habitat for larval fish. Summer surface water temperatures during the summer stratification period are predicted to increase in Lakes Michigan and Huron (Trumpickas et al., 2009), making the surface waters an area of poor habitat for larvae if zooplankton densities remain low at the surface during summer. Past time series data and predictive climate change models forecast that thermal stratification is likely to occur sooner in the season with time (Austin and Colman 2007, Trumpickas et al., 2009), possibly limiting the period of overlap between high quality habitat occurs in surface waters and larvae emergence. In Lake Huron, habitat quality in June is highest for larval fish in surface waters throughout the transect as the water column is weakly stratified and prey availability is highest in surface waters. Additionally, June is when larval fish were first observed in offshore bathymetric depths of transects in this study. High growth during June before strong thermal stratification sets in may be important for larvae in southern Lake Huron, considering larger larvae with increased visual acuity and foraging abilities experienced high habitat quality in surface waters offshore, but small larvae experiences poor habitat quality in the same environment. As spring warming rates increase in the future, hatch dates and advection rate of larvae may not coincide with high quality habitat offshore during weak thermal stratification.

In conclusion, the locations of best habitat quality for larval yellow perch and smelt shift throughout the summer, with more consistency of high quality locations in both Lake Michigan and Lake Huron later in the summer. For many transects of these lakes, the shallow, nearshore areas provide better suited habitat for larval fish than offshore areas, with Lake Huron having high quality habitat for larger larvae in July. Considering these observations, factors that affect the duration of the offshore pelagic stage such as hatch date, wind speed/direction, and larval growth rate should be investigated further to understand recruitment dynamics of these species. The lack of prey availability in surface waters offshore during May and July might limit the habitat quality and growth of larval fish, which supports the presence of a recruitment bottleneck during their offshore pelagic stage.

3.5 Tables and Figures

Table 3. 1 Nearshore-offshore TUV transects location, length, depth station range, month(s) sampled, TUV used in data collection, and transect group used for figures and summary analysis.

Transect lengths are listed in chronological order for Lake Huron (May, June July) and Lake Michigan (May, July).

Transect Location	Transect Length (km)	Depth Station Range (m)	Months Sampled	TUV	Transect Group	LOPC Calibration Value
Saugeen River	11.25, 10.5, 8.75	15-70 May/June, 30-60 July	May, June, July	TRIAXUS	Southern Lake Huron	2.30
Maitland River	10.5, 10.5, 10	15-70				
Harbor Beach	28, 28, 27	15-70				
Frankfort	7.5, 7.5	15-100	May, July	Vfin	Central Lake Michigan	1.73
Ludington	13, 13.25	15-100				
Manitowoc	14.75, 17.5	15-100				
Sturgeon Bay	13, 13.25	15-100				

Table 3. 2 Description of zooplankton groups used as prey types in the foraging model. The median length of the size bin is used in the model for all particles of that size bin. All particles in the LOPC size bin are assumed to have similar energy densities, according to reported energy densities of the taxonomic group designated. Energy densities sourced from Cummings and Wuycheck (1971), as grouped by Fernandez et al (2009).

LOPC Size Bin (mm)	Length (mm)	Taxonomic Group	Energy density (J/ug DW)
0.2-0.25	0.225	Copepod Nauplii	0.02461
0.25-0.30	0.275	Copepod Nauplii	0.02461
0.30-0.50	0.40	75% small cladocerans, 25% copepods	0.02412
0.50-0.70	0.60	75% small cladocerans, 25% copepods	0.02412
0.70-1.0	0.85	75% large cladocerans, 25% copepods	0.02383
1.0-1.5	1.25	75% large cladocerans, 25% copepods	0.02383
1.5-3.0	2.25	75% large cladocerans, 25% copepods	0.02383

Table 3. 3 Yellow perch and European Smelt bioenergetic parameters. Yellow perch equations and parameters sourced from post 1990 and Worishka and Mehner (1998). European smelt paramters sourced from Karjalainen et al (1997a).

	Yellow Perch <i>Perca Flavescens</i>	European Smelt <i>Osmerus mordax</i>
Consumption g g-1 day-1	$C_{max} = C_A * M^{C_B} * V^X * e^{X*(1-V)}$ $V = \frac{CTM - T}{CTM - CTO}$ $X = \frac{Z^2 * \left(1 + \left(1 + \frac{40}{Y}\right)^{0.5}\right)^2}{400}$ $Z = \ln(CQ) * (CTM - CTO)$ $Y = \ln(CQ) * (CTM - CTO + 2)$	$C_{max} = C_A * M^{C_B} * (K_A * K_B)$ $K_A = (CK1 * L1) / (1 + CK1 * (L1 - 1))$ $L1 = e^{G1*(T-CQ)}$ $G1 = \left(\frac{1}{CTO - CQ}\right) * \ln\left(\frac{0.98 * (1 - CK1)}{CK1 * 0.02}\right)$ $K_B = \frac{CK4 * L2}{1 + CK4 * (L2 - 1)}$ $L2 = e^{G2*(CTL-T)}$ $G2 = \left(\frac{1}{CTL - CTM}\right) * \ln\left(\frac{0.98 * (1 - CK4)}{CK4 * 0.02}\right)$
C_A	0.51	0.18
C_B	-0.42	-0.275
CQ	2.3	3
CTM	32	21
CTO	29	16
CTL	NA	26
$CK1$	NA	0.40
$CK2, CK3$	NA	0.98
$CK4$	NA	0.01
Respiration gO2 g-1 day-1	$R = R_A * M^{R_B} * V^X * e^{X*(1-V)}$ $V = \frac{RTM - T}{RTM - RTO}$ $X = \frac{Z^2 * \left(1 + \left(1 + \frac{40}{Y}\right)^{0.5}\right)^2}{400}$ $Z = \ln(RQ) * (RTM - RTO)$ $Y = \ln(RQ) * (RTM - RTO + 2)$	$R = R_A * M^{R_B} * e^{RQ*T} * A$
R_A	0.0065	0.00189
R_B	-0.2	-0.1057
RQ	2.1	0.073
RTM	35	NA
RTO	32	NA
SDA	0.15	0.175
UA	0.15	0.10
FA	0.15	0.16
Larvae Energy Density J WW g-1	2512	2997

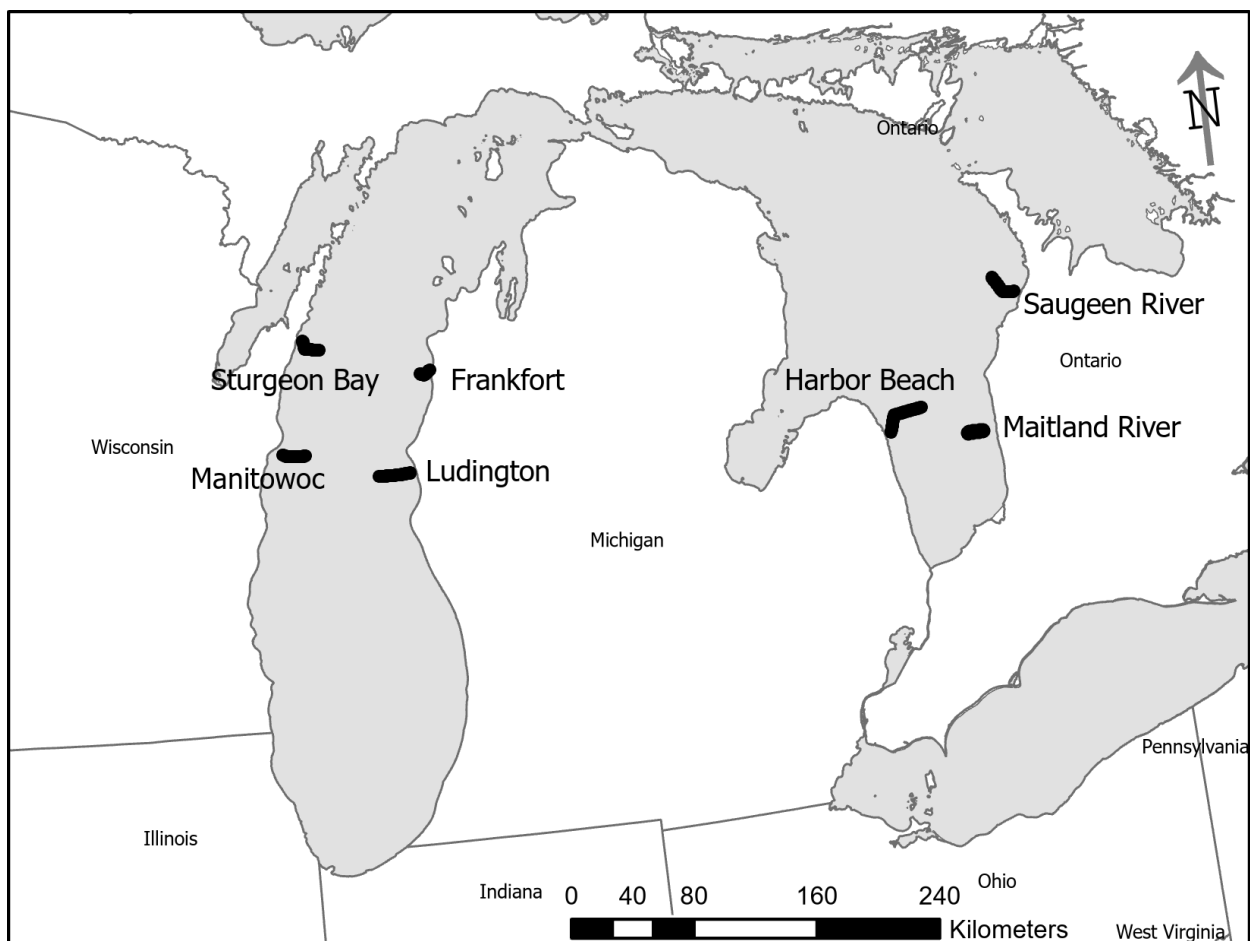


Figure 3. 1. Locations of nearshore-offshore TUV transects in Lake Michigan (2015) and Lake Huron (2017).

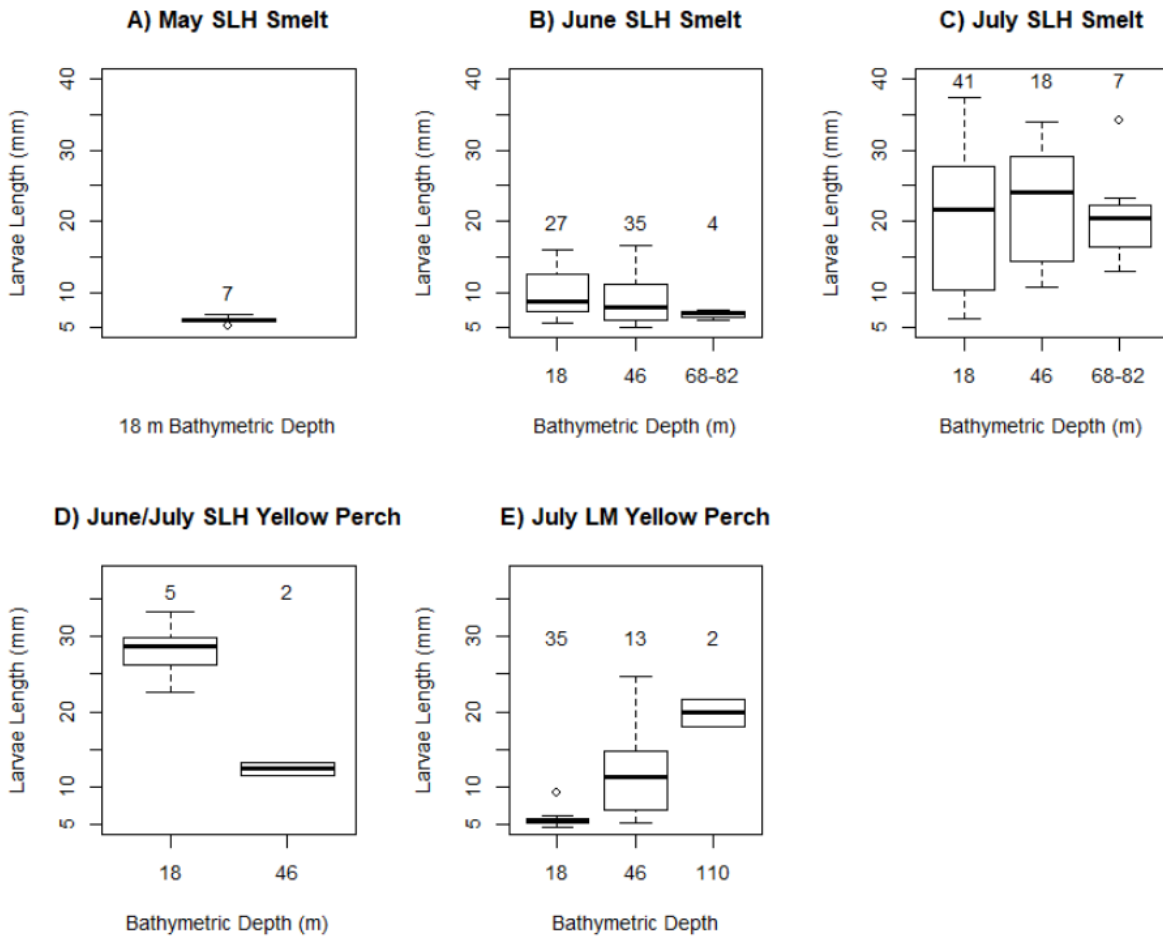


Figure 3. 2 Boxplots of lengths of a subset of larvae collected in oblique larval fish tows at bathymetric depths of 18, 46, and an additional offshore site (68-110 m depth contour) in Lake Huron in 2017 and Lake Michigan in 2015. For rainbow smelt, larvae were only collected at 18 m bathymetric depth in May (A), but in all depth stations in June (B) and July (C) in southern Lake Huron transects. Larval yellow perch were only collected at 18 and 46 m bathymetric depths in June and July (combined data of these 2 months, D). Larval yellow perch from central and southern lake Michigan transects were only collected in July (E). Numbers placed above each boxplot represent sample size.

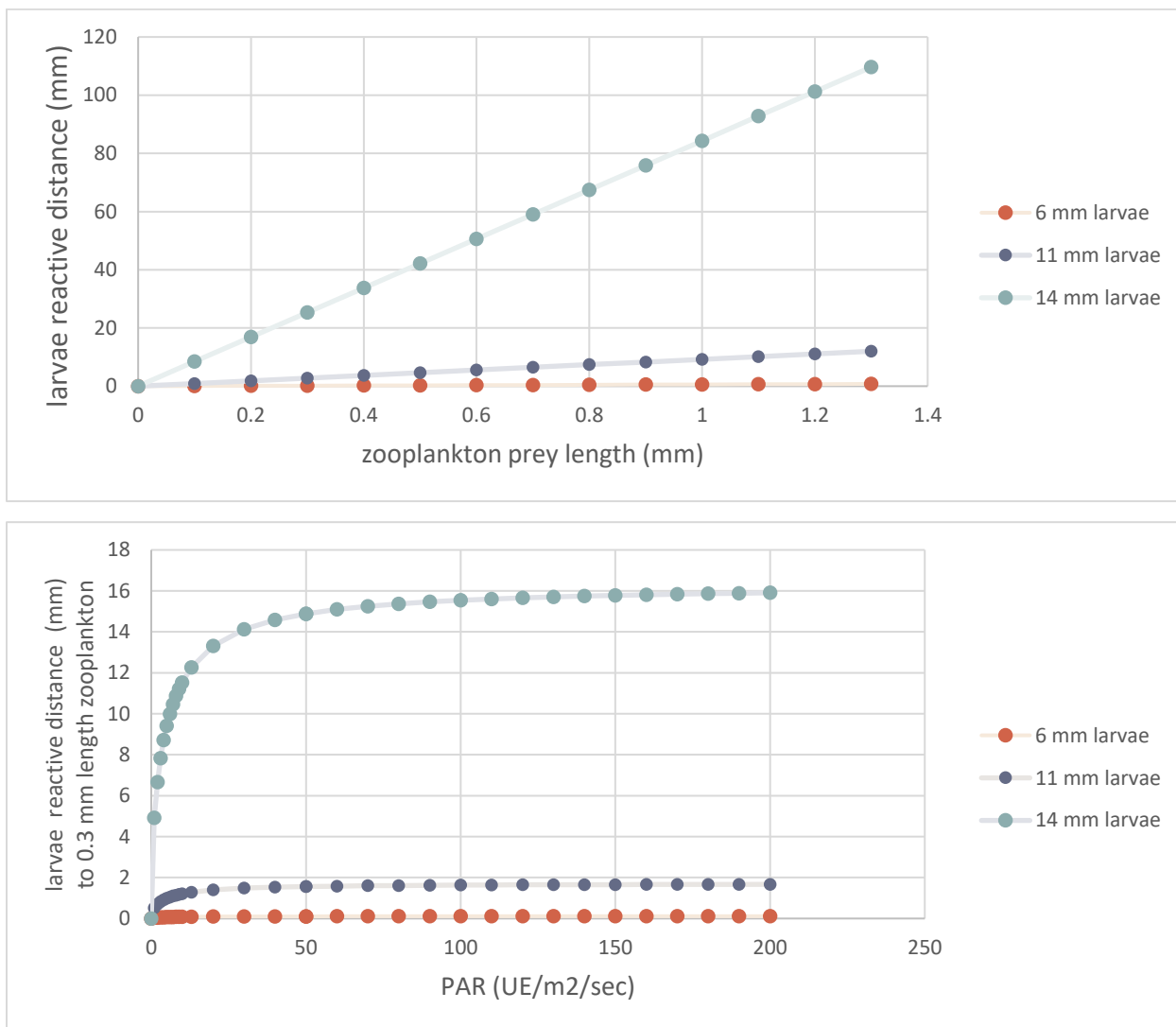


Figure 3. 3 Relationship between larvae reactive distance and zooplankton length (top), and the relationship between larvae reactive distance and light availability ($\mu\text{E m}^{-2} \text{sec}^{-1}$) (bottom) for 6 mm, 11 mm, and 14 mm larvae.

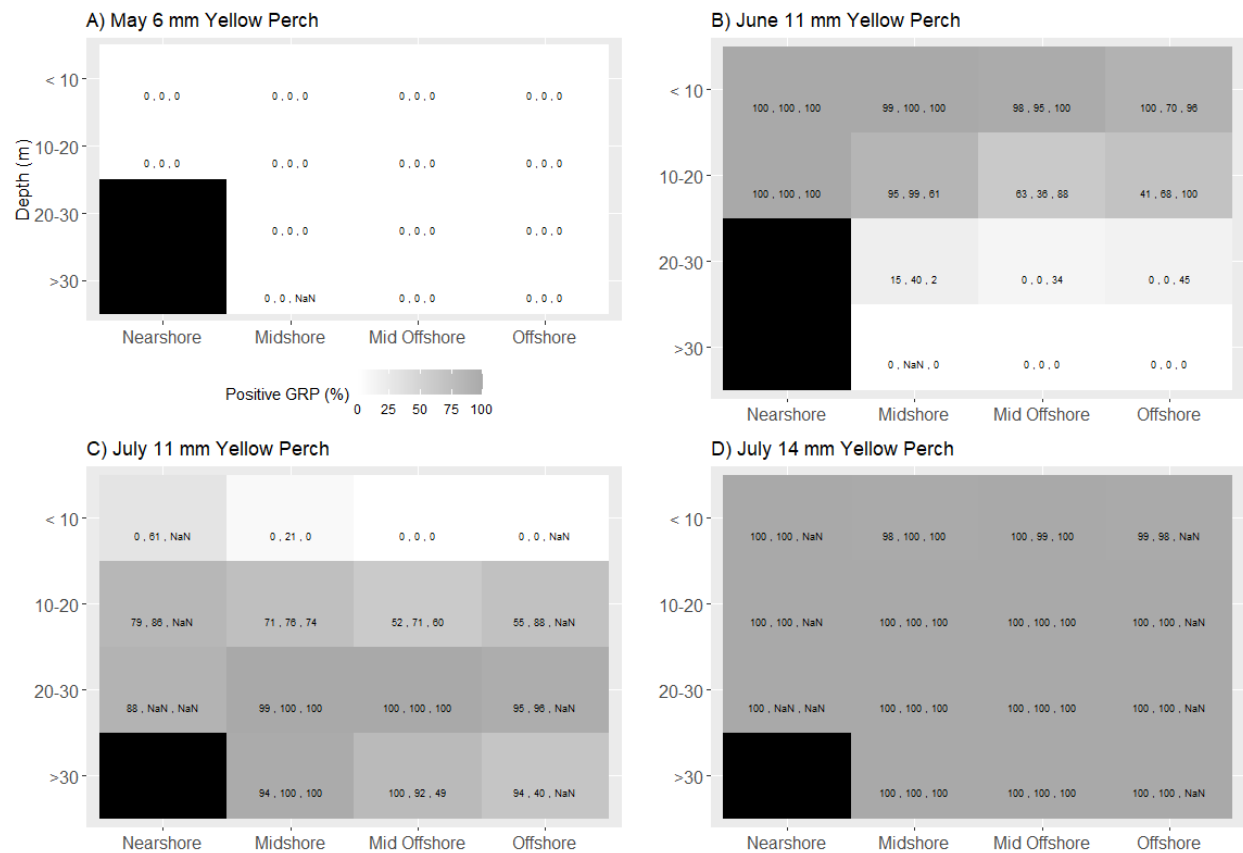


Figure 3. 4 Mean percent positive GRP in 16 sections of the water column among southern Lake Huron transects for 6 mm yellow perch in May (A), 11 mm yellow perch in June (B), and 11 mm and 14 mm yellow perch in July (C,D). Labels are the percent positive GRP value for each transect in the following order: Maitland, Harbor Beach, Saugeen River.

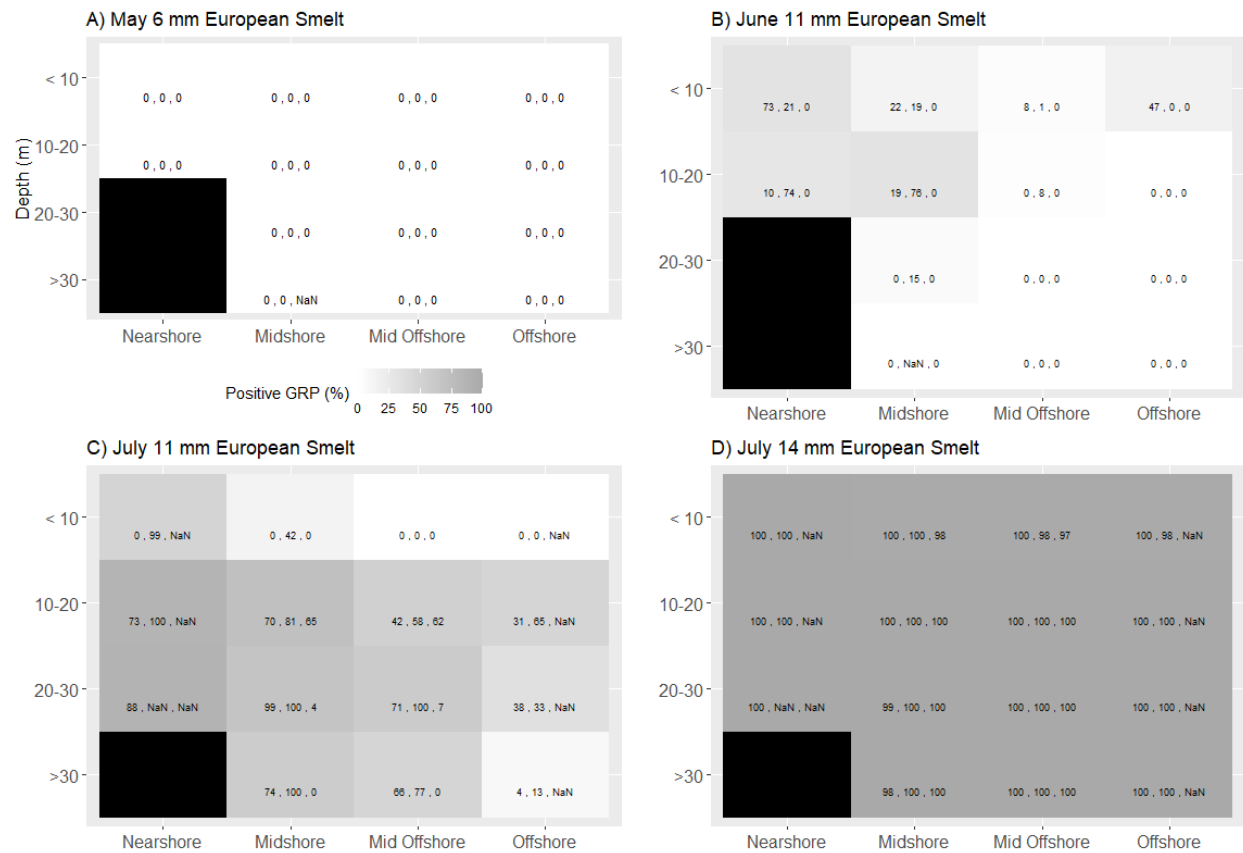


Figure 3. 5 Mean percent positive GRP in 16 sections of the water column among southern Lake Huron transects for 6 mm smelt in May (A), 11 mm smelt in June (B), and 11 mm and 14 mm smelt in July (C,D). Labels are the percent positive GRP value for each transect in the following order: Maitland, Harbor Beach, Saugeen River.



Figure 3. 6 Mean percent positive GRP in 16 sections of the water column among southern Lake Michigan transects for 11 mm and 14 mm yellow perch (A,B) and smelt (C,D). Labels are the percent positive GRP value for each transect in the following order: : Frankfort, Sturgeon Bay, Manitowoc, Ludington.

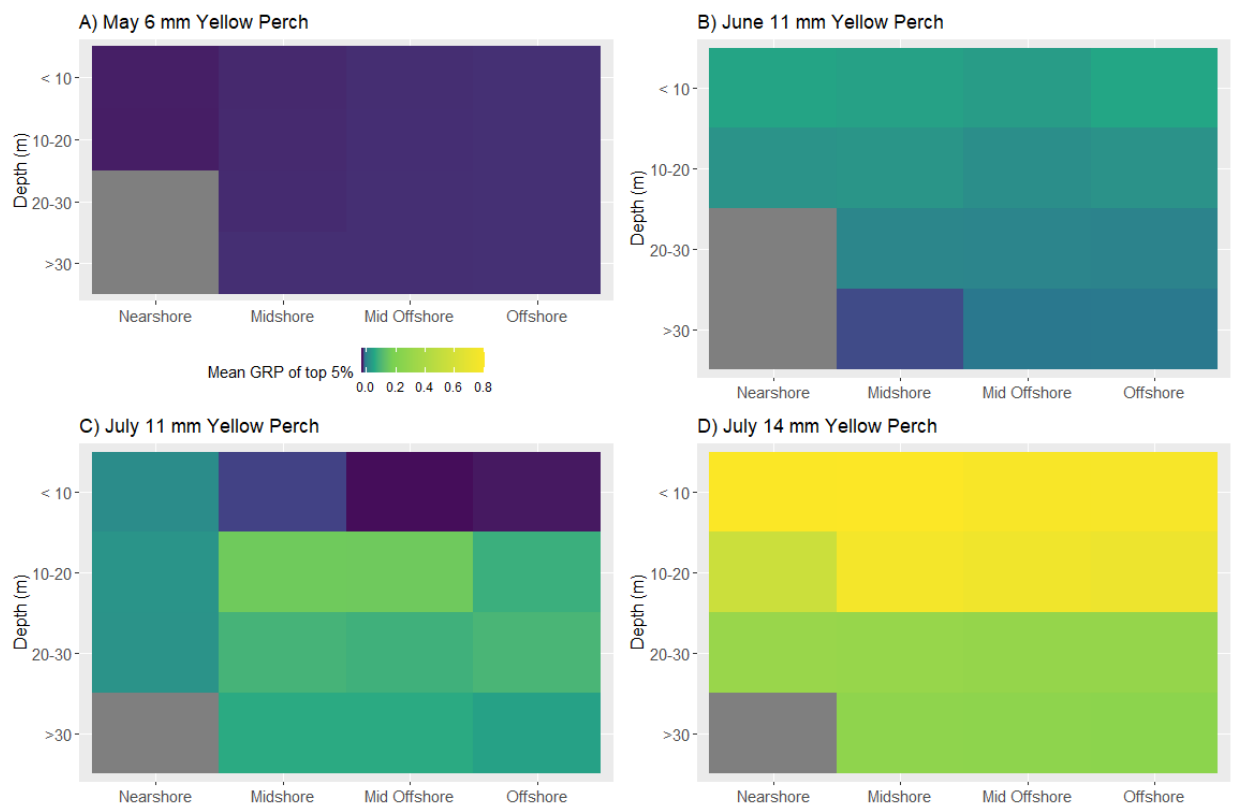


Figure 3. 7 Southern Lake Huron means of mean individual transect averages of GRP in cells within the 95th percentile for 16 designated areas of the water column in May for 6 mm yellow perch (A), June for 11 mm yellow perch (B), and July for 11 mm and 14 mm yellow perch (C,D).

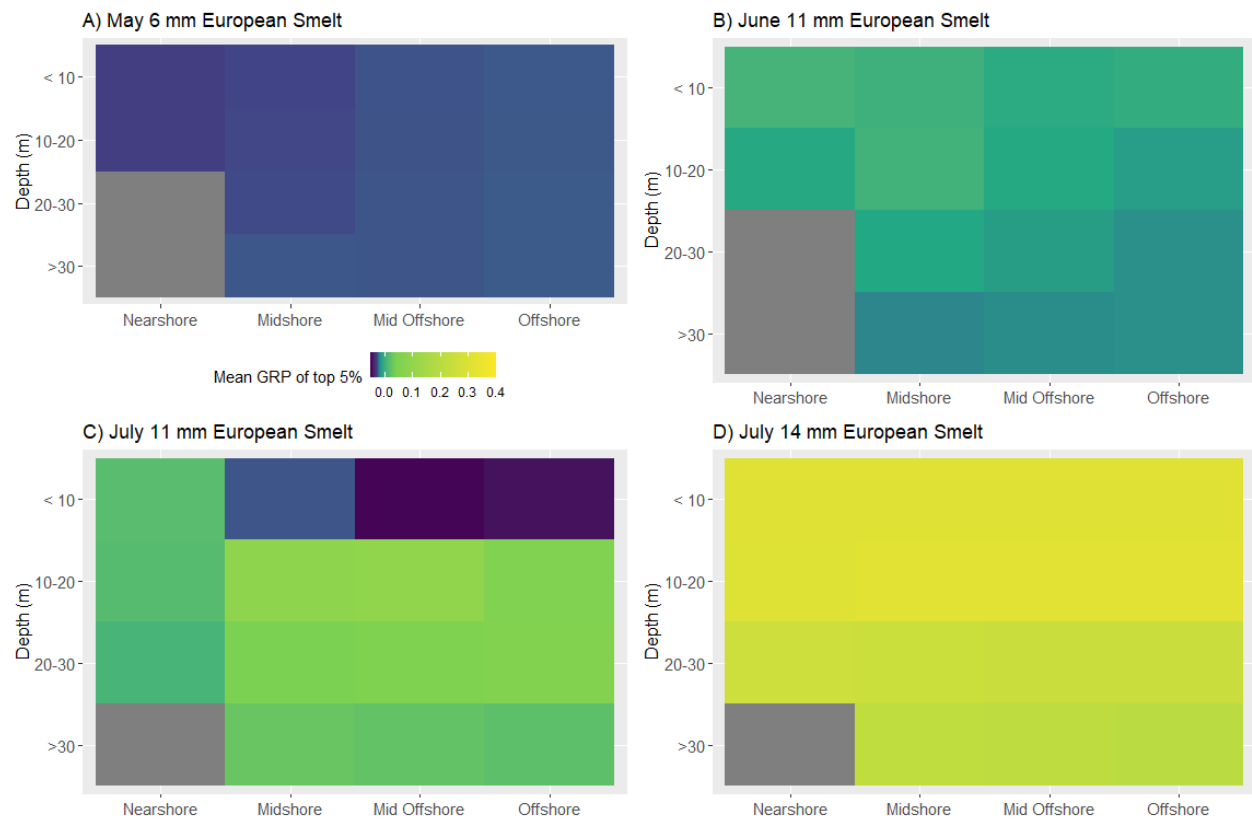


Figure 3. 8 Southern Lake Huron means of mean individual transect averages of GRP in cells within the 95th percentile for 16 designated areas of the water column in May for 6 mm smelt (A), June for 11 mm smelt (B), July for 11 mm and 14 mm smelt (C,D).

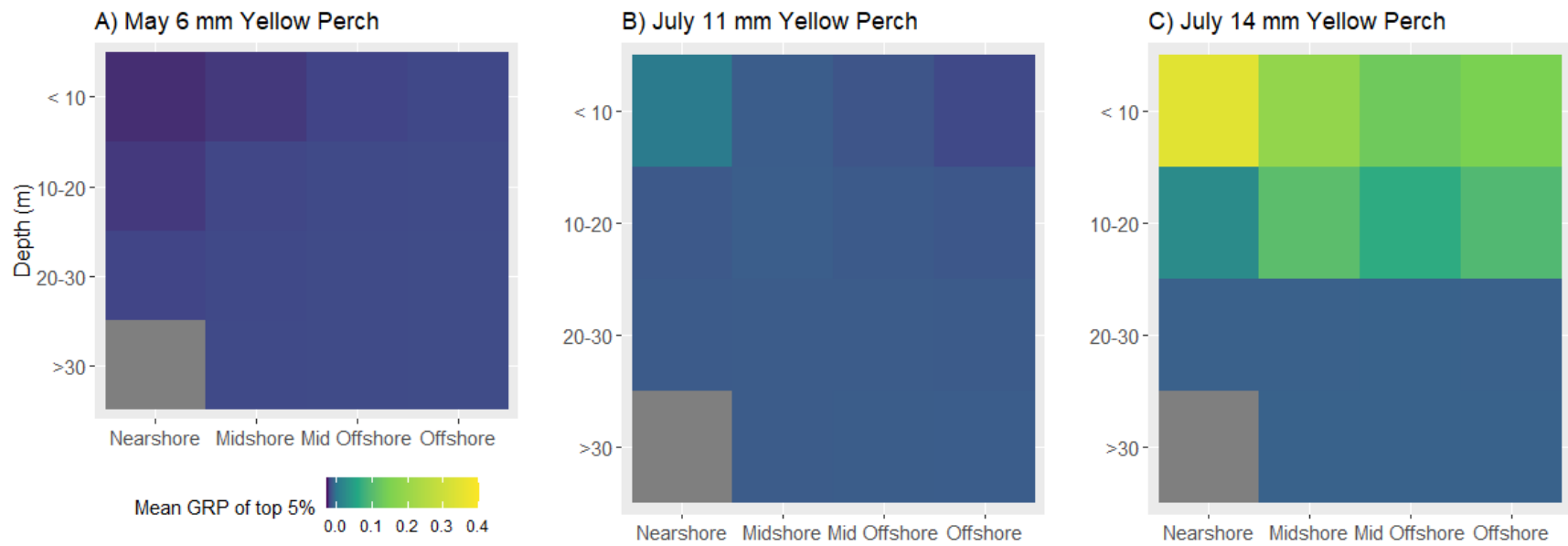


Figure 3. 9 Central Lake Michigan means of mean individual transect averages of GRP in cells within the 95th percentile for 16 designated areas of the water column by month and species in May for 6 mm yellow perch (A) and July for 11 mm and 14 mm yellow perch (B,C).

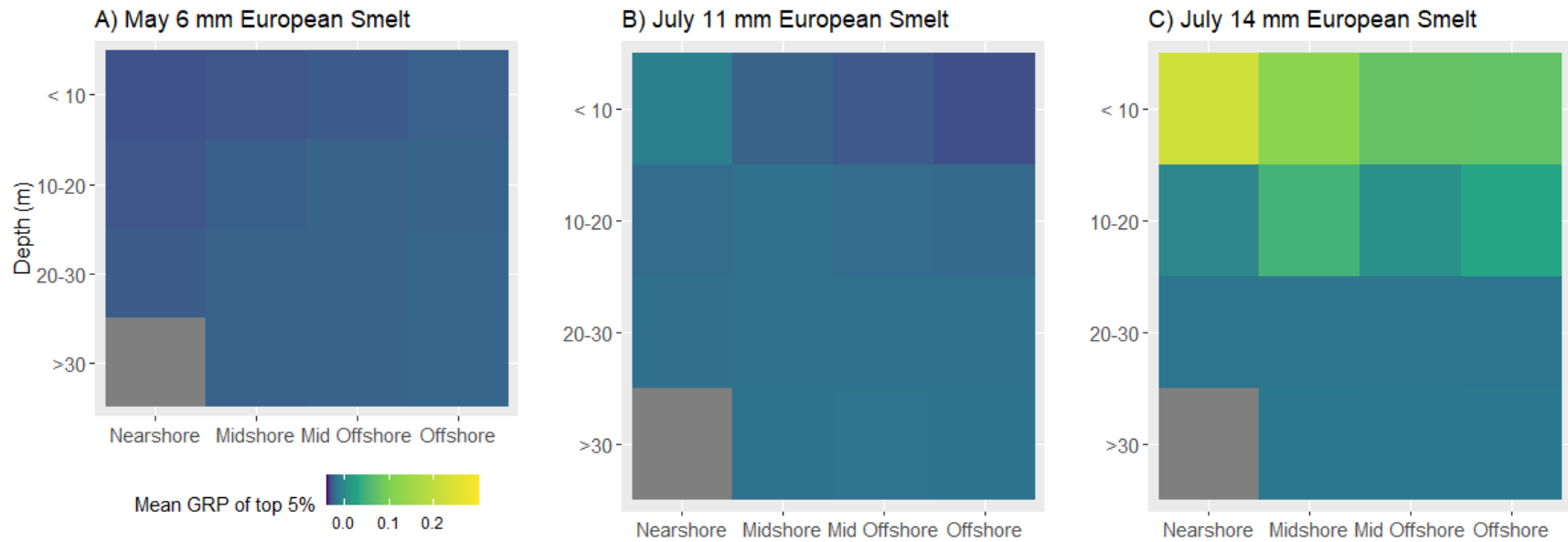


Figure 3. 10 Central Lake Michigan means of mean individual transect averages of GRP in cells within the 95th percentile for 16 designated areas of the water column by month and species in May for 6 mm smelt (A) and July for 11 mm and 14 mm smelt (B,C).

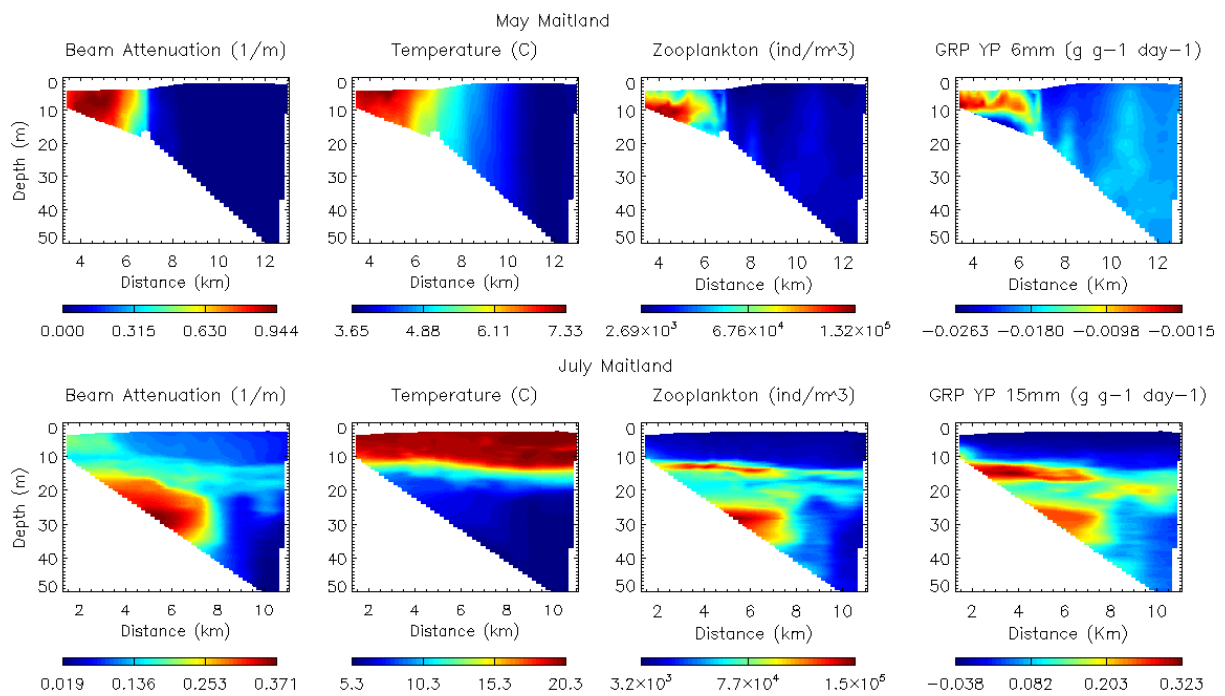


Figure 3. 11 Dissolved oxygen, temperature, zooplankton density, and GRP for Maitland transects in May (top row) and July (bottom row)

3.6 References

- Aksnes, D.L. and Utne, A.C.V., 1997. A revised model of aquatic visual feeding. *Sarsia*, 82, pp.137-147.
- Anneville, O., Berthon, V., Glippa, O., Mahjoub, M.S., Molinero, J.C. and Souissi, S., 2011. Ontogenetic dietary changes of whitefish larvae: insights from field and experimental observations. *Environmental biology of fishes*, 91(1), pp.27-38.
- Arend, K.K., Beletsky, D., DePINTO, J.V., Ludsin, S.A., Roberts, J.J., Rucinski, D.K., Scavia, D., Schwab, D.J. and Höök, T.O., 2011. Seasonal and interannual effects of hypoxia on fish habitat quality in central Lake Erie. *Freshwater Biology*, 56(2), pp.366-383.
- Austin, J. and Colman, S., 2008. A century of temperature variability in Lake Superior. *Limnology and Oceanography*, 53(6), pp.2724-2730.
- Barbiero, R.P., Rudstam, L.G., Watkins, J.M. and Lesht, B.M., 2019. A cross-lake comparison of crustacean zooplankton communities in the Laurentian Great Lakes, 1997–2016. *Journal of Great Lakes Research*, 45(3), pp.672-690.

- Beletsky, D., Mason, D.M., Schwab, D.J., Rutherford, E.S., Janssen, J., Clapp, D.F. and Dettmers, J.M., 2007. Biophysical model of larval yellow perch advection and settlement in Lake Michigan. *Journal of Great Lakes Research*, 33(4), pp.842-866.
- Bottrell, H.C. and HH, B., 1976. A review of some problems in zooplankton production studies.
- Bourdeau, P.E., Pangle, K.L. and Peacor, S.D., 2015. Factors affecting the vertical distribution of the zooplankton assemblage in Lake Michigan: The role of the invasive predator *Bythotrephes longimanus*. *Journal of Great Lakes Research*, 41, pp.115-124.
- Brandt, S.B., Costantini, M., Kolesar, S., Ludsins, S.A., Mason, D.M., Rae, C.M. and Zhang, H., 2011. Does hypoxia reduce habitat quality for Lake Erie walleye (*Sander vitreus*)? A bioenergetics perspective. *Canadian Journal of Fisheries and Aquatic Sciences*, 68(5), pp.857-879.
- Bunnell, D.B., Ludsins, S.A., Knight, R.L., Rudstam, L.G., Williamson, C.E., Höök, T.O., Collingsworth, P.D., Lesht, B.M., Barbiero, R.P., Scofield, A.E. and Rutherford, E.S., 2021. Consequences of changing water clarity on the fish and fisheries of the Laurentian Great Lakes. *Canadian Journal of Fisheries and Aquatic Sciences*, 78(10), pp.1524-1542.
- Cummins, K.W. and Wuycheck, J.C., 1971. Caloric Equivalents for Investigations in Ecological Energetics: With 2 figures and 3 tables in the text. *Internationale Vereinigung für Theoretische und Angewandte Limnologie: Mitteilungen*, 18(1), pp.1-158.
- Dettmers, J.M., Janssen, J., Pientka, B., Fulford, R.S. and Jude, D.J., 2005. Evidence across multiple scales for offshore transport of yellow perch (*Perca flavescens*) larvae in Lake Michigan. *Canadian Journal of Fisheries and Aquatic Sciences*, 62(12), pp.2683-2693.
- Evans, M.A., Fahnenstiel, G. and Scavia, D., 2011. Incidental oligotrophication of North American great lakes. *Environmental science & technology*, 45(8), pp.3297-3303.
- Fahnenstiel, G., Pothoven, S., Vanderploeg, H., Klarer, D., Nalepa, T. and Scavia, D., 2010. Recent changes in primary production and phytoplankton in the offshore region of southeastern Lake Michigan. *Journal of Great Lakes Research*, 36, pp.20-29.
- Fernandez, R.J., Rennie, M.D. and Sprules, W.G., 2009. Changes in nearshore zooplankton associated with species invasions and potential effects on larval lake whitefish (*Coregonus clupeaformis*). *International review of hydrobiology*, 94(2), pp.226-243.
- Fiksen, Ø., Utne, A.C.W., Aksnes, D.L., Eiane, K., Helvik, J.V. and Sundby, S., 1998. Modelling the influence of light, turbulence and ontogeny on ingestion rates in larval cod and herring. *Fisheries Oceanography*, 7(3-4), pp.355-363.
- Fuiman, L.A. and Werner, R.G. eds., 2009. *Fishery science: the unique contributions of early life stages*. John Wiley & Sons.

- Gorman, O.T., 2019. Prey fish communities of the Laurentian Great Lakes: A cross-basin overview of status and trends based on bottom trawl surveys, 1978-2016. *Aquatic Ecosystem Health & Management*, 22(3), pp.263-279.
- Hewett, S. W. and BL Johnson. 1992. A generalized bioenergetics model of fish growth for microcomputers. University of Wisconsin Sea Grant Institute, Madison, Wisconsin. UW Sea Grant Tech. Rep. WIS-SG-92-250. 79 pp.
- Hoagman, W.J., 1974. Vital activity parameters as related to the early life history of larval and post-larval lake whitefish (*Coregonus clupeaformis*). In *The early life history of fish* (pp. 547-558). Springer, Berlin, Heidelberg.
- Holbrook, B.V., Hrabik, T.R., Branstrator, D.K. and Mensinger, A.F., 2013. Foraging mechanisms of age-0 lake trout (*Salvelinus namaycush*). *Journal of Great Lakes Research*, 39(1), pp.128-137.
- Holling, C.S., 1965. The functional response of predators to prey density and its role in mimicry and population regulation. *The Memoirs of the Entomological Society of Canada*, 97(S45), pp.5-60.
- Höök, T.O., Rutherford, E.S., Brines, S.J., Geddes, C.A., Mason, D.M., Schwab, D.J. and Fleischer, G.W., 2004. Landscape scale measures of steelhead (*Oncorhynchus mykiss*) bioenergetic growth rate potential in Lake Michigan and comparison with angler catch rates. *Journal of Great Lakes Research*, 30(4), pp.545-556.
- Hrabik, T.R., Carey, M.P. and Webster, M.S., 2001. Interactions between young-of-the-year exotic rainbow smelt and native yellow perch in a northern temperate lake. *Transactions of the American Fisheries Society*, 130(4), pp.568-582.
- Karjalainen, J., Turunen, T., Helminen, H., Sarvala, J. and Huuskonen, H., 1997. Food selection and consumption of O+ smelt (*Osmerus eperlanus* (L.)) and vendace (*Coregonus albula* (L.)) in pelagial zone of Finnish lakes (with 5 figures and 3 tables). *Ergebnisse der Limnologie*, (49), pp.37-50.
- Letcher, B.H., Rice, J.A., Crowder, L.B. and Rose, K.A., 1996. Variability in survival of larval fish: disentangling components with a generalized individual-based model. *Canadian Journal of Fisheries and Aquatic Sciences*, 53(4), pp.787-801.
- Mahjoub, M.S., Anneville, O., Molinero, J.C., Souissi, S. and Hwang, J.S., 2008. Feeding mechanism and capture success of European whitefish (*Coregonus lavaretus* L.) larvae. *Knowledge and Management of Aquatic Ecosystems*, (388), p.05.
- Mason, D. M., and Brandt, S.B., 1996. Effects of Spatial Scale and Foraging Efficiency on the Predictions Made by Spatially-Explicit Models of Fish Growth Rate Potential. *Environmental Biology of Fishes* 45(3), pp. 283–98.

- Miller, T.J., Crowder, L.B., Rice, J.A. and Marschall, E.A., 1988. Larval size and recruitment mechanisms in fishes: toward a conceptual framework. *Canadian Journal of Fisheries and Aquatic Sciences*, 45(9), pp.1657-1670.
- Nislow, K.H., Folt, C.L. and Parrish, D.L., 2000. Spatially explicit bioenergetic analysis of habitat quality for age-0 Atlantic salmon. *Transactions of the American Fisheries Society*, 129(5), pp.1067-1081.
- Nowicki, C.J., Bunnell, D.B., Armenio, P.M., Warner, D.M., Vanderploeg, H.A., Cavaletto, J.F., Mayer, C.M. and Adams, J.V., 2017. Biotic and abiotic factors influencing zooplankton vertical distribution in Lake Huron. *Journal of Great Lakes Research*, 43(6), pp.1044-1054.
- Ord, J.K. and Getis, A., 1995. Local spatial autocorrelation statistics: distributional issues and an application. *Geographical analysis*, 27(4), pp.286-306.
- Post, J.R., 1990. Metabolic allometry of larval and juvenile yellow perch (*Perca flavescens*): in situ estimates and bioenergetic models. *Canadian Journal of Fisheries and Aquatic Sciences*, 47(3), pp.554-560.
- Pothoven, S.A., Höök, T.O. and Roswell, C.R., 2014. Feeding ecology of age-0 lake whitefish in Saginaw Bay, Lake Huron. *Journal of Great Lakes Research*, 40, pp.148-155.
- Pothoven, S.A. and Fahnenstiel, G.L., 2015. Spatial and temporal trends in zooplankton assemblages along a nearshore to offshore transect in southeastern Lake Michigan from 2007 to 2012. *Journal of Great Lakes Research*, 41, pp.95-103.
- Puvanendran, V. and Brown, J.A., 2002. Foraging, growth and survival of Atlantic cod larvae reared in different light intensities and photoperiods. *Aquaculture*, 214(1-4), pp.131-151.
- Richmond, H. E., Hrabik, T. R., & Mensinger, A. F. (2004). Light intensity, prey detection and foraging mechanisms of age 0 year yellow perch. *Journal of Fish Biology*, 65(1), 195-205.
- Richmond, H.E., Hrabik, T.R. and Mensinger, A.F., 2004. Light intensity, prey detection and foraging mechanisms of age 0 year yellow perch. *Journal of Fish Biology*, 65(1), pp.195-205.
- Roseman, E.F. and O'Brien, T.P., 2013. Spatial distribution of pelagic fish larvae in the northern main basin of Lake Huron. *Aquatic Ecosystem Health & Management*, 16(3), pp.311-321.
- Schael, D.M., Rudstam, L.G. and Post, J.R., 1991. Gape limitation and prey selection in larval yellow perch (*Perca flavescens*), freshwater drum (*Aplodinotus grunniens*), and black crappie (*Pomoxis nigromaculatus*). *Canadian Journal of Fisheries and Aquatic Sciences*, 48(10), pp.1919-1925.
- Scofield, A.E., Watkins, J.M. and Rudstam, L.G., 2020. Heterogeneity in zooplankton distributions and vertical migrations: Application of a laser optical plankton counter in offshore Lake Michigan. *Journal of Great Lakes Research*, 46(4), pp.780-797.

- Stadig, M.H., Collingsworth, P.D., Lesht, B.M. and Höök, T.O., 2020. Spatially heterogeneous trends in nearshore and offshore chlorophyll a concentrations in lakes Michigan and Huron (1998–2013). *Freshwater Biology*, 65(3), pp.366-378.
- Trumpickas, J., Shuter, B.J. and Minns, C.K., 2009. Forecasting impacts of climate change on Great Lakes surface water temperatures. *Journal of Great Lakes Research*, 35(3), pp.454-463.
- Utne-Palm, A.C., 1999. The effect of prey mobility, prey contrast, turbidity and spectral composition on the reaction distance of *Gobiusculus flavescens* to its planktonic prey. *Journal of Fish Biology*, 54(6), pp.1244-1258.
- Utne-Palm, A.C., 2002. Visual feeding of fish in a turbid environment: physical and behavioural aspects. *Marine and Freshwater Behaviour and Physiology*, 35(1-2), pp.111-128.
- Utne-Palm, A.C. and Stiansen, J.E., 2002. Effect of larval ontogeny, turbulence and light on prey attack rate and swimming activity in herring larvae. *Journal of experimental marine biology and ecology*, 268(2), pp.147-170.
- Varpe, Ø. and Fiksen, Ø., 2010. Seasonal plankton–fish interactions: light regime, prey phenology, and herring foraging. *Ecology*, 91(2), pp.311-318.
- Walton, W.E., Hairston Jr, N.G. and Wetterer, J.K., 1992. Growth-related constraints on diet selection by sunfish. *Ecology*, 73(2), pp.429-437.
- Watkins, J.M., Collingsworth, P.D., Saavedra, N.E., O'Malley, B.P. and Rudstam, L.G., 2017. Fine-scale zooplankton diel vertical migration revealed by traditional net sampling and a Laser Optical Plankton Counter (LOPC) in Lake Ontario. *Journal of Great Lakes Research*, 43(5), pp.804-812.
- Weber, M.J., Dettmers, J.M. and Wahl, D.H., 2011. Growth and survival of age-0 yellow perch across habitats in southwestern Lake Michigan: early life history in a large freshwater environment. *Transactions of the American Fisheries Society*, 140(5), pp.1172-1185.
- Withers, J.L., Sesterhenn, T.M., Foley, C.J., Troy, C.D. and Höök, T.O., 2015. Diets and growth potential of early stage larval yellow perch and alewife in a nearshore region of southeastern Lake Michigan. *Journal of Great Lakes Research*, 41, pp.197-209.
- Worischka, S. and Mehner, T., 1998. Comparison of field-based and indirect estimates of daily food consumption in larval perch and zander. *Journal of Fish Biology*, 53(5), pp.1050-1059.
- Xu, W., Collingsworth, P., Bailey, B., Mazur, M.C., Schaeffer, J. and Minsker, B., 2017. Detecting spatial patterns of rivermouth processes using a geostatistical framework for near-real-time analysis. *Environmental modelling & software*, 97, pp.72-85. Xu, Wenzhao. 2018. Towed Undulating Vehicles Analyzing Tool. (<https://doi.org/10.1016/j.envsoft.2017.06.049>): Stormxuwz/TUVTool. R.

Yurista, P.M., Kelly, J.R. and Miller, S.E., 2009. Lake Superior zooplankton biomass: alternate estimates from a probability-based net survey and spatially extensive LOPC surveys. *Journal of Great Lakes Research*, 35(3), pp.337-346.

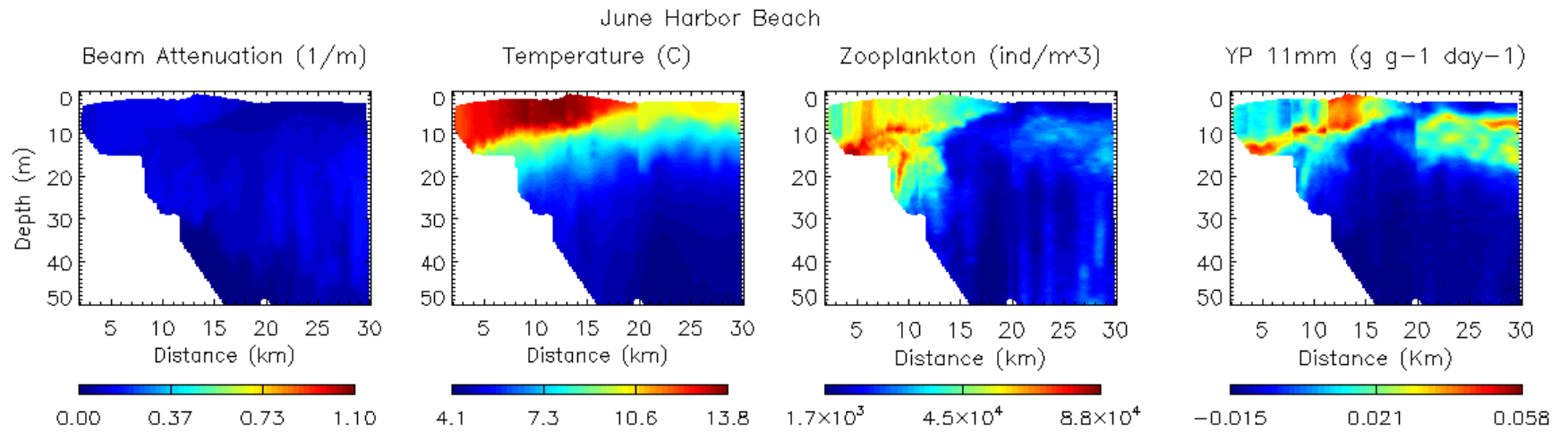


Figure 1: June Harbor Beach transect environmental conditions (temperature, beam attenuation, zooplankton density) and GRP of 10 mm yellow perch

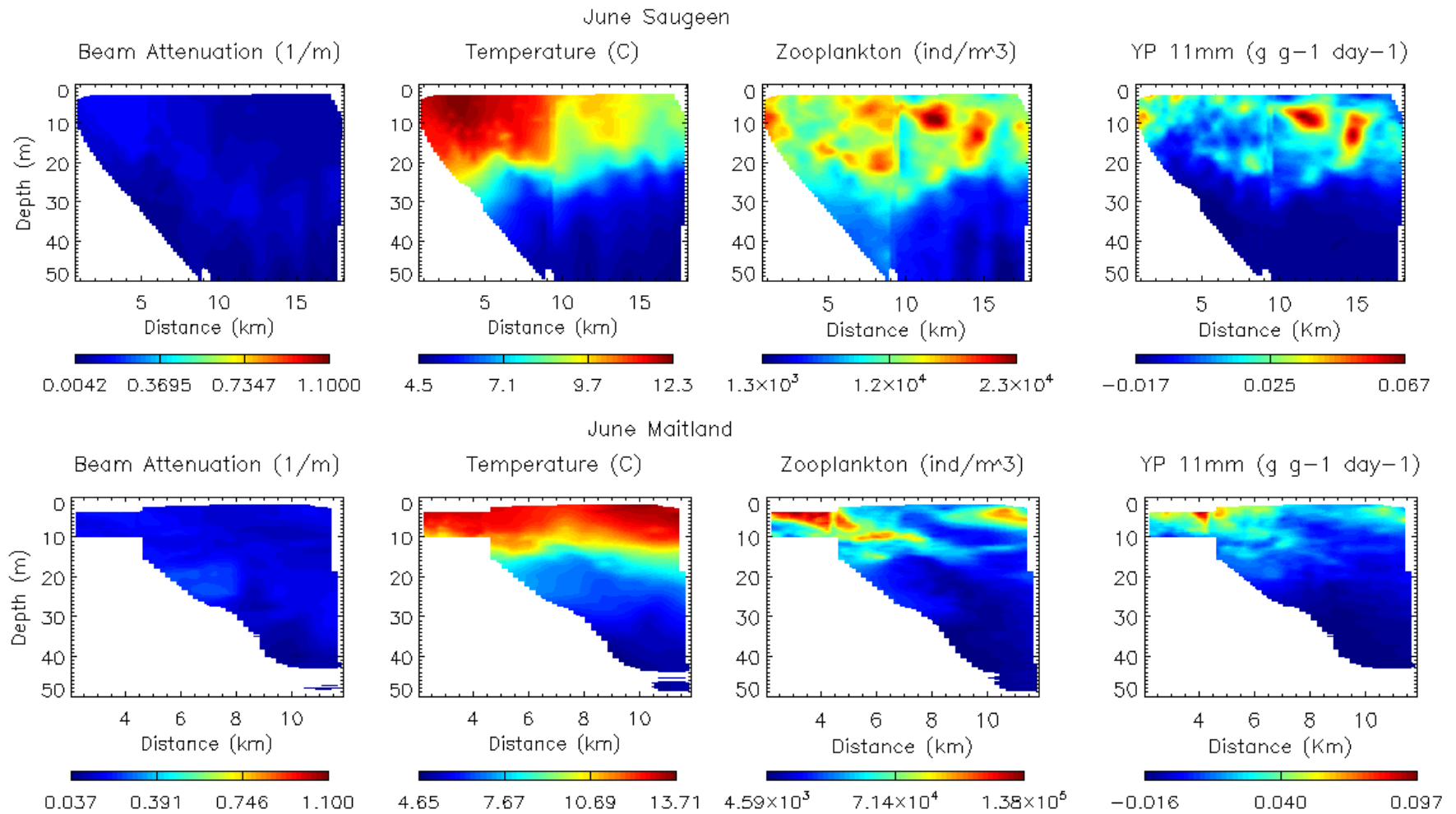


Figure 2: June Saugeen (top row) and June Maitland (bottom row) transect environmental conditions (temperature, beam attenuation, zooplankton density) and GRP of 10 mm yellow perch.

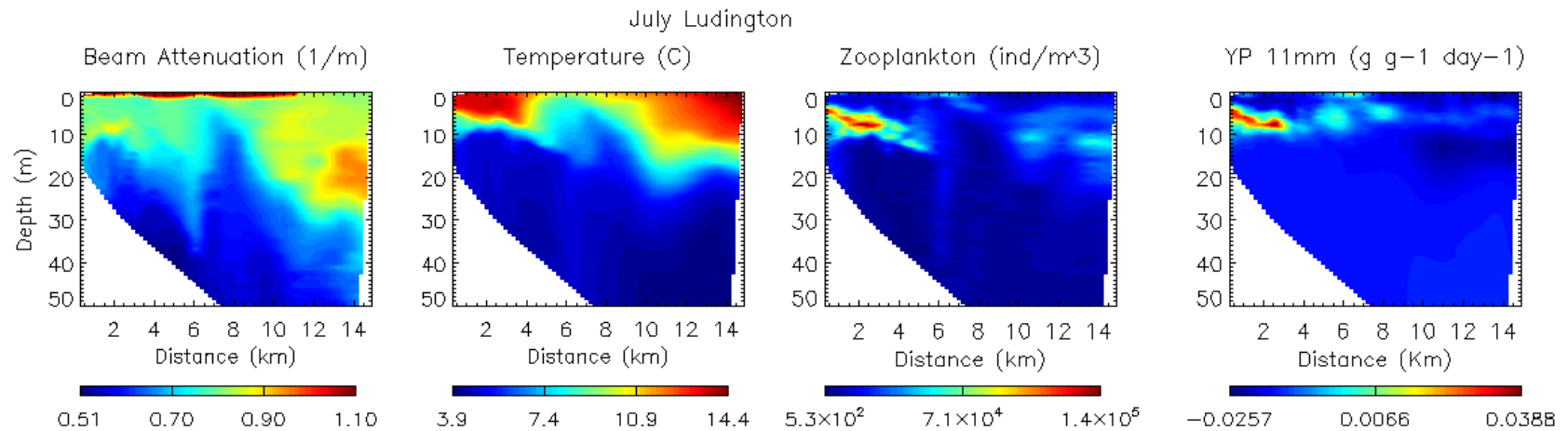
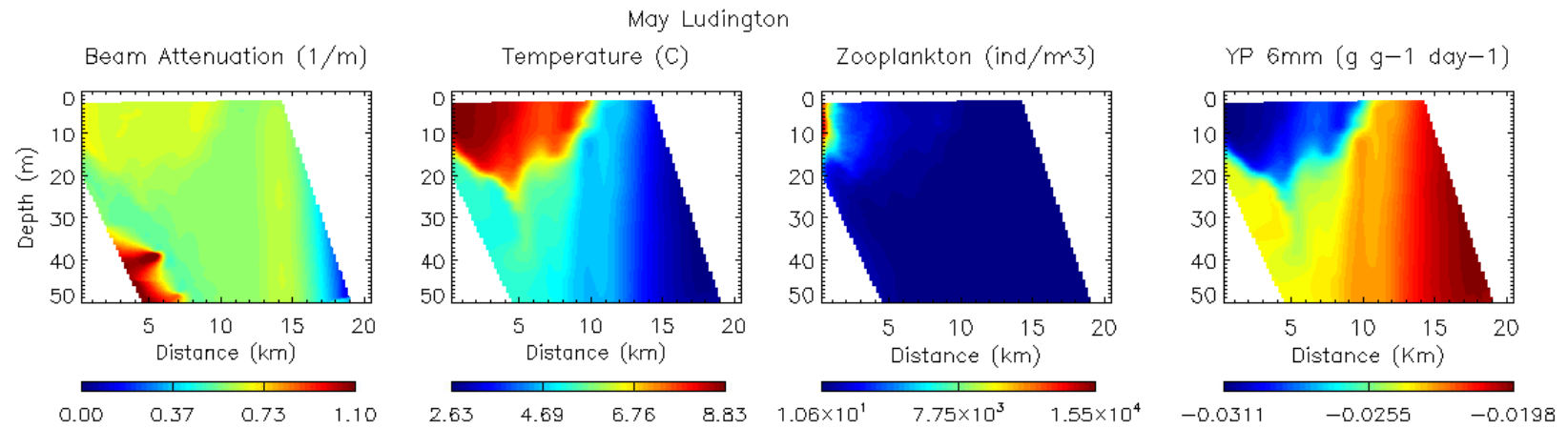


Figure 3: May Ludington (top row) and July Ludington (bottom row) transect environmental conditions (temperature, beam attenuation, zooplankton density) and GRP of 6 mm (top) or 15 mm (bottom) yellow perch.

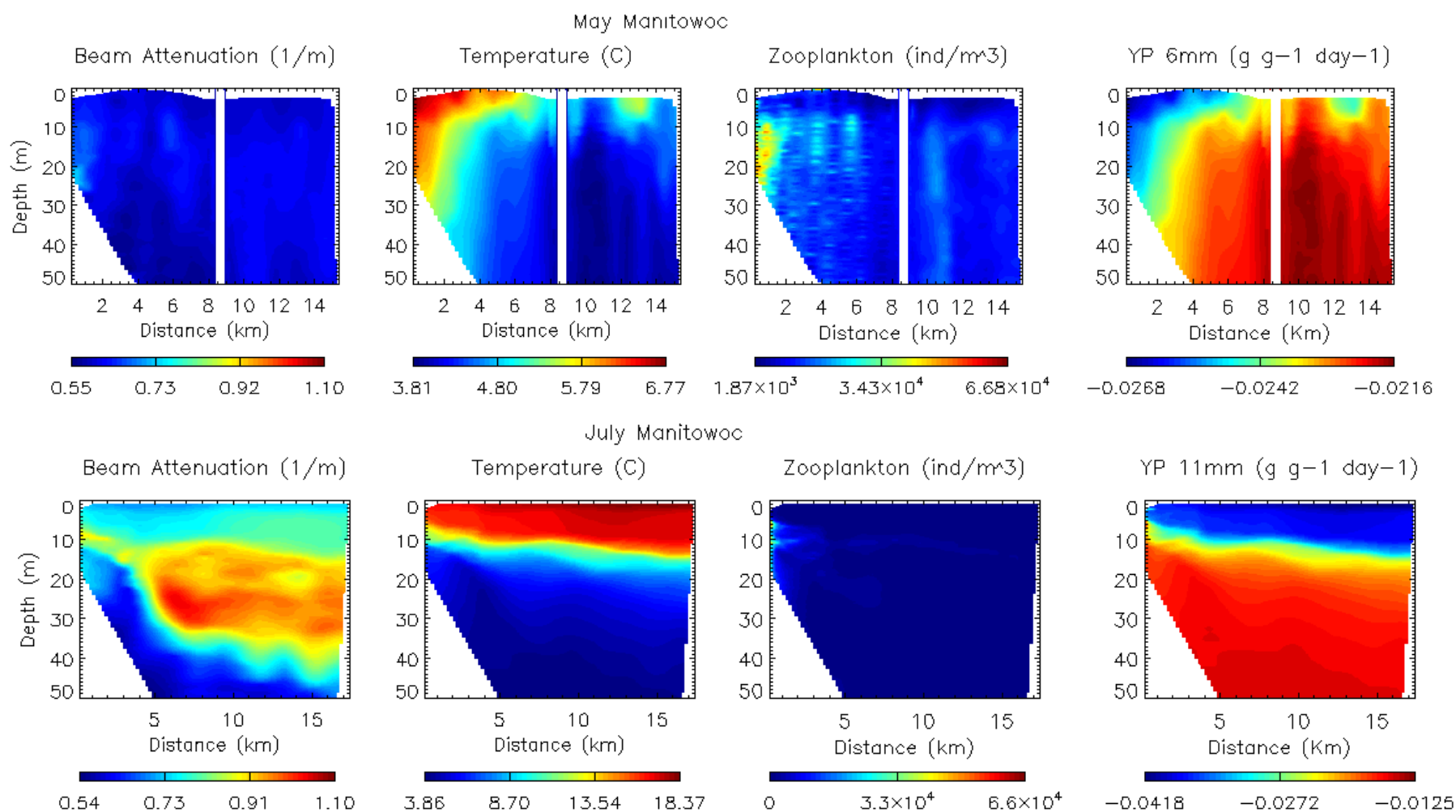


Figure 4: May Manitowoc (top row) and July Manitowoc (bottom row) transect environmental conditions (temperature, beam attenuation, zooplankton density) and GRP of 6 mm (top) or 15 mm (bottom) yellow perch.

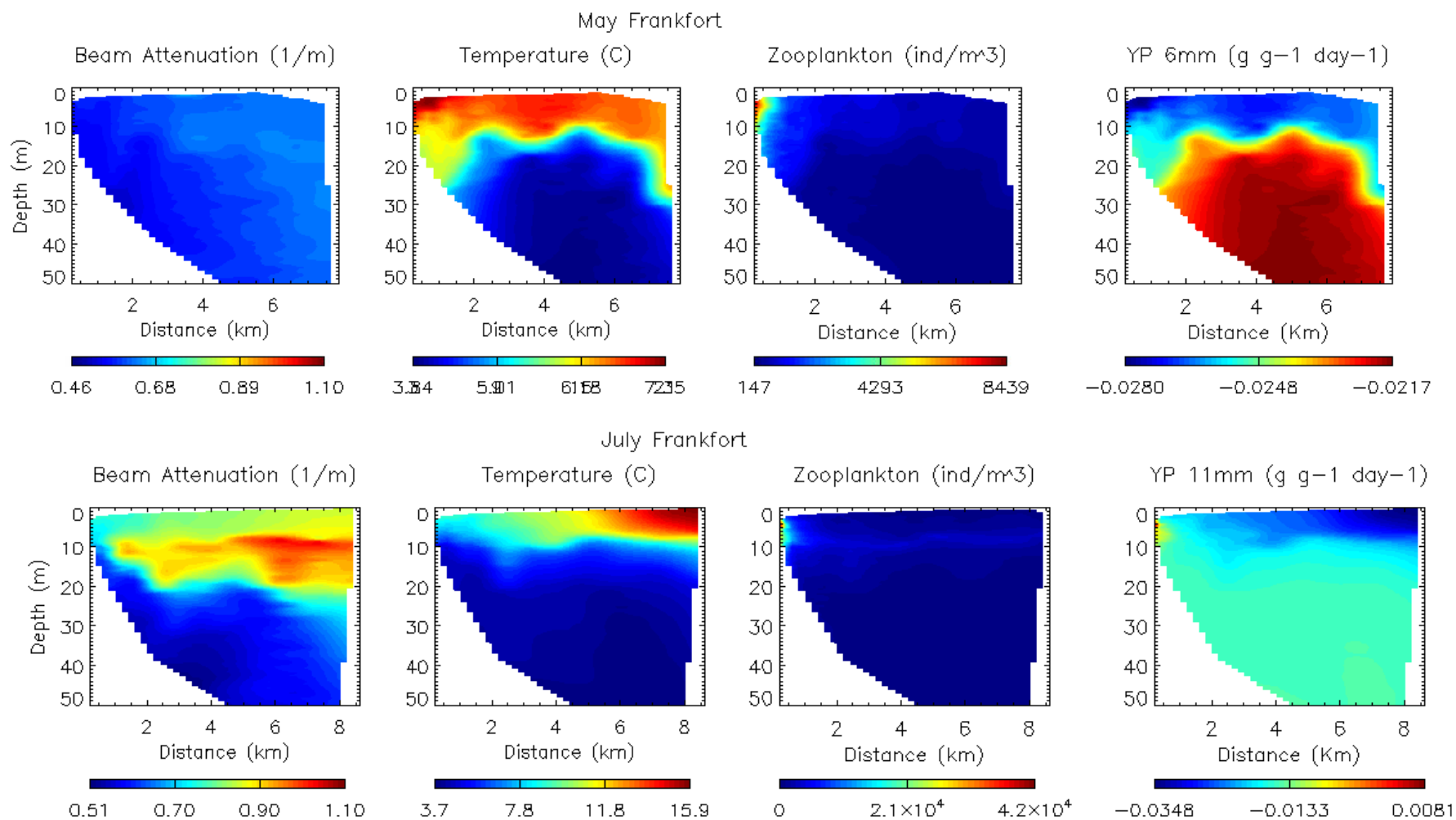


Figure 5: May Frankfort (top row) and July Frankfort (bottom row) transect environmental conditions (temperature, beam attenuation, zooplankton density) and GRP of 6 mm (top) or 15 mm (bottom) yellow perch.

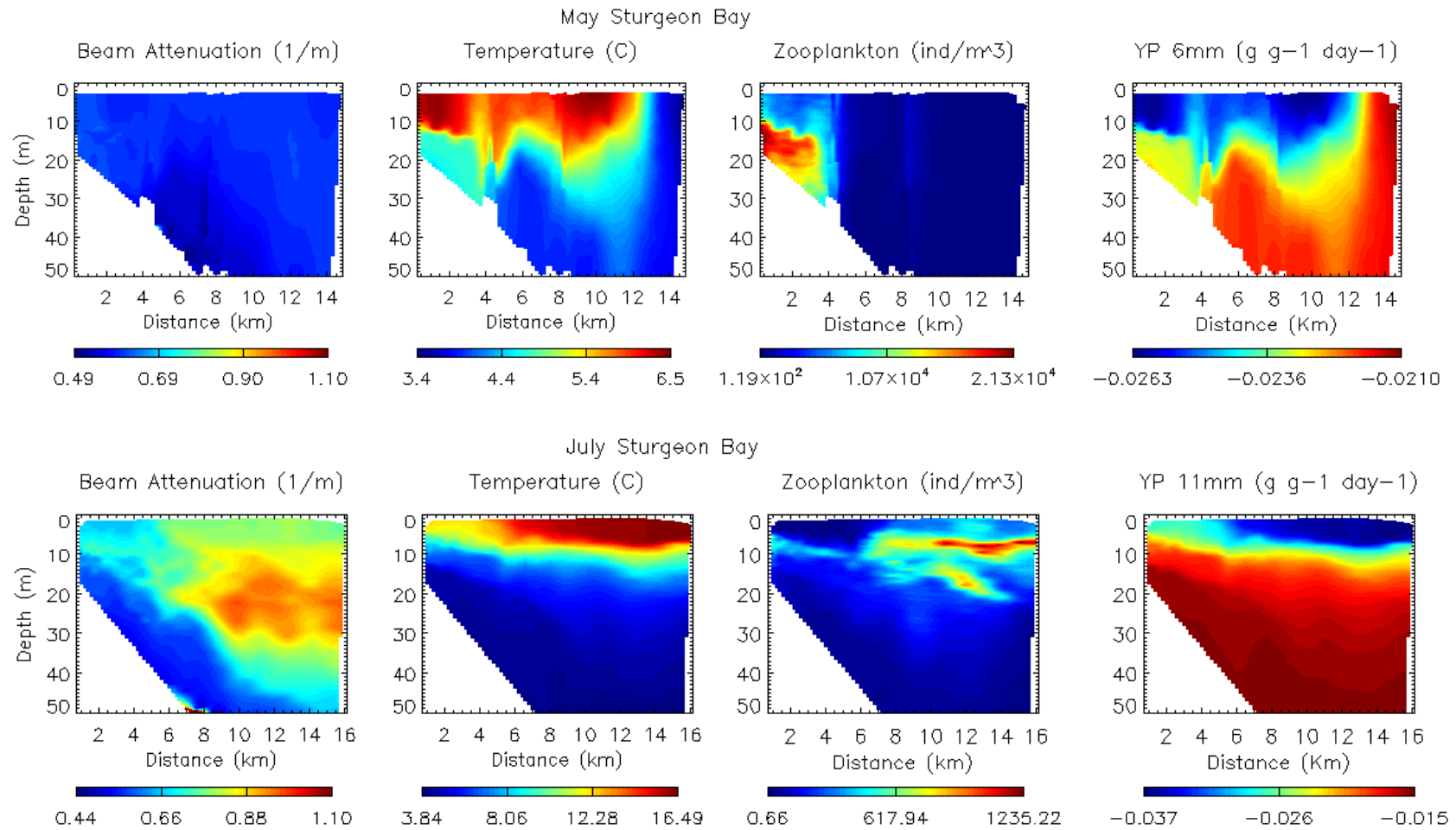


Figure 6: May Sturgeon Bay (top row) and July Sturgeon Bay (bottom row) transect environmental conditions (temperature, beam attenuation, zooplankton density) and GRP of 6 mm (top) or 15 mm (bottom) yellow perch.

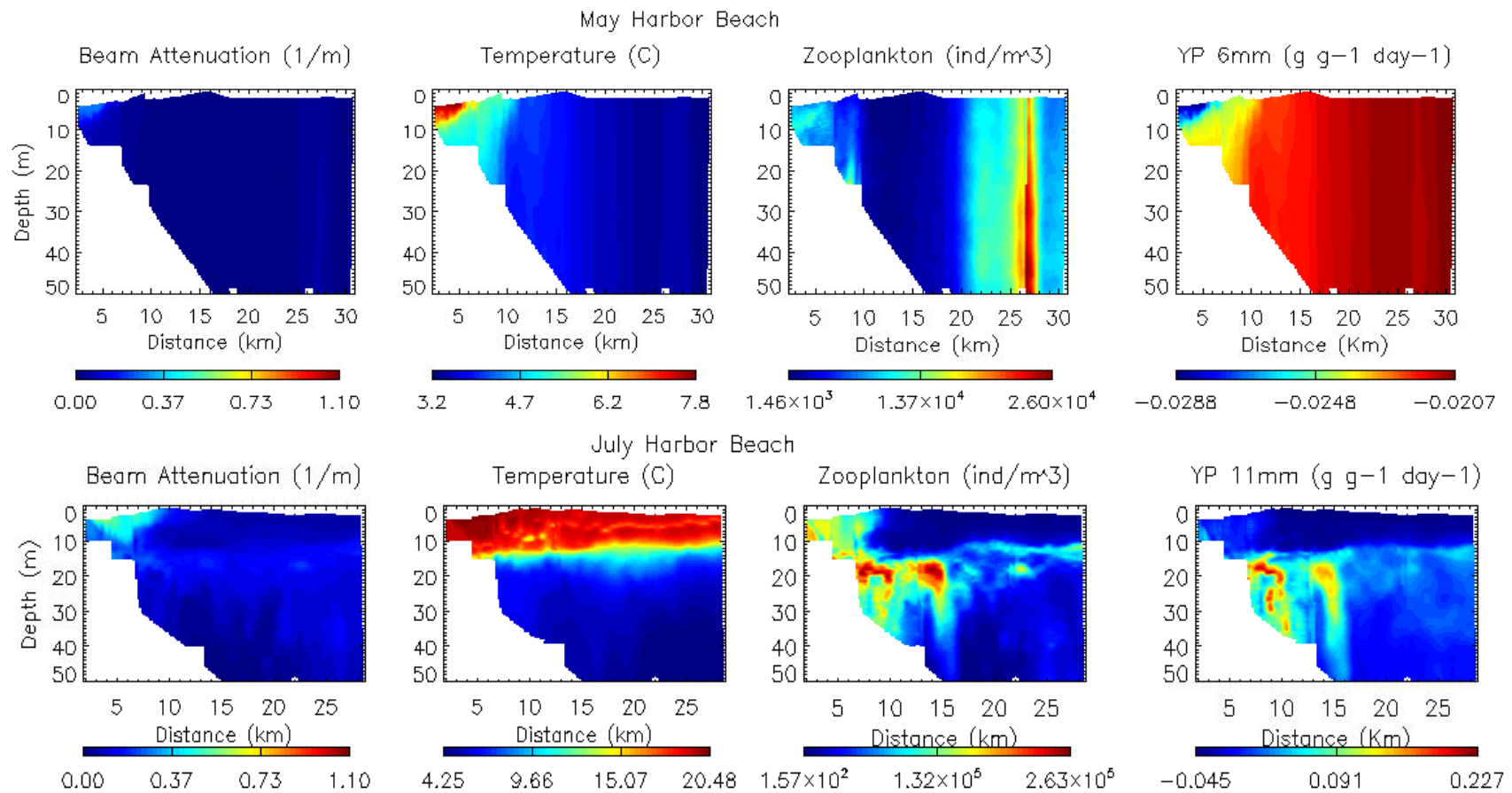


Figure 7: May Harbor Beach (top row) and July Harbor Beach (bottom row) transect environmental conditions (temperature, beam attenuation, zooplankton density) and GRP of 6 mm (top) or 15 mm (bottom) yellow perch.

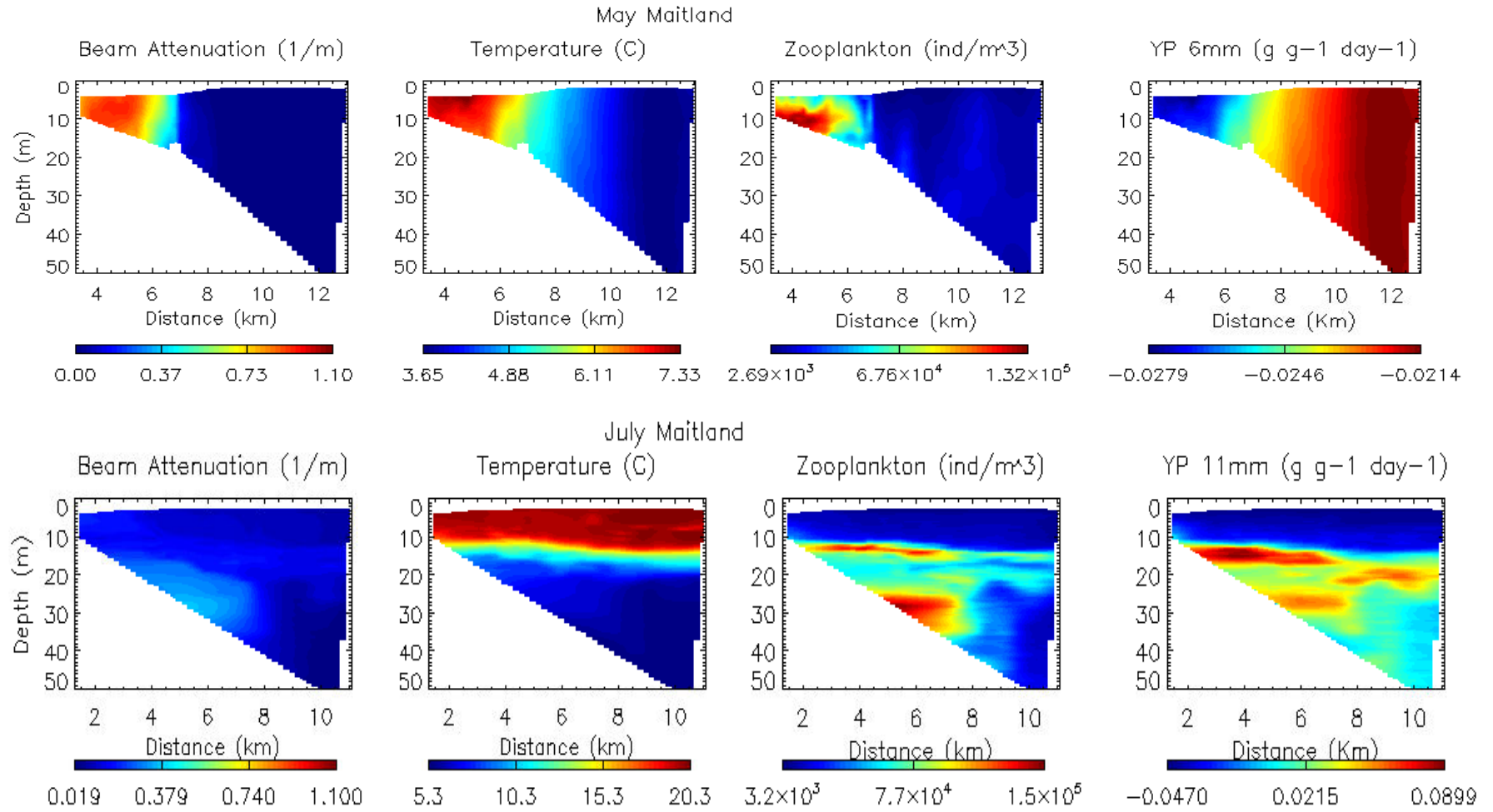


Figure 8: May Maitland (top row) and July Maitland (bottom row) transect environmental conditions (temperature, beam attenuation, zooplankton density) and GRP of 6 mm (top) or 15 mm (bottom) yellow perch.

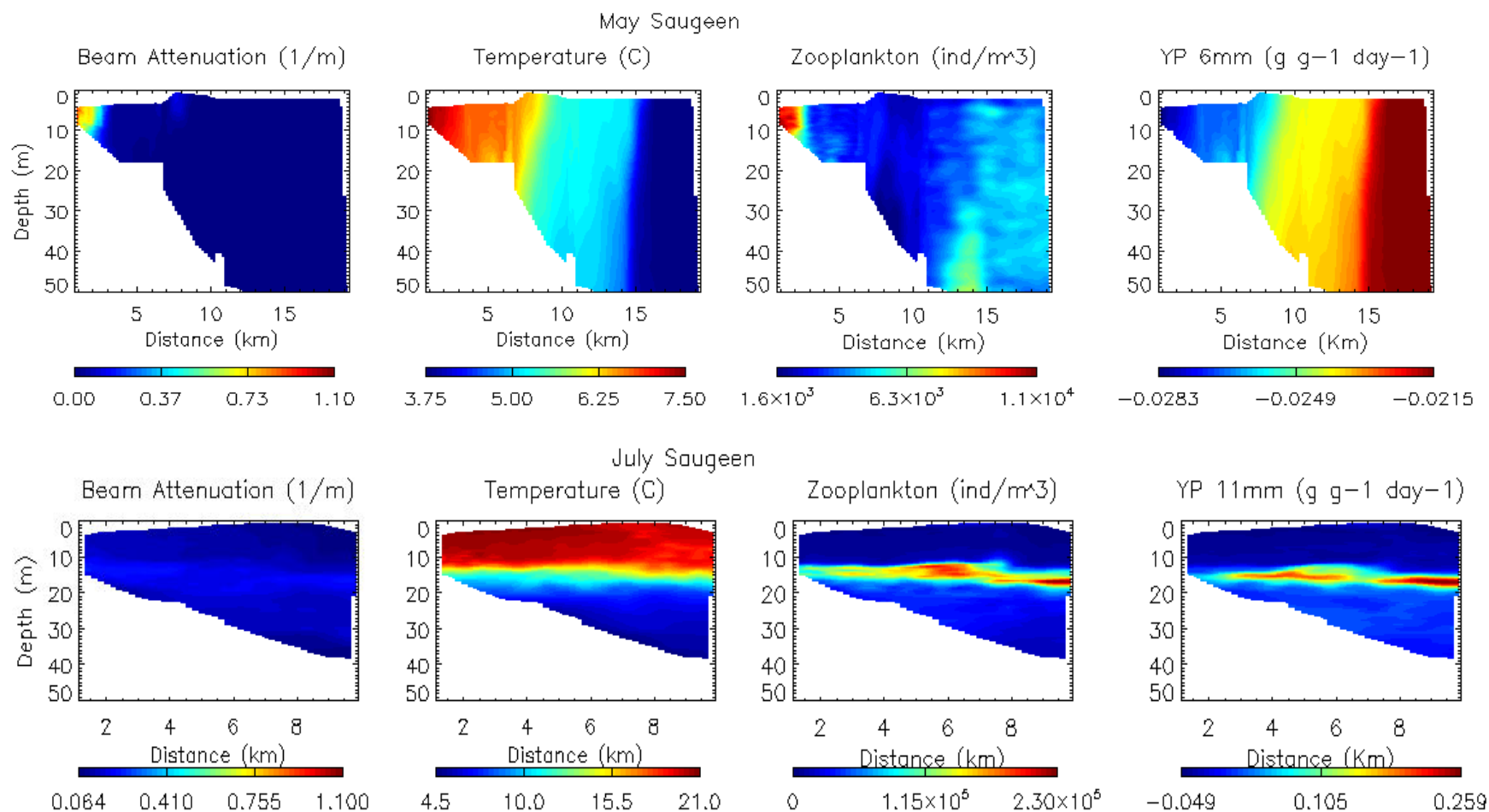


Figure 9: May Saugeen (top row) and July Saugeen (bottom row) transect environmental conditions (temperature, beam attenuation, zooplankton density) and GRP of 6 mm (top) or 15 mm (bottom) yellow perch.